

***The Development of Techniques for the Identification  
of Novel Viruses Associated with Acute Infantile  
Gastroenteritis in South Africa***

Thesis submitted in the fulfilment of the requirements of the degree

**Master of Science (Microbiology)**

**At Rhodes University**

Brittany J. Jaquet

Department of Biochemistry and Microbiology, Rhodes University, Grahamstown 6140, Eastern  
Cape, South Africa.

## ***Abstract***

Gastroenteritis is a serious disease affecting both children and adults globally, but is more predominant in children with over half a million deaths reported each year. The leading cause of this disease is rotavirus, which accounts for 38% of all hospitalised cases. There has, however, been a significant decrease in the number of deaths associated with rotavirus worldwide since the introduction of the two vaccines, Rotarix® and RotaTeq®. A large number of cases are therefore either associated with other viruses, such as norovirus, Aichi virus (AiV) or Saffold virus (SAFV), or are of unknown aetiology. This study thus aims to develop techniques for the identification of viruses associated with gastroenteritis. Theiler's murine encephalomyelitis virus (TMEV) was used to develop the sample preparation, transmission electron microscopy and RT-PCR techniques used in this study. This virus was chosen as a replication system using baby hamster kidney cells can be used to create high concentrations of viral particles from which RNA can be extracted preventing the waste of the limited samples. The virus particles are also similar in size and morphology to the viruses to be identified in this study, as it belongs to the same family. After sample preparation, TEM analysis showed the presence of small, round, non-enveloped virus particles in the TMEV sample. Due to the low concentration of virus particles, PEG precipitation was performed using both 0.15 M and 0.25 M NaCl and 8% (w/v) PEG 6000. TEM analysis then showed an increase in viral particle concentration, with the highest concentration observed at 0.25 M NaCl and 8% PEG 6000. RNA was successfully extracted and RT-PCR assays were performed for both the VP1 and 2B coding regions of TMEV. A method for creating a positive control for the RT-PCR assay was developed by the *in vitro* transcription of RNA from pTMEV, which contains the cDNA of TMEV. The RNA was then used as the template for the 2B two-step RT-PCR assay. A product of 412 bp was successfully amplified from the *in vitro* transcribed RNA and the sensitivity of the RT-PCR assay was determined. Using a Norovirus GII positive stool sample provided by Maureen Taylor, a nested RT-PCR assay was developed for the NoV GII N/S domain using a previously-published primer set and cycling parameters. A 342 bp product was successfully amplified from the RNA extracted from the stool sample and cloned into pGEM®-T Easy to produce pNoVGII. Using the plasmid containing the AiV 5'UTR and the PCR amplicon for AiV 3CD, RT-PCR assays were developed for AiV 5'UTR and partial 3CD. The RT-PCR assays produced a 1008 bp product for AiV 5'UTR and 266 bp for AiV 3CD, which were cloned into pGEM®-T Easy to produce pAiV5'UTR and pAiV3CD, respectively. Using *in vitro* transcribed RNA from

pNoVGII, pAiV5'UTR, pAiV3CD and pSAFV, which contains the SAFV cDNA, positive controls were developed for the RT-PCR assays for NoV GII, AiV 5'UTR, AiV 3CD and SAFV 2C. The sensitivity of these assays was determined. The samples chosen for this study include wastewater collected from the Belmont Valley water treatment plant, oysters suspected to be infected with viruses collected from Port Elizabeth, South Africa and 30 stool samples from symptomatic patients. With the methods developed using TMEV, the wastewater, oysters and 30 stool samples were filter-sterilised, concentrated and screened by TEM. All samples showed the presence of virus particles. RNA was successfully extracted and the wastewater, oyster and 30 stool samples were screened for NoV GII using the NoV GII RT-PCR assay. The wastewater, oysters and 11 of the stool samples produced the 342 bp NoV GII PCR product and BLAST analysis determined the nucleotide sequences to be NoV GII.4. This shows that this study was able to develop sample preparation techniques and TEM analysis for selected samples and RT-PCR assays for NoV GII, AiV and SAFV. The NoV GII RT-PCR assay was successfully used for the screening of the wastewater, oysters and 30 stool samples for NoV GII. Due to the high number of gastroenteritis cases with unknown aetiology in South Africa, the development of techniques for the identification of NoV, AiV, SAFV and other viruses is very important. The identification of these viruses will allow for better surveillance, treatment and prevention of gastroenteritis in South Africa.

## *Research Outputs*

### **Conferences:**

**Williams, B. J., de Felipe, P., Knox, C. M. (2013).** Identification of Novel Viruses Associated with Acute Infantile Gastroenteritis in South Africa. *Oral presentation, SASM 2013 conference, held at Forever Resorts Warm Baths, Bela-Bela, Limpopo province, South Africa.* 24-27 November.

### **Articles:**

**Knox, C. M., Luke, G. A., Dewar, J., de Felipe, P. & Williams, B. J. (2012).** Rotaviruses and Emerging Picornaviruses as Aetiological Agents of Acute Gastroenteritis. *South African Journal of Epidemiological Infection* **27**, 141-148.

# *Table of Contents*

<b>Abstract</b> .....	<b>i</b>
<b>Research Outputs</b> .....	<b>iii</b>
<b>List of Figures</b> .....	<b>viii</b>
<b>List of Tables</b> .....	<b>xii</b>
<b>List of Abbreviations</b> .....	<b>xiii</b>
<b>Acknowledgments</b> .....	<b>xvi</b>
<b>Chapter 1: Literature Review</b> .....	<b>1</b>
1.1 An Overview of Gastroenteritis.....	1
1.2 Causative Agents.....	2
1.3 Viral Pathogens.....	4
1.3.1 Rotavirus.....	5
1.3.2 Norovirus.....	8
1.3.3 Picornaviridae.....	11
1.3.3.1 Enteroviruses.....	13
1.3.3.2 Cosavirus.....	13
1.3.3.3 Cardioviruses and Saffold Virus.....	13
1.3.3.4 Aichi Virus.....	15
1.3.4 Adenovirus.....	16
1.3.5 Astrovirus.....	18
1.4 Gastroenteritis in South Africa.....	19
1.5 Methods of Virus Detection.....	20
1.6 Motivation.....	26
1.7 Primary Aim and Objectives.....	27
<b>Chapter 2: The Development of Sample Preparation Techniques and RT-PCR Assays Using Theiler’s Murine Encephalomyelitis Virus</b> .....	<b>32</b>
2.1 Introduction.....	32
2.2 Materials and Methods.....	34
2.2.1 TMEV Sample Preparation.....	34
2.2.2 Filter Sterilisation and Concentration of TMEV Infected Lysates.....	34
2.2.3 Transmission Electron Microscopy Analysis of the TMEV Sample.....	35
2.2.4 PEG 6000 Precipitation of Virus Particles.....	35
2.2.5 Viral RNA Extraction.....	35
2.2.6 First-Strand cDNA Synthesis and RT-PCR Assay.....	36
2.2.7 In Vitro Transcription.....	37
2.2.8 First-Strand cDNA Synthesis and RT-PCR Assay from In Vitro Transcribed RNA.....	39

2.2.9 Sensitivity of the RT-PCR Assay.....	39
2.3 Results.....	40
2.3.1 Transmission Electron Microscopy .....	40
2.3.2 RNA Extraction from TMEV Particles.....	41
2.3.3 RT-PCR Assays for the Detection of TMEV 2B and VP1 Sequences .....	42
2.3.4 In Vitro Transcription of RNA from pTMEV.....	43
2.3.5 Development of a Two-Step RT-PCR Assay from In Vitro Transcribed RNA.....	44
2.3.6 Sensitivity of the Two-Step RT-PCR Assay .....	44
2.4 Discussion.....	45
<b>Chapter 3: The Development of Positive Controls for the Detection of Norovirus GII, Aichi Virus and Saffold Virus Sequences in RT-PCR Assays .....</b>	<b>48</b>
3.1 Introduction.....	48
3.2 Materials and Methods.....	50
3.2.1 Norovirus .....	50
3.2.1.1 Viral RNA Extraction .....	50
3.2.1.2 Development of a Two-Step RT-PCR Assay for the Amplification of the N/S Domain of the VP1 Sequence .....	50
3.2.1.3 Cloning and Sequencing of the RT-PCR Product.....	52
3.2.1.4 In Vitro Transcription of RNA from pNoVGII.....	52
3.2.1.5 Sensitivity of the Norovirus GII RT-PCR Assay .....	53
3.2.2 Aichi Virus.....	53
3.2.2.1 PCR Assays for the 5'UTR and 3CD Coding Sequence.....	53
3.2.2.2 Cloning of the Aichi Virus 5'UTR and 3CD PCR Products.....	56
3.2.2.3 In Vitro Transcription of RNA from pAiV5'UTR and pAiV3CD.....	56
3.2.2.4 Two-Step RT-PCR Assay from the Aichi Virus 5'UTR and 3CD In Vitro Transcribed RNA .....	56
3.2.2.5 Sensitivity of the Two-Step RT-PCR Assays for the Aichi Virus 5'UTR and 3CD Coding Region .....	57
3.2.3 Saffold Virus.....	57
3.2.3.1 pSAFV .....	57
3.2.3.2 In Vitro Transcription of RNA from pSAFV.....	58
3.2.3.3 Developing a Two-Step RT-PCR Assay for the Detection of Saffold Virus 2C Coding Region .....	58
3.2.3.4 Sensitivity of the Saffold Virus 2C RT-PCR Assay .....	59
3.2.4 Plasmids .....	59
3.3 Results.....	60
3.3.1 Norovirus .....	60
3.3.1.1 The Development of a Two-Step RT-PCR Assay for the Detection of NoV GII.....	60
3.3.1.2 Cloning of the PCR Amplicon from NoV GII into pGEM®-T Easy .....	61

3.3.1.3 In Vitro Transcription of NoV GII RNA from pNoVGII and RT-PCR Assay .....	63
3.3.1.4 Sensitivity of the Two-Step RT-PCR Assay for NoV GII .....	63
3.3.2 Aichi Virus .....	64
3.3.2.1 PCR Amplification of the AiV 5'UTR Coding Region .....	64
3.3.2.2 PCR Amplification of the AiV partial 3CD Coding Region .....	65
3.3.2.3 Cloning of the PCR Amplicons into pGEM®-T Easy to create pAiV5'UTR and pAiV3CD .....	66
3.3.2.4 Development of a Two-Step RT-PCR Assay for AiV 5'UTR .....	67
3.3.2.5 Development of a Two-Step RT-PCR Assay for AiV 3CD .....	68
3.3.2.6 Sensitivity of the Two-Step RT-PCR Assay for AiV 5'UTR and AiV3CD .....	68
3.3.3 Saffold Virus .....	69
3.3.3.1 In Vitro Transcription of SAFV RNA from pSAFV .....	69
3.3.3.2 Development of a Two-Step RT-PCR Assay for SAFV .....	70
3.3.3.3 Sensitivity of the Two-Step RT-PCR Assay for SAFV .....	71
3.4 Discussion .....	72
<b>Chapter 4: Preparation of Samples and Morphological Analysis of Virus Particles .....</b>	<b>76</b>
4.1 Introduction .....	76
4.2 Materials and Methods .....	77
4.2.1 Wastewater Sample .....	77
4.2.1.1 Sample Preparation and Transmission Electron Microscopy .....	77
4.2.1.2 Precipitation with PEG 6000 .....	78
4.2.2 Oyster Samples .....	78
4.2.2.1 Sample Preparation and Transmission Electron Microscopy .....	78
4.2.3 Stool Samples .....	79
4.2.3.1 Sample Preparation and Transmission Electron Microscopy .....	79
4.3 Results .....	81
4.3.1 Transmission Electron Microscopy Wastewater Sample .....	81
4.3.2 Transmission Electron Microscopy of Oyster Extracts .....	82
4.3.3 Transmission Electron Microscopy of Stool Samples .....	83
4.4 Discussion .....	86
<b>Chapter 5: Detection of Norovirus GII in the Wastewater, Oyster and Stool Samples using an RT-PCR assay .....</b>	<b>89</b>
5.1 Introduction .....	89
5.2 Materials and Methods .....	90
5.2.1 Viral RNA Extraction from the Wastewater, Oyster and Stool Samples .....	90
5.2.2 Nested Two-Step Norovirus GII RT-PCR Assay Performed on the Wastewater, Oyster and Stool Samples First-Strand cDNA .....	90
5.2.3 Cloning, Sequencing and BLAST analysis of NoV RT-PCR Products .....	91

5.2.4 Bioinformatics Analysis of the Sequences from the Wastewater, Oyster and Stool Samples .....	91
5.3 Results .....	91
5.3.1 Viral RNA Extraction from the Wastewater, Oyster and Stool Samples.....	91
5.3.2 Norovirus GII RT-PCR Assay Performed on the Wastewater and Oyster Samples .....	93
5.3.3 Norovirus GII RT-PCR Assay Performed on the Stool Samples.....	95
5.3.4 BLAST Analysis of the NoV GII Sequences.....	97
5.3.5 Multiple Alignment of the NoV GII Sequences .....	99
5.4 Discussion .....	102
<b>Chapter 6: General Conclusions and Future Work .....</b>	<b>104</b>
<b>References .....</b>	<b>112</b>
<b>Appendix I: Aichivirus Nucleotide Sequences and Multiple Alignments.....</b>	<b>125</b>
<b>Appendix II: Norovirus Nucleotide Sequences and Multiple Alignments.....</b>	<b>129</b>

## *List of Figures*

### **Chapter 1**

Figure 1.1: Map showing the estimated global distribution of 215 000 deaths associated with rotavirus infections in 2013.....	6
Figure 1.2: A schematic diagram of the rotavirus viral particle. ....	6
Figure 1.3: Schematic diagram of the Calicivirus (A): virus particle and (B): genome structure. ....	10
Figure 1.4 (A): A schematic diagram of a picornavirus viral particle. (B) A schematic diagram of the picornavirus polyprotein, and post translational processing. ....	12
Figure 1.5: A schematic diagram of the AiV genome. ....	16
Figure 1.6: A schematic diagram of an adenovirus viral particle. ....	17
Figure 1.7: A schematic diagram of the Astrovirus viral particle. ....	19
Figure 1.8: Flow diagram of the study design (Chapters 1-3). ....	30
Figure 1.9: Flow diagram of the study design (Chapters 4-6). ....	31

### **Chapter 2**

Figure 2.1: Schematic diagram of the VP1 and 2B forward (→) and reverse (←) oligonucleotides and the position of binding to the VP1 and 2B coding sequences.....	36
Figure 2.2: Schematic diagram of pTMEV. Essential features include the TMEV GDVII cDNA, lacZα and lacO promoter encoding sequence, T3 and T7 RNA polymerase promoter. ....	38
Figure 2.3: TEM images of the TMEV samples before and after PEG precipitation. ....	41
Figure 2.4: Agarose gel electrophoresis of the RNA extracted from the TMEV cell lysate.....	42
Figure 2.5: Agarose gel electrophoresis of the RT-PCR assays for TMEV 2B and VP1 performed on the RNA extracted from the TMEV sample treated with 8% PEG 6000 and 0.25M NaCl. ....	42
Figure 2.6: (A) Agarose gel electrophoresis of pTMEV before and after linearization with <i>Bam</i> HI. (B) Agarose gel electrophoresis of the <i>in vitro</i> transcribed RNA from the linearised pTMEV.....	43
Figure 2.7: Agarose gel electrophoresis of the two-step RT-PCR assay for the TMEV 2B and VP1 coding sequences from the TMEV <i>in vitro</i> transcribed RNA.....	44
Figure 2.8: Agarose gel electrophoresis of the dilution series RT-PCR assay for TMEV 2B from the <i>in vitro</i> transcribed RNA.....	45

### **Chapter 3**

Figure 3.1: A schematic diagram of the forward (→) and reverse (←) primer binding sites for the NoV GII VP1 N/S domain coding region.....	51
Figure 3.2: Schematic diagram of the forward (→) and reverse (←) primer binding sites for 5'UTR. ....	54
Figure 3.3: Schematic diagram of the forward (→) and reverse (←) primer binding sites for 3CD.....	55
Figure 3.4: Schematic diagram of the plasmid map of pSAFV. ....	57
Figure 3.5: Schematic diagram of the forward and reverse primer binding site for SAFV 2C. ....	58
Figure 3.6: (A) Agarose gel electrophoresis of the first round of the RT-PCR assay performed on the NoV GII RNA. (B) Agarose gel electrophoresis of the second round of the RT-PCR assay performed on the NoV GII RNA.....	61

Figure 3.7: (A) Agarose gel electrophoresis of pNoVGII before and after digestion with the restriction enzyme Eco RI. (B) A schematic diagram of the plasmid map of pNoVGII. ....	62
Figure 3.8: (A) Agarose gel electrophoresis of the <i>in vitro</i> transcribed RNA from pNoVGII. (B) Agarose gel electrophoresis of the RT-PCR assay from the NoV GII <i>in vitro</i> transcribed RNA. ...	63
Figure 3.9: Agarose gel electrophoresis of the dilution series RT-PCR assay from the <i>in vitro</i> transcribed RNA from NoV GII. ....	64
Figure 3.10: Agarose gel electrophoresis of the PCR assay from the AiV 5' UTR plasmid provided by Jan Drexler. ....	65
Figure 3.11: Agarose gel electrophoresis of the PCR assay performed on the 3CD cDNA. ....	65
Figure 3.12: A schematic diagram of the plasmid maps of: (A) pAiV5'UTR and (B) pAiV3CD. ....	66
Figure 3.13: Agarose gel electrophoresis of the two-step RT-PCR assays from the <i>in vitro</i> transcribed RNA from pAiV5'UTR. ....	67
Figure 3.14: Agarose gel electrophoresis of the two-step RT-PCR assays from the <i>in vitro</i> transcribed RNA from pAiV3CD. ....	68
Figure 3.15: Agarose gel electrophoresis of the dilution series RT-PCR assay from the <i>in vitro</i> transcribed RNA from: (A) pAiV5'UTR. ....	69
Figure 3.16: (A) Agarose gel electrophoresis of pSAFV before and after linearization. (B) Agarose gel electrophoresis of the <i>in vitro</i> transcribed RNA from the linearised pSAFV. ....	70
Figure 3.17: Agarose gel electrophoresis of the two-step RT-PCR assay for the SAFV 2C, full and partial, coding sequences from the SAFV <i>in vitro</i> transcribed RNA. ....	71
Figure 3.18: Agarose gel electrophoresis of the dilution series RT-PCR assay for SAFV full 2C from the <i>in vitro</i> transcribed RNA. ....	72

## Chapter 4

Figure 4.1: A schematic diagram of the internal organs of an oyster (adapted from <a href="http://lanwebs.lander.edu/faculty/rsfox/invertebrates/crassostrea.html">http://lanwebs.lander.edu/faculty/rsfox/invertebrates/crassostrea.html</a> ; drawn by Kate Bryan [Rhodes University, South Africa]). ....	79
Figure 4.2: TEM images of the wastewater sample after PEG precipitation. ....	82
Figure 4.3: TEM images of the oyster samples after PEG precipitation. ....	83
Figure 4.4: TEM images of selected stool samples after PEG precipitation. ....	84
Figure 4.5: TEM images of selected stool samples showing the variety of virus particles present. ....	85

## Chapter 5

Figure 5.1: Agarose gel electrophoresis of the viral RNA extracted from the (A) wastewater sample and (B) oyster sample. ....	92
Figure 5.2: Agarose gel electrophoresis of the viral RNA extracted from selected stool samples (A-C). ....	92
Figure 5.3: Agarose gel electrophoresis of the wastewater NoV GII nested RT-PCR assay. ....	94
Figure 5.4: Agarose gel electrophoresis of the oyster sample NoV GII nested RT-PCR assay. ....	94
Figure 5.5: Agarose gel electrophoresis of the NoV GII nested RT-PCR assay performed on selected stool samples. ....	95
Figure 5.6: Multiple amino acid sequence Alignment of NoV GII sequences in comparison to the reference sequence (Accession no. HQ008055.1). ....	99

## Appendix I

- Figure 1S: The nucleotide sequence of the AiV 3CD insert in pAiV3CD. The blue boxes highlight the pGEM®-T Easy nucleotide sequence which surrounds the AiV 3CD insert. .... 125
- Figure 2S: The nucleotide sequence of the AiV 5'UTR insert in pAiV5'UTR. The blue boxes highlight the pGEM®-T Easy nucleotide sequence which surrounds the AiV 5'UTR insert. .... 126
- Figure 3S: A multiple sequence alignment of the nucleotide sequence of the AiV 5'UTR insert of pAiV5'UTR to the AiV reference strain (Accession no. AB010145.1). The red blocks indicate changes in the bases of the nucleotide sequences nucleotide. .... 127
- Figure 4S: A multiple sequence alignment of the nucleotide sequence of the AiV 3CD insert of pAiV3CD to the AiV reference strain (Accession no. AB010145.1). The red blocks indicate changes in the bases of the nucleotide sequences nucleotide. .... 128

## Appendix II

- Figure 5S: The nucleotide sequence of the NoV GII N/S Domain PCR product insert in pNoVGII The blue boxes highlight the pGEM®-T Easy nucleotide sequence which surrounds the NoV GII N/S Domain insert. .... 129
- Figure 6S: The nucleotide sequence of the NoV GII N/S Domain PCR product from the sewage sample inserted into pGEM®-T Easy. The blue boxes highlight the pGEM®-T Easy nucleotide sequence which surrounds the NoV GII N/S Domain insert. .... 129
- Figure 7S: The nucleotide sequence of the NoV GII N/S Domain PCR product from the oyster sample inserted into pGEM®-T Easy. The blue boxes highlight the pGEM®-T Easy nucleotide sequence which surrounds the NoV GII N/S Domain insert. .... 130
- Figure 8S: The nucleotide sequence of the NoV GII N/S Domain PCR product from the P1 stool sample inserted into pGEM®-T Easy. The blue boxes highlight the pGEM®-T Easy nucleotide sequence which surrounds the NoV GII N/S Domain insert. .... 130
- Figure 9S: The nucleotide sequence of the NoV GII N/S Domain PCR product from the P5 stool sample inserted into pGEM®-T Easy. The blue boxes highlight the pGEM®-T Easy nucleotide sequence which surrounds the NoV GII N/S Domain insert. .... 131
- Figure 10S: The nucleotide sequence of the NoV GII N/S Domain PCR product from the P7 stool sample inserted into pGEM®-T Easy. The blue boxes highlight the pGEM®-T Easy nucleotide sequence which surrounds the NoV GII N/S Domain insert. .... 131
- Figure 11S: The nucleotide sequence of the NoV GII N/S Domain PCR product from the P8 stool sample inserted into pGEM®-T Easy. The blue boxes highlight the pGEM®-T Easy nucleotide sequence which surrounds the NoV GII N/S Domain insert. .... 132
- Figure 12S: The nucleotide sequence of the NoV GII N/S Domain PCR product from the P9 stool sample inserted into pGEM®-T Easy. The blue boxes highlight the pGEM®-T Easy nucleotide sequence which surrounds the NoV GII N/S Domain insert. .... 132
- Figure 13S: The nucleotide sequence of the NoV GII N/S Domain PCR product from the P17 stool sample inserted into pGEM®-T Easy. The blue boxes highlight the pGEM®-T Easy nucleotide sequence which surrounds the NoV GII N/S Domain insert. .... 133
- Figure 14S: The nucleotide sequence of the NoV GII N/S Domain PCR product from the P18 stool sample inserted into pGEM®-T Easy. The blue boxes highlight the pGEM®-T Easy nucleotide sequence which surrounds the NoV GII N/S Domain insert. .... 133
- Figure 15S: The nucleotide sequence of the NoV GII N/S Domain PCR product from the P19 stool sample inserted into pGEM®-T Easy. The blue boxes highlight the pGEM®-T Easy nucleotide sequence which surrounds the NoV GII N/S Domain insert. .... 134

Figure 16S: The nucleotide sequence of the NoV GII N/S Domain PCR product from the P20 stool sample inserted into pGEM®-T Easy. The blue boxes highlight the pGEM®-T Easy nucleotide sequence which surrounds the NoV GII N/S Domain insert. .... 134

Figure 17S: The nucleotide sequence of the NoV GII N/S Domain PCR product from the P21 stool sample inserted into pGEM®-T Easy. The blue boxes highlight the pGEM®-T Easy nucleotide sequence which surrounds the NoV GII N/S Domain insert. .... 135

Figure 18S: The nucleotide sequence of the NoV GII N/S Domain PCR product from the P29 stool sample inserted into pGEM®-T Easy. The blue boxes highlight the pGEM®-T Easy nucleotide sequence which surrounds the NoV GII N/S Domain insert. .... 135

Figure 19S: A multiple alignment of the NoV GII PCR product nucleotide sequences from the NoV GII positive sample, wastewater, oyster and 11 stool samples and the reference strain (Accession no. HQ008055.1). The red blocks highlight changes in the bases of the nucleotide sequences. Continues on next page. .... 136

Figure 19S: (Continued from previous page) A multiple alignment of the NoV GII PCR product nucleotide sequences from the NoV GII positive sample, wastewater, oyster and 11 stool samples and the reference strain (Accession no. HQ008055.1). The red blocks highlight changes in the bases of the nucleotide sequences. .... 137

## *List of Tables*

### **Chapter 1**

Table 1.1: Selected Genera and Species of the <i>Picornaviridae</i> Family (ICTV, 2014).....	11
--	----

### **Chapter 2**

Table 2.1: Forward and Reverse Oligonucleotide Sequences for TMEV 2B and VP1. ....	37
--	----

### **Chapter 3**

Table: 3.1: The Forward and Reverse Oligonucleotides for the NoV GII VP1 N/S Domain Coding Region as Described by Kojima <i>et al.</i> (2002).....	51
Table 3.2: Forward and Reverse Oligonucleotides for AiV 5'UTR as Described by Drexler <i>et al.</i> (2011).....	54
Table 3.3: Forward and Reverse Oligonucleotides for AiV Partial 3CD Coding Sequence Described by Pham <i>et al.</i> (2007).....	55
Table 3.4: Forward and Reverse Oligonucleotide Sequences for SAFV Full Length 2C and Internal Region of 2C.....	59
Table 3.5: The Vector, Insert Size, Insert Product and Reference of the Plasmids used to Synthesis <i>In Vitro</i> Transcribed RNA.....	60

### **Chapter 4**

Table 4.1: Data Pertaining to the Patients from which the Stool Samples were Collected.....	80
---	----

### **Chapter 5**

Table 5.1: RNA Concentrations Obtained for the Oyster, Wastewater and Stool Samples.....	93
Table 5.2: Presence of NoV GII in the Stool Samples Analysed.....	96
Table 5.3: The BLAST Analysis of the NoV GII PCR Products for Wastewater, Oyster and Stool Samples.....	98
Table 5.4: The Sequence Identity and Similarity of the NoV GII Amino Acid Sequences.....	100
Table 5.5: Amino Acid Changes in the Nov GII Sequences for the Nov GII Positive Control, Wastewater, Oyster and Stool Samples. ....	101

## *List of Abbreviations*

aa	Amino acid
AFP	Acute flaccid paralysis
AIDS	Acquired Immune Deficiency Syndrome
Amp	Ampicillin
BHK-21 Cells	Baby hamster kidney -21 cells
BLAST	Basic local alignment search tool
BSC-1 Cells	Monkey kidney epithelial cells
cDNA	Copy Deoxyribonucleic acid
CO <sub>2</sub>	Carbon dioxide
CPE	Cytopathic effect
ddH <sub>2</sub> O	Double distilled water
DMEM	Dulbecco's modified Eagle's medium
DNA	Deoxyribonucleic acid
EDTA	Ethylenediaminetetraacetate
ELISA	Enzyme linked immunosorbent assays
EPI [SA]	Extended Programme on Immunisation in South Africa
ER	Endoplasmic reticulum
F	Forward
FBS	Foetal bovine serum
GI	Genogroup I
GII	Genogroup II
IF	Immunofluorescence
IPTG	Isopropyl $\beta$ -D-1-thiogalactopyranoside
LA	Luria bertani agar
LB	Luria bertani broth
NaCl	Sodium chloride
NICD	National Institute for Communicable Diseases
NSP	Non-structural protein
ORF	Open reading frame
P domain	Protruding domain
PBS	Phosphate-buffered saline
PCR	Polymerase chain reaction

PEG	Polyethylene glycol
PSF	Penicillin, Streptomycin and Fungizone
PTSAGs	Pyrogenic Toxin Superantigens
qPCR	real-time polymerase chain reaction
qRT-PCR	quantitative reverse-transcription polymerase chain reaction
R	Reverse
RdRp	RNA dependent RNA polymerase
RNA	Ribonucleic acid
RT-PCR	Reverse transcriptase- polymerase chain reaction
S domain	Shell domain
Stx 1	Shigella toxin 1
TAE	Tris acetate edta
TEM	Transmission electron microscope
UK	United Kingdom
USA	United States of America
UTR	Untranslated region
UV	Ultraviolet
VLP	Virus-like particles
VP	Virion protein
WHO	World health organisation

### **Viruses**

SAFV	Saffold Virus
AiV	Aichi virus
NoV	Norovirus
EMCV	Encephalomyocarditis virus
TMEV	Theiler's murine encephalomyelitis virus
VHEV	Vilyuisk human encephalomyelitis virus
HIV	Human Immunodeficiency Virus

### **Units and Symbols**

%	Per cent
°C	Degrees Celsius
µg	Micro gram

μl	Microlitre
μM	Micro molar
bp	Base pair
cm <sup>2</sup>	Square centimetres
hr	Hour
kb	Kilo base pair
M	Molar
ml	Millilitre
mM	Milli molar
ng	Nano gram
nm	Nanometre
rpm	Revolutions per minute
s	Seconds
U	Unit
V	Volts
w/v (wt/vol)	Weight/volume
xg	Times gravity

## *Acknowledgments*

I would like to acknowledge and thank the South African Medical Research Council, the Poliomyelitis Research Foundation (South Africa) and the Research Council (Rhodes University) for their financial support.

Special thanks to Jan Drexler (University of Bonn Medical Centre, Germany), Hiroshi Ushijima (University of Tokyo, Japan), and Maureen Taylor (University of Pretoria, South Africa) for providing the positive controls used in this study; Prof. Mike Lee and Dr Jaco Olivier (Physics Department, NMMU) for their assistance with TEM; Geoff Butler (NHLS, Settlers Hospital, Grahamstown) for providing space to work in the Pathogen Laboratory; Ina Peenze (MRC Diarrhoeal Pathogen Research Unit, Medunsa) for supplying stool samples and John Dewar (UNISA), and Pablo de Felipe (AEMPS, Spain).

I would also like to thank the following Lab 425 members for their help and support: Michael Jukes, Boitumelo Motsoeneng and Oikwathaile Onosi (Rhodes University). Finally I would like to thank Professor Caroline Knox for all her help and support, Christopher Jaquet for many hours of proofreading and Marc Jaquet for all his love, support and many hours of proofreading.

## ***Chapter 1: Literature Review***

### ***1.1 An Overview of Gastroenteritis***

Gastroenteritis is a common, yet potentially serious, disease affecting many people worldwide. It is one of the leading causes of morbidity and mortality in developing and first world countries alike. This disease affects both adults and children but is more predominant in young children and the elderly. The World Health Organization (WHO) reported over 6280 000 deaths in children under the age of five years during 2013 and diarrhoeal disease accounted for 9% of these (WHO, 2015).

Acute gastroenteritis is a diarrhoeic disease often caused by the ingestion of food or water which is contaminated by an infectious organism, virus or toxin (Bennett, 1998). Gastroenteritis may also occur by the infection with a pathogen through the faecal-oral route, as is often the case with viruses (reviewed by Wilhelmi *et al.*, 2003). The pathogen causes the inflammation of the mucosa of the stomach and/or the small intestines. The inflammation is caused by the invasion of the epithelial cells by the pathogen which results in cell death or by the production of an enterotoxin which may inhibit cell function or result in cell death. The dead cells are replaced by new, immature cells which cannot perform their function adequately which results in the malabsorption of fluids and essential nutrients resulting in diarrhoea (Bennett, 1998). Other symptoms of this disease include vomiting, fever, abdominal pain, dehydration, abdominal cramps and bloating. In severe cases blood may be present in the stool or vomit.

In most cases, gastroenteritis is non-fatal and will often resolve itself within 3 days (Bennett, 1998). Recovery is aided by rehydration with fluids which contain glucose and electrolytes. Treatment is seldom required and is often limited to the symptoms rather than the cause of the disease. Severe gastroenteritis may, however, result in the hospitalisation of the patient, and could be fatal.

## 1.2 Causative Agents

Pathogens which are associated with gastroenteritis include many bacteria, parasites and viruses. Protozoan parasites are rare causative agents of this disease as they are generally unable to survive the pH conditions of the stomach (Verweij *et al.*, 2004; Bennett, 1998). The most common parasites which cause gastroenteritis are *Giardia lamblia*, *Cryptosporidium* and *Entamoeba histolytica* (Iyaloo *et al.*, 2015; Verweij *et al.*, 2004; Bennett, 1998). *G. lamblia* is thought to be one of the main causative agents of non-viral gastroenteritis, as infections with this pathogen are common. *E. histolytica* is the cause of amoebic colitis, amoebic dysentery and amoebic liver abscess, resulting in 100 000 deaths annually. *Cryptosporidium parvum* has been recognized as the cause of large water- and food-borne outbreaks of gastroenteritis and is a fairly common infection in patients with Acquired Immune Deficiency Syndrome (AIDS). *Isospora belli* is an opportunistic parasite, which causes an infection in immune-compromised hosts. This parasite is very common in patients with Human Immunodeficiency Virus (HIV) (Kumar *et al.*, 2015; Ghadage *et al.*, 2014; Verweij *et al.*, 2004). Protozoan parasite infections occur worldwide.

Bacterial gastroenteritis is caused by bacteria or a toxin produced by a bacterium (Bennett 1998). Both food and water supplies can be contaminated. Once the bacteria has been ingested, they may cause gastroenteritis by attaching to the intestinal epithelium where they produce a toxin which damages the cells or the bacterium may invade the mucosal cells and destroy them resulting in bloody diarrhoea with fever and abdominal pain (dysentery) (Bennett, 1998). Bacterial gastroenteritis may be caused by the following bacteria: *Staphylococcus aureus*, *Bacillus cereus*, *Escherichia coli*, *Campylobacter jejuni*, *Salmonella* spp, *Shigella* spp, *Vibro* spp and others (Iyaloo *et al.*, 2015; Bennet, 1998). *Salmonella*, *S. aureus*, *B. cereus* and *E. coli* are discussed below.

*Salmonella* is the leading cause of bacterial gastroenteritis and affects people of all ages (WHO, 2016; Majowicz *et al.*, 2010). *S. typhi* is responsible for typhoid fever and infection occurs through the consumption of contaminated water (Rahman, 2012). Other *Salmonella* spp are responsible for Salmonellosis. This disease is caused by the ingestion of contaminated food, in particular poultry, or through person-to-person contact via the faecal-oral route. Symptoms occur 6-72 hours after ingestion of the bacteria and they include fever,

abdominal pain, diarrhoea, nausea and vomiting (WHO, 2016; Rahman, 2012). The illness will generally resolve itself in 2 to 7 days and treatment is often limited to electrolyte replacement and rehydration (WHO, 2016). In severe cases and immuno-susceptible patients, such as infants and the elderly, antimicrobial treatment may be used. The bacteria invade the hosts epithelial cells and hide in vacuoles where they replicate. The bacteria are released from the cells through cell death resulting in diarrhoea.

*Staphylococcus aureus* and *Bacillus cereus* cause a mild form of gastroenteritis, which normally resolves itself within 24-48 hours (reviewed by Dinges *et al.*, 2000; Bennett, 1998; reviewed by Granum and Lund, 1997). These bacteria will produce toxins after an incubation period of one to six hours. *S. aureus* produces many toxins, but pyrogenic toxin superantigens (PTSAgs) are the toxins responsible for gastroenteritis (reviewed by Dinges *et al.*, 2000). These toxins cause gastroenteritis by causing lesions and the inflammation of the gastrointestinal tract. *B. cereus* produces enterotoxins which cause the accumulation of liquids in the intestines resulting in watery diarrhoea (reviewed by Granum and Lund, 1997).

*E. coli* strains are commonly found in the intestinal tract and are generally non-pathogenic (reviewed by Besser, 1999; Bennett, 1998). Some strains have, however, become pathogenic by acquiring virulence factors from other bacteria for example the enterohemorrhagic *E. coli* strains which have acquired the shiga toxin from *Shigella dysenteriae* (Lim *et al.*, 2010; reviewed by Besser, 1999). The toxins are known as Shiga toxins because of the essentially-identical structure of Shiga toxin 1 (Stx 1) to the Shiga toxin produced by *S. dysenteriae* type 1. These strains of *E. coli* are responsible for causing haemorrhagic colitis (bloody diarrhoea) and haemolytic uremic syndrome as the toxin often destroys the intestinal epithelial cells (Lim *et al.*, 2010). *E. coli* O157:H7 is one of the most important enterohemorrhagic *E. coli* strains as, while the infection rates are lower than other pathogenic bacteria, the hospitalisation and fatality rate is much higher than *Salmonella* and *Campylobacter* spp. Most infections with *E. coli* O157 present with non-bloody diarrhoea and will resolve themselves (Lim *et al.*, 2010). Several patients, children and the elderly in particular, will develop bloody diarrhoea and of these 5-10 % will develop haemolytic uremic syndrome, sequelae or thrombocytopenic purpura. This bacteria is transmitted through the consumption of

contaminated food or water, or through person-to-person contact and the faecal-oral route (Lim *et al.*, 2010).

While bacteria and parasites are a common cause of gastroenteritis, viral pathogens are the leading cause of this disease. The leading viral pathogens and viruses commonly associated with viral gastroenteritis are discussed in the next section along with novel viruses associated with this disease.

### ***1.3 Viral Pathogens***

Viruses are some of the most important pathogens associated with acute gastroenteritis. The first identification of viruses as a causative agent of this disease was described by Kapikian and colleagues in 1972, where Norwalk virus was found in faecal matter after a recent outbreak of diarrhoea (Kapikian *et al.*, 1972). Over the next few years rotavirus, astrovirus and enteric adenovirus were all identified in association with gastroenteritis. Since their initial identification, a number of viruses have been found in association with this disease in humans including rotavirus, caliciviruses and picornaviruses such as enterovirus, coxsackie virus group A and B, human parechovirus, Saffold virus (SAFV) and Aichi virus (AiV). Enteric adenovirus, astrovirus, *Picobirnavirus*, and coronaviruses, such as *Torovirus* and *Coronavirus*, have also been associated with gastroenteritis in humans (Knowles *et al.*, 2012; reviewed by Wilhelmi *et al.*, 2003).

Of the viruses associated with gastroenteritis, rotavirus (*Reoviridae*) and norovirus (NoV) (*Caliciviridae*) are the two leading causes of the disease (Esposito *et al.*, 2013; reviewed by Bernstein, 2009; reviewed by Wilhelmi *et al.*, 2003). Rotavirus is mainly limited to, and is the leading cause of this disease in, children under the age of 5 years. NoV affects all age groups, but mainly the young and the elderly and is the leading cause of community-acquired gastroenteritis, causing frequent outbreaks in nursing homes and hospitals (Esposito *et al.*, 2013; reviewed by Bernstein, 2009; Ferson *et al.*, 2000).

Other viruses associated with acute infantile gastroenteritis include adenovirus (*Adenoviridae*), astrovirus (*Astroviridae*) and picornaviruses (*Picornaviridae*) (reviewed by

Wilhelmi *et al.*, 2003). Adenovirus commonly infects children and may cause respiratory or gastrointestinal symptoms (Russell, 2000; Doefler, 1996). Astrovirus causes diarrhoea in children either on its own or as part of a mixed infection with other viruses associated with this disease (Bosch *et al.*, 2014).

Picornaviruses are an important family of viruses associated with this disease (reviewed by Wilhelmi *et al.*, 2003). The more commonly known picornaviruses, which are causative agents of this disease, include coxsackie virus group A and B (genus *Enterovirus*), enterovirus (genus *Enterovirus*) and echovirus (genus *Enterovirus*) but in the past few years, several newer viruses have been associated with the disease. These viruses include SAFV (SAFV) (genus *Cardiovirus*) and common stool-associated virus (Cosavirus) (genus *Cosavirus*) (Holtz *et al.*, 2008; Jones, 2007). But one of the most important picornaviruses to cause gastroenteritis is AiV (genus *Kobuvirus*) as the prevalence of this virus has increased in the past few years (Reuter *et al.*, 2009; Oh *et al.*, 2006; Yamashita *et al.*, 1991). The biology of rotavirus, NoV, picornaviruses, adenovirus and astrovirus are discussed below.

### ***1.3.1 Rotavirus***

Rotavirus is the leading cause of severe infantile gastroenteritis, causing approximately 215 000 (37%) of all deaths, due to gastroenteritis, in children under the age of 5 years in 2013 and accounts for an average of 38% of hospitalised cases in 2012 (Tate *et al.*, 2016; WHO, 2013) This virus mainly infects children under the age of 5 years, particularly those 6 to 36 months, but may also infect the elderly (reviewed by Midthun and Kapikian, 1996). This virus occurs worldwide with the highest death rates found in the following developing countries: India, Nigeria, Afghanistan and Democratic Republic of Congo, which account for approximately 49% of all rotavirus death, as shown in Figure 1.1 below.

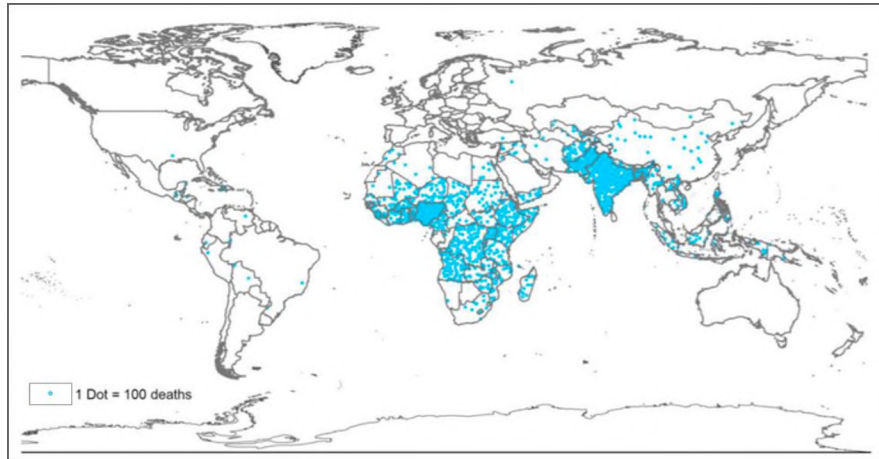


**Figure 1.1:** Map showing the estimated global distribution of 215 000 deaths associated with rotavirus infections in 2013. 1 dot represents 100 deaths (Tate *et al.*, 2016).

Rotavirus belongs to the family *Reoviridae*. The virion is approximately 70 nm in diameter and spherical in shape with a distinctive double capsid as shown in Figure 1.2 (reviewed by Knox *et al.*, 2012; reviewed by Dennehy, 2008). The genome is encapsulated in the inner capsid and consists of 11 double-stranded RNA segments, which encode six structural and six non-structural proteins (Matthijnsens *et al.*, 2009). The six structural proteins are as follows: VP1, VP2 and VP3 are the core proteins; VP6 is the inner capsid protein and VP4 and VP7 are the outer capsid proteins. VP4, VP6 and VP7 are important in determining the antigenic specificities, group, subgroup and serotype, of rotavirus. VP6 is responsible for determining the group specificity and also mediates the subgroup specificity.

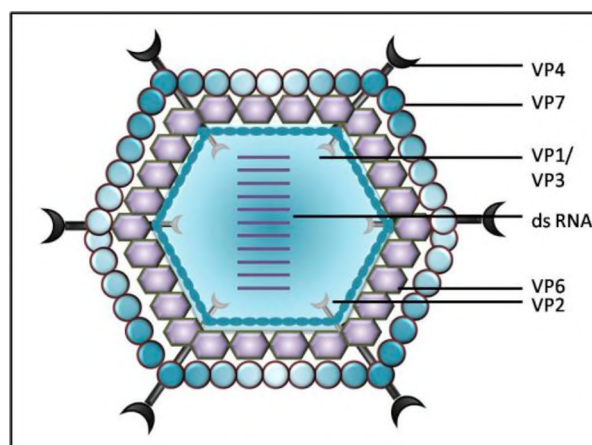


**Figure 1.2:** A schematic diagram of the rotavirus viral particle. Three protein layers enclose the 11 segments of dsDNA. VP4 and VP7 form part of the outer capsid and are neutralization antigens and mediate the P and G serotypes. VP6 forms the inner capsid while VP1, VP3 and VP2 form the internal core (adapted from Dennehy, 2008).

The Rotavirus genus contains 7 serogroups (Group A-G). Human rotaviruses belong to serogroups A, B, and C; with the most epidemiologically important human and animal rotaviruses belonging to rotavirus group A (reviewed by Knox *et al.*, 2012; Knowles *et al.*, 2012; reviewed by Midthun and Kapikian, 1996). Rotavirus group B and C infections occur in both adults and children, but the detection rates of these viruses remain low. Therefore, the role of these viruses in diarrhoeal disease is not fully known (Rahman *et al.*, 2005; Anderson and Weber, 2004; Sanekata *et al.*, 2003). Studies have shown that rotavirus group B is limited to Asian and Indian continent. Rotavirus group B and C are not detected by the rotavirus group A ELISA (Anderson and Weber, 2004).

Classification of rotavirus is currently achieved by the serotyping of VP6, sero- and genotyping of VP4 and VP7 and analysis of the amino acids of Non-Structural Protein 4 (NSP4). Group A rotavirus is divided into subgroup I and II specificities using VP6, although some viruses contain both or neither specificities. VP4 (P) and VP7 (G) mediate genotype and serotype specificity. There are currently 15 G genotypes (14 G serotypes), and 27 P genotypes (14 P serotypes). Of these 11 G and 12 P serotypes have been found in association with human rotavirus infections (Matthijnssens *et al.*, 2009). There are four groups which are the most common serotypes in human infections; these are P8G1, P4G2, P8G3 and P8G4 (reviewed by Dennehy, 2008).

In recent years, a new classification system of rotavirus has been proposed due to the lack of immunological reagents in many laboratories as well as the cross-reactivity of some of the serotypes (Matthijnssens *et al.*, 2009). This system involves the analysis of all 11 segments of the dsRNA, allowing for the classification of rotavirus using VP1 to VP3, VP4, VP6, VP7 and NSP1-NSP5. As this system uses nucleotide sequences, higher cut off values can be used allowing for greater identification of distinct rotaviruses genotypes and better analysis of the trends of rotavirus infections in humans and other animals (Matthijnssens *et al.*, 2009).

Rotavirus causes disease after a 1-3 day incubation period (reviewed by Bernstein, 2009; reviewed by Midthun and Kapikian, 1996). The virus replicates in the villus tip epithelial cells of the small intestines and the infection results in cell death. New, immature cells are promoted to replace the dead cells. These new cells are inefficient in absorption, resulting in

osmotic diarrhoea and dehydration. Rotavirus is transmitted through the faecal-oral route, and an infection sheds large numbers of virions during a diarrhoea episode. This allows for a high transmission rate.

Due to the severity of rotavirus infections, several vaccines have been developed and tested using live attenuated bovine and rhesus strains of rotavirus as well as human-bovine assortment virus vaccines (reviewed by Dennehy, 2008). Two vaccines are currently in use; these are Rotarix® (GlaxoSmithKline Biologicals, Belgium) and RotaTeq® (Merk, USA). Rotarix® uses a live attenuated virus vaccine while RotaTeq® uses a human-bovine assortment virus. The Rotarix® and RotaTeq® vaccines are administered orally to babies as follows: Rotarix® is administered in two doses, at two and four months while RotaTeq® is administered in three doses at two, four and six months. The vaccines are administered to lessen the severity of the disease rather than to eliminate the disease entirely as there are a large number of seasonal variations between strains (reviewed by Dennehy, 2008).

Routine vaccination with Rotarix® was started in 2004 in Mexico and the Dominican Republic and by 2007 over 90 countries were licensing Rotarix® for the routine vaccination of infants (reviewed by Dennehy, 2008). Vaccination with RotaTeq® was started in the USA in 2006 and over 100 countries applied for licensing of this vaccine during 2007. In South Africa and the UK, routine vaccination with Rotarix® was started in 2009 and 2013 respectively (National Health Service, 2013b; Cohen *et al.*, 2010; reviewed by Dennehy, 2008) Since the implementation of routine vaccination, industrialised countries report an efficacy of 80-98% of the vaccines while developing countries report an efficacy of 39-77%, thus showing a decrease in the burden of disease of rotavirus worldwide (Tshangela *et al.*, 2012).

### ***1.3.2 Norovirus***

NoV is one of the leading causes of acute gastroenteritis worldwide with up to 21 million cases reported in the United States each year (Centre for Disease Control and Prevention, 2013). This virus affects people of all ages, but the more severe infections are mainly found in children under the age of 5 years and the elderly, with over 200 000 deaths worldwide reported in children annually (Centre for Disease Control and Prevention, 2013). This virus

is commonly associated with outbreaks of gastroenteritis in community environments such as hospitals, child care facilities and nursing homes. The virus infections in these environments may be so severe that the facility or wards may have to be closed down (National Health Service, 2013a).

The virus belongs to the family *Caliciviridae*, which are small (27 - 40 nm in diameter), non-enveloped, icosahedral viruses which have a positive-sense, single-stranded RNA genome as shown in Figure 1.3 (A) (reviewed by Robilotti *et al.*, 2015; Green, 2007). The family contains four genera, *Norovirus*, *Saprovirus*, *Lagovirus* and *Vesivirus*. Human caliciviruses belong to the *Norovirus* and the *Saprovirus* genera, both of which contain viruses associated with gastroenteritis (reviewed by Robilotti *et al.*, 2015). The *Norovirus* genus is further divided into five genogroups, GI – GV. Of these GI, GII and GIV contain the human noroviruses. Currently, the GII.4 strains are the leading cause of NoV outbreaks worldwide (Zakikhany *et al.*, 2012; Green, 2007).

The NoV genome is a single strand of RNA approximately 7.5 kb in length which encodes three open reading frames (ORF's), as shown in Figure 1.3 (B) below. ORF1 encodes a polyprotein which is cleaved to form six non-structural proteins including a 3C-like protein and the RNA-dependent RNA polymerase (RdRp) (reviewed by Robilotti *et al.*, 2015; Green, 2007). ORF 2 and 3 encode the major structural protein VP1 a minor structural protein VP2. The VP1 protein is folded into two dominant domains: the shell (S) domain and the protruding (P) domain; with a third domain found at the N-terminal of VP1 (10-49 amino acids). The P domain consists of two sub-domains P1 and P2. The N/S domain junction is frequently used for the identification and genotyping of NoV.

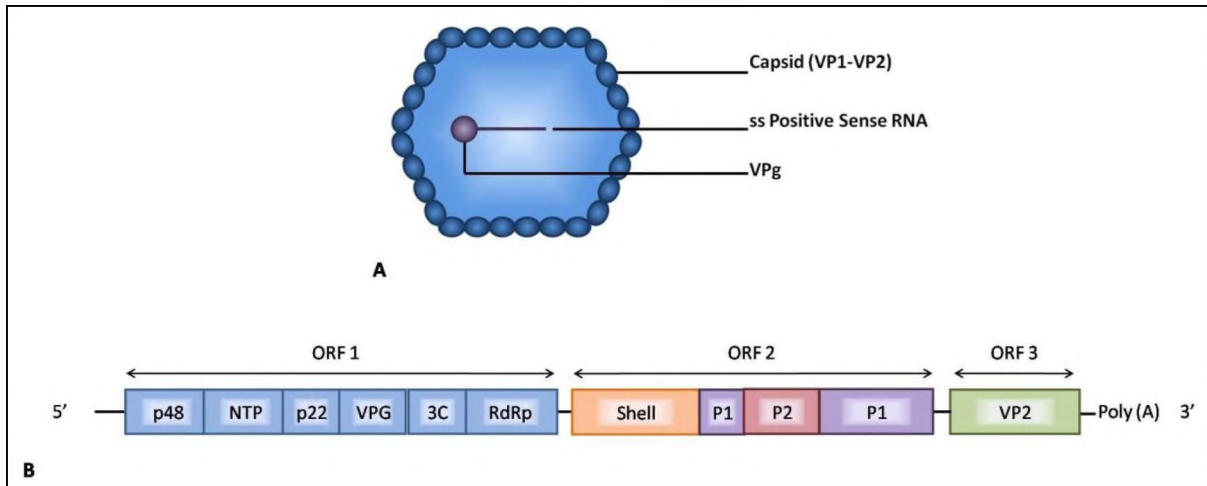


**Figure 1.3: Schematic diagram of the Calicivirus (A): virus particle and (B): genome structure.** ORF 1 encodes for six non-structural proteins while ORF 2 and ORF 3 encode for the capsid proteins VP1 and VP2 (adapted from Donaldson *et al.*, 2010).

NoV infections result from the ingestion of contaminated food or water, or by person-to-person contact. After the initial infection, there is a 24 - 48 hour incubation period and a typical infection lasts between one and three days (reviewed by Robilotti *et al.*, 2015; Le Pendu *et al.*, 2006). NoV infections cause vomiting, diarrhoea, stomach cramps, mild fever and nausea. These viruses infect the epithelium of the proximal small intestines, where they cause blunting of the villi, resulting in a decrease in the absorptive surface of the epithelium. The contaminated food and water sources, from which NoV has been isolated, include wastewater, sewage-polluted water sources and shellfish, such as oysters and mussels (da Silva *et al.*, 2007; Loisy *et al.*, 2005). This group of viruses have been found on their own or as part of a mixed infection with other viruses associated with gastroenteritis including astrovirus (Le Guyader *et al.*, 2008).

Although NoV is the leading cause of gastroenteritis worldwide, there is limited surveillance of this virus (Centre for Disease Control and Prevention, 2013). Surveillance is limited as many cases are not reported, either because the patients do not receive medical attention or because medical practitioners do not have the facilities to test for NoV, and hence only treat the symptoms. Much of the surveillance which is performed comes from the outbreaks of NoV which occur throughout the year. While there is no vaccine currently available, a GI.1/GII.4 bivalent vaccine is undergoing clinical trials. This bivalent vaccine contains 50 µg Norwalk virus (GI.1) virus-like particles (VLP's) and 50 µg GII.4 VLP's developed using the

consensus amino acid residues of three capsid protein sequences. The VLP's were produced in a baculovirus expression system (Bernstein *et al.*, 2015; Esposito *et al.*, 2013).

### 1.3.3 Picornaviridae

Picornaviruses belong to the family *Picornaviridae*. There are 29 genera in this family, including the recently-added *Cosavirus* genus (International Committee on Taxonomy of Viruses (ICTV) (ICTV, 2014; Racaniello, 2007). The family contains many important human and animal pathogens including foot-and-mouth disease virus, poliovirus and hepatitis A virus. Table 1.1 shows several of the genera belonging to the family along with examples of species within the genera.

**Table 1.1: Selected Genera and Species of the *Picornaviridae* Family (ICTV, 2014).**

Family	Genus	E.g. Species
<i>Picornaviridae</i>	<i>Aphthovirus</i>	Foot-and-Mouth Disease Virus (FMDV)
	<i>Cardiovirus</i>	Encephalomyocarditis Virus (EMCV)
		Theiler's Murine Encephalomyelitis Virus (TMEV)
		Vilyuisk Human Encephalomyelitis Virus (VHEV)
		Saffold Virus (SAFV)
	<i>Enterovirus</i>	Enteroviruses
		Poliovirus
		Echovirus
		Rhinovirus
<i>Hepatovirus</i>	Hepatitis A Virus	
<i>Kobuvirus</i>	Aichi Virus	
	Bovine Kobuvirus	
<i>Parechovirus</i>	Human Parechovirus	
<i>Cosavirus</i>	Human Cosavirus A	

Picornaviruses are non-enveloped, icosahedra viruses with a diameter of approximately 30 nm, Figure 1.4 (A). The genome is a single-stranded positive sense RNA molecule approximately 8-9 kb in size, encoding a single polyprotein which is cleaved to form several viral proteins, Figure 1.4 (B). These proteins either form part of the capsid or are involved in genome replication (Racaniello, 2007). The genome encodes 4 structural proteins, VP1-4 which form the capsid of the virus, and 8 replication proteins including 2B, which is involved with the altering of the host Golgi and endoplasmic reticulum (ER) membranes which results in the formation of virus-vesicles, as well as a change in the permeability of the plasma membrane which, in turn, results in cell lyses (Racaniello, 2007).

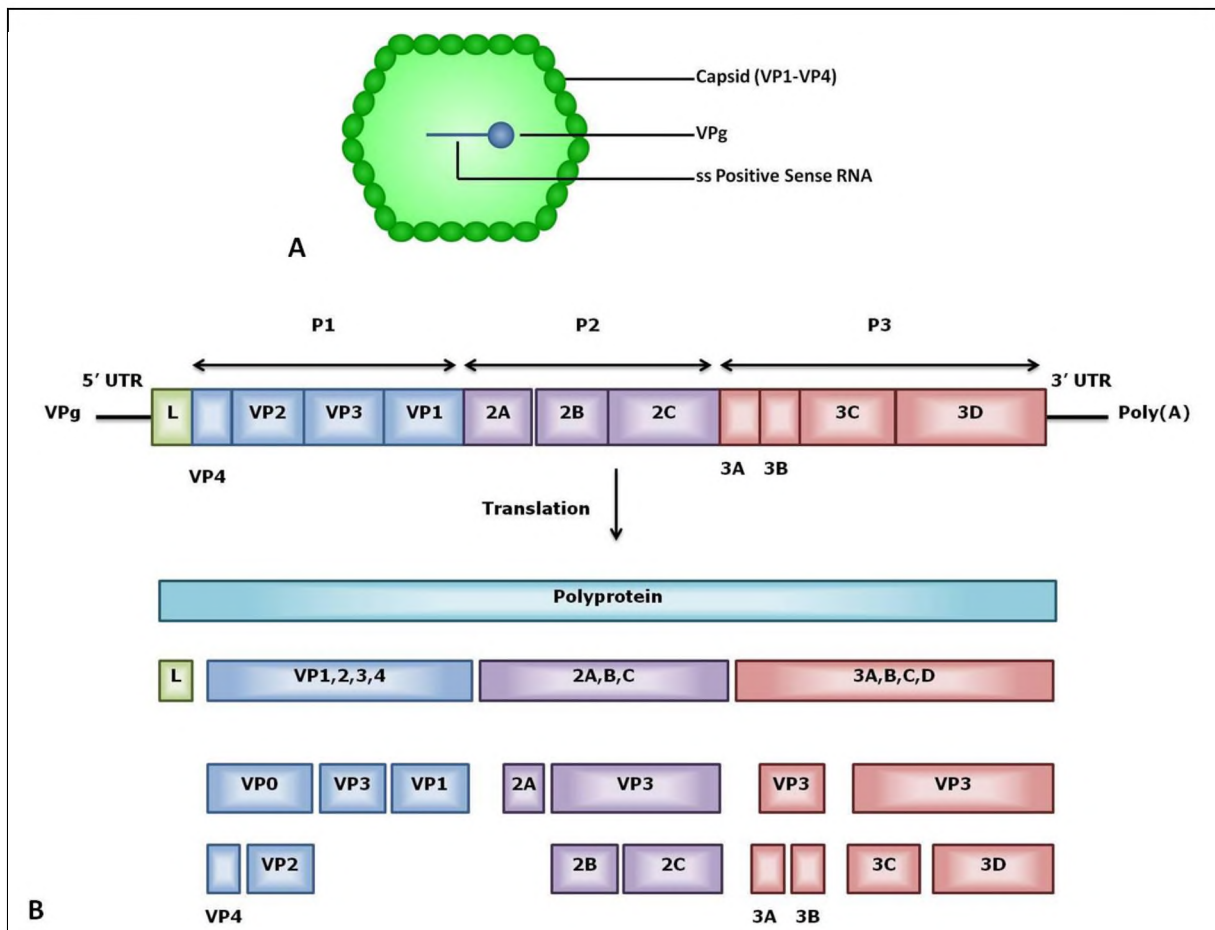


**Figure 1.4 (A):** A schematic diagram of a picornavirus viral particle. **(B)** A schematic diagram of the picornavirus polyprotein, and post translational processing. P1 encodes the structural proteins of the viral capsid (blue), while P2 (purple) and P3 (red) encode the replication proteins, including 2B (adapted from [www.viralzone.expasy.org](http://www.viralzone.expasy.org)).

There are several viruses within this family that are associated with gastroenteritis, the most common of which are the *Enteroviruses*, including enteroviruses, coxsackie viruses groups A and B, and echoviruses (Griffin *et al.*, 2003). In recent years several new viruses have, however, been associated with gastroenteritis. These include SAFV (*Cardiovirus*), Cosavirus (*Cosavirus*) and AiV (*Kobuvirus*). AiV was mainly associated with oyster-associated gastroenteritis, but is now considered a serious pathogen of gastroenteritis (Holtz *et al.*, 2008; Jones *et al.*, 2007; Oh *et al.*, 2006).

#### ***1.3.3.1 Enteroviruses***

Enteroviruses, such as coxsackie viruses group A and B and echovirus, are responsible for 10-15 million infections per year in the United States; a large number of these may result in gastroenteritis (Centre for Disease Control and Prevention, 2013). Most infections occur in children under the age of 10 years. These viruses are transmitted through the faecal-oral route and an infection may occur after the consumption of contaminated food or water, or through person-to-person contact. These viruses have been commonly found in water sources such as rivers, dams and bore-holes, are very stable in the environment and may survive wastewater treatment (Ehlers *et al.*, 2005; Formiga-Cruz *et al.*, 2005; Fuhrman *et al.*, 2005). Most infections are asymptomatic or result in a mild illness; however some cases result in a serious or fatal infection.

#### ***1.3.3.2 Cosavirus***

In 2008, Cosavirus was isolated from stool samples taken from children with acute flaccid paralysis (AFP) and diarrhoea (Holtz *et al.*, 2008; Kapoor *et al.*, 2008). This novel virus was found to be closely related to Cardioviruses but was significantly divergent in the amino acid sequence; therefore it was classified as a new genus in the *Picornaviridae*. Cosavirus has been identified in South Asia, Pakistan, Afghanistan, the United Kingdom and the United States, in healthy children as well as those with AFP (Blinkova *et al.*, 2008). To date, the ecological role and pathogenesis of Cosavirus is unknown.

#### ***1.3.3.3 Cardioviruses and Saffold Virus***

Cardioviruses have, until recently, been associated with rodents. Members of this genus include Encephalomyocarditis virus (EMCV) and Theiler's murine encephalomyelitis virus

(TMEV). These viruses infect and replicate in cells of the gastrointestinal tract of rodents and may cause mild or severe enteric illnesses (Racaniello, 2007). In the case of TMEV there are two species, one of which is highly neurovirulent. The other is low-neurovirulent or persistent (Oleszak *et al.*, 2004; Lipton *et al.*, 1998). There are two strains belonging to each species: GDVII and FA strains belong to the neurovirulent species while BeAn and DA belong to the low-neurovirulent species (Oleszak *et al.*, 2004). The neurovirulent strains cause a rapidly-fatal encephalitis in mice but do not persist in the animal while the less-virulent strains are less fatal and are able to persist in the central nervous systems (Lipton *et al.*, 1998). The low-neurovirulent strains have been widely studied as they serve as a model for multiple sclerosis (Oleszak *et al.*, 2004; Lipton *et al.*, 1998). TMEV GDVII, which is highly neurovirulent, has also been widely characterized (Oleszak *et al.*, 2004; Lipton *et al.*, 1998).

The first human cardiovirus to be isolated was Vilyuisk human encephalomyelitis virus (VHEV) (reviewed by Lipton, 2008). Identified over 50 years ago, this virus is restricted to the Yakuts people of Siberia as it has not been found elsewhere in the world.

In 2007 a new human cardiovirus, SAFV, was identified and classified in the *Cardiovirus* genus (reviewed by Knox *et al.*, 2012; Jones *et al.*, 2007). SAFV was isolated from the stool sample collected in 1981 from a child displaying a fever of unknown origin. Electron microscopy showed viral particles of 28 to 30 nm in diameter and molecular and phylogenetic analysis showed this virus to be closely related to TMEV. SAFV has been isolated from many countries around the world, including Germany, America, Canada, Japan and Brazil. It has been isolated from clinical samples collected from patients suffering with several diseases including respiratory symptoms, influenza-like illnesses, non-polio AFP, as well as patients with no overt neurological symptoms of AFP, but most commonly gastroenteritis (reviewed by Knox *et al.*, 2012; Blinkova *et al.*, 2009; Zoll *et al.*, 2009). Transmission electron microscopy (TEM) analysis and reverse transcriptase-polymerase chain reaction (RT-PCR) assays are used for the identification of SAFV from clinical samples and phylogenetic analysis of the VP1 and VP2 regions have shown the presence of eleven genotypes for SAFV (Naeem *et al.*, 2014). SAFV has been detected in low frequencies ranging from 0.5% - 3% globally, but in Afghanistan and Pakistan higher

incidences of 10% - 12% have been reported (Blinkova *et al.*, 2009). The aetiological role of SAFV and its association with gastroenteritis is, however, unknown.

#### ***1.3.3.4 Aichi Virus***

AiV was first isolated from the Aichi region in Japan in 1989 where it was thought to be a likely cause of an oyster-associated non-bacterial diarrhoeal case (Oh *et al.*, 2006; Yamashita *et al.*, 1991). After it was first detected, AiV was found in many stool samples from gastroenteritis outbreaks in Japan and tourists returning from Southeast Asia (Oh *et al.*, 2006; Yamashita *et al.*, 1995; Yamashita *et al.*, 1993). In recent years, however, AiV has been isolated from many countries around the world including Japan, Pakistan, Germany, Hungary, Vietnam, Thailand, France and Tunisia; and shows a high prevalence in many of these countries (Chang *et al.*, 2013; Lodder *et al.*, 2013; reviewed by Knox *et al.*, 2012; Pham *et al.*, 2007; Yamashita *et al.*, 1995; Yamashita *et al.*, 1993).

AiV was first identified using transmission electron microscopy and enzyme-linked immunosorbent assays (ELISA), where small, round virus particles 30 nm in diameter were present and caused cytopathic effects in BSC-1 cells (Oh *et al.*, 2006, Yamashita *et al.*, 1991). In 2000 a RT-PCR assay was developed for the identification of AiV from clinical samples (Yamashita *et al.*, 2000). Full-length genomes have been obtained for AiV by RNA extraction followed by cDNA synthesis, cloning and nucleotide sequencing, allowing for further study of AiV (Chang *et al.*, 2013; Lodder *et al.*, 2013; Yamashita *et al.*, 1998).

The genome organisation showed that this virus was part of the *Picornaviridae* family, but the amino acid sequences only showed a 15% - 36% homology to other picornaviruses (reviewed by Reuter *et al.*, 2011). One of the most noticeable differences in the organisation of the genome of AiV is the lack of the cleavage of VP4 from VP1 resulting in three capsid proteins, namely VP0, VP2 and VP3, as shown in Figure 1.5 below. It was therefore placed into its own genus, *Kobuvirus*, which also contains bovine kobuvirus, porcine kobuvirus and canine kobuvirus. Three genotypes have been identified in AiV to date. These are A, B and C, where A and B have been identified in Asia and Europe and C has only been identified in Africa (Di Martino *et al.*, 2013; Oh *et al.*, 2006). This classification is based on phylogenetic analysis of the 3C/3D and VP1 nucleotide sequences.

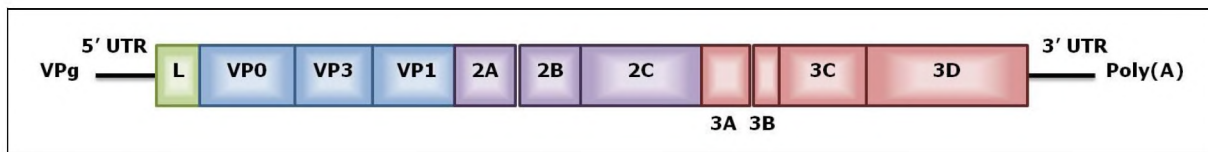


**Figure 1.5: A schematic diagram of the AiV genome.** The capsid proteins, VP0-VP3, are shown in blue while the replication proteins, 2A-2C and 3A-3D, are shown in purple and red, respectively. (adapted from Yamashita *et al.*, 1998)

An infection with AiV may be non-symptomatic or may occur as a respiratory or gastrointestinal infection, where the patient may suffer from vomiting, diarrhoea, stomach cramps and nausea (Pham *et al.*, 2007; Oh *et al.*, 2006). Transmission occurs through the ingestion of contaminated food or water or by person-to-person contact.

Several studies have shown the worldwide presence of AiV in clinical samples collected from outbreaks from infected food sources, such as oysters and other shellfish; while other studies have identified AiV from water sources, such as sewage and surface waters (Di Martino *et al.*, 2013; Lodder *et al.*, 2013; Pham *et al.*, 2007; Yamashita *et al.*, 1995; Yamashita *et al.*, 1991). Sporadic cases of AiV have also been reported in many countries. It has been isolated from both adults and children alike but is predominantly studied in children. Several of these studies have shown the presence of a mixed infection with other viruses associated with gastroenteritis, such as NoV, rotavirus and astrovirus (Pham *et al.*, 2007, Oh *et al.*, 2006).

Due to the worldwide presence of this virus, the high numbers of mono-infections of AiV and the ability to cause infections through person-to-person contact, AiV is now considered an important pathogen in human disease. While there are many studies which have identified the epidemiological relevance of this virus, and are continuing to do so, there is limited knowledge on the pathogenesis of this virus.

### ***1.3.4 Adenovirus***

Adenovirus was first isolated in the 1950's and has since been found to cause a variety of diseases, including respiratory and gastrointestinal infections, in humans as well as other

animals (Russell, *et al.*, 2000). These viruses are large (70 - 100 nm), non-enveloped, icosahedral viruses with a non-segmented, linear double-stranded DNA genome. The viral capsid consist of 3 major proteins, 5 minor proteins and 3 proteins which associate with the viral DNA in the core of the plasmid, as shown in Figure 1.6 below (Nemerow *et al.*, 2012; Russell, 2000; Doerfler, 1996). The 3 major proteins constitute 252 capsomers, 12 of these are pentons (protein III), with a slender projection called a fibre (protein IV), which occur on the 12 vertices of the icosahedron. The edges and 20 faces of the icosahedron are made up of 240 capsomers called hexons (protein II). The minor proteins are IIIa, VI, VIII and IX (Nemerow *et al.*, 2012; Russell, 2000). Protein VII is intimately associated with the DNA genome as well as a minor protein called mu to form a DNA-protein complex which is linked to protein VI of the capsid by protein V.

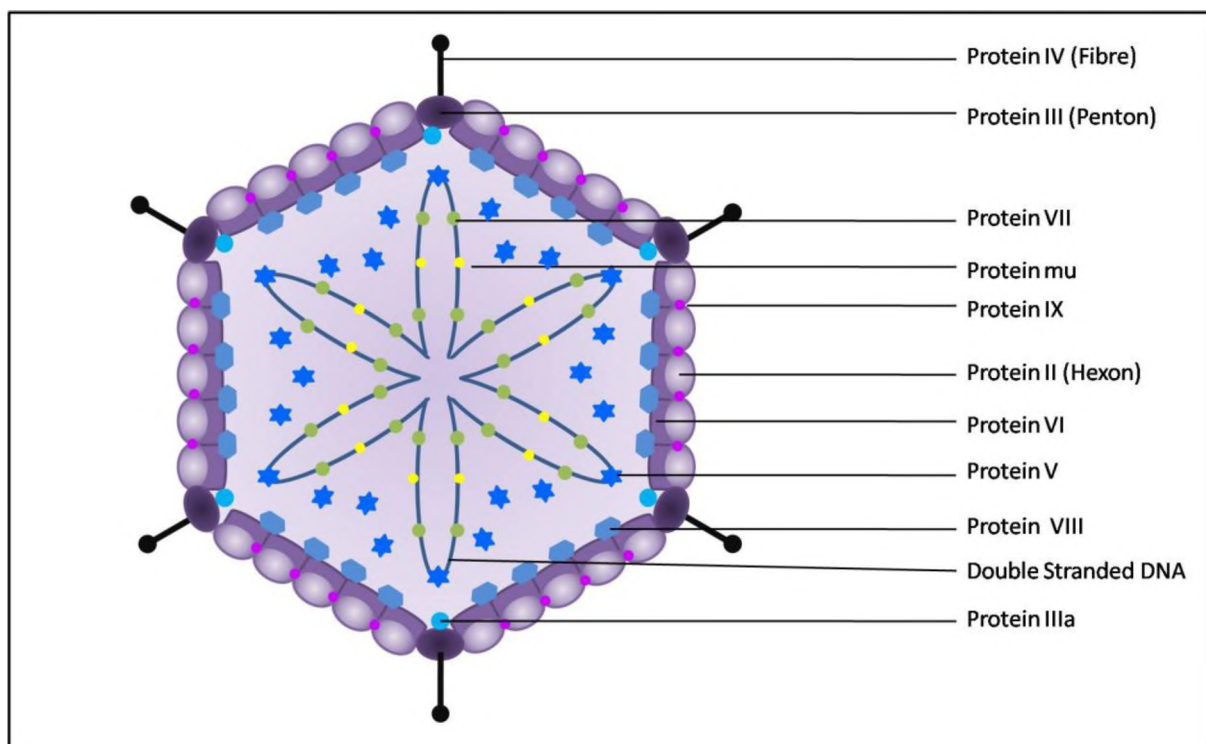


**Figure 1.6: A schematic diagram of an adenovirus viral particle (Adapted from Russell, 2000).**

These viruses belongs to the family *Adenoviridae* (Doefler, 1996). There are 5 genera within this family, *Atadenovirus*, *Aviadenovirus*, *Ichtadenovirus*, *Mastadenovirus* and *Siadenovirus*. Since their first identification, 57 types have been observed in humans. These viruses belong to the *Atadenovirus and Mastadenovirus* genera, and are further classified into 7 species (A-

G). Of the 57 serotypes, 40 and 41, which belong to group F, are most commonly associated with gastroenteritis (Russell, 2000; Doerfler, 1996).

Infection with adenovirus occurs through contact with the conjunctiva, aerosolised droplets, infected tissue and blood or, in the case of gastroenteritis, the faecal-oral route (Doerfler, 1996). This virus mainly infects children under the age of 5, and most infections are asymptomatic. Symptoms of gastroenteritis caused by adenovirus include fever, headache, vomiting, loss of appetite, fainting, stomach cramps, dehydration and watery diarrhoea. Symptoms may last for up to a week but will often resolve themselves (Doerfler, 1996).

### **1.3.5 Astrovirus**

Astroviruses are small (28-41 nm in diameter), non-enveloped, icosahedra viruses, with a 5 to 6 star-like shape when observed with electron microscopy (Arias and DuBois, 2017; Bosch *et al.*, 2014). These viruses belong to the *Astroviridae* family, which contains 2 genera, *Mamastrovirus* (mammals) and *Avastrovirus* (avian) (Bosch *et al.*, 2014). Currently there are 22 species of astrovirus, 19 which belong to the *Mamastrovirus* genus and 3 which belong to the *Avastrovirus* genus.

The genome consists of a 6.2-7.8 kb positive-sense single-stranded RNA molecule that contains 3 ORFs; ORF1a, ORF1b and ORF2 (Bosch *et al.*, 2014). ORF1a encodes the polyprotein NSP1a, while ORF1b encodes the polyprotein NSP1b, both of which are cleaved to form the non-structural proteins, including the protease, VPg and RNA dependent-RNA polymerase. ORF2 encodes the polyprotein VP90 which is cleaved to form the capsid proteins VP34, VP27 and VP25 (Arias and DuBois, 2017). Figure 1.7 below shows a schematic diagram of the viral particle of astrovirus.

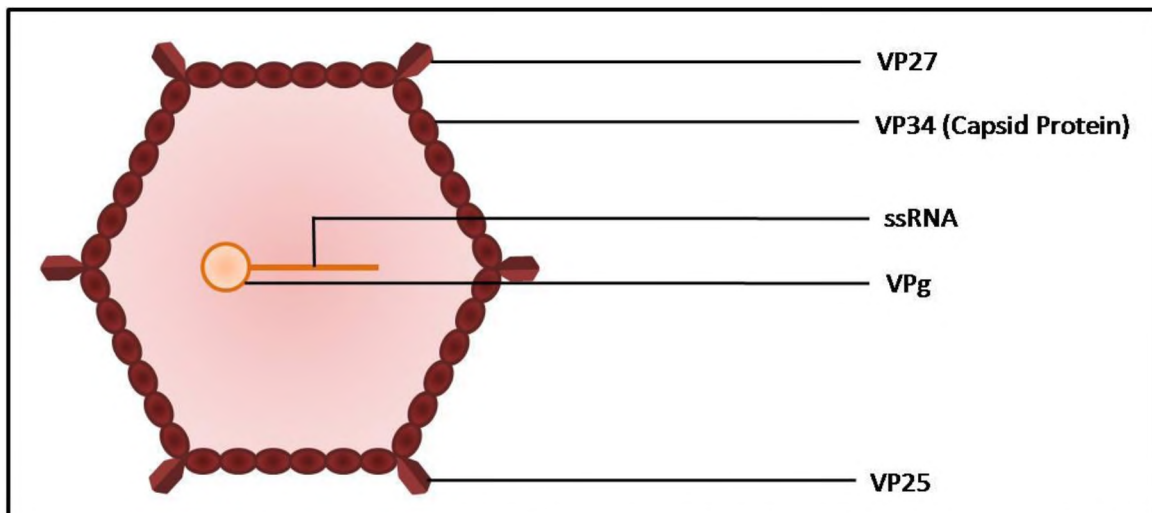


Figure 1.7: A schematic diagram of the Astrovirus viral particle. (Adapted from [http://viralzone.expasy.org/all\\_by\\_species/27.html](http://viralzone.expasy.org/all_by_species/27.html))

While astroviruses are detected at a lower rate than norovirus and rotavirus, these viruses are still an important virus associated with gastroenteritis (Jeong *et al.*, 2012). Astroviruses have been detected in 2-16 % of diarrhoeal cases which resulted in hospitalisation in children under the age of 5 years (Jeong *et al.*, 2012). There are a large number of outbreaks in adults associated with astrovirus as well as a frequent outbreaks which occur in schools and nursing homes.

#### ***1.4 Gastroenteritis in South Africa***

According to the National Institute for Communicable Diseases (NICD), gastroenteritis is responsible for approximately 20% of child mortalities, under the age of four years, in South Africa (reviewed by Lanata *et al.*, 2013). The leading cause of the disease in South Africa is rotavirus (Cohen *et al.*, 2010; Steele *et al.*, 2002).

Due to the severity of this disease, routine vaccination is performed using both Rotarix® and RotaTeq®. Trials for vaccination were started in 2007 and in August 2009 the routine vaccination against rotavirus was incorporated into the Extended Programme on Immunisation in South Africa [EPI (SA)] (Cohen *et al.*, 2010). Rotavirus and the vaccine Rotarix® has been monitored by the Viral Gastroenteritis Unit, NICD and the Diarrhoeal Pathogens Research Unit, MEDUNSA since 2009. These groups monitor the number of rotavirus-positive cases from selected hospitals around South Africa and they test for the

presence of rotavirus using standard immunoassays, ProSpecT Rotavirus ELISA kit (Oxoid, UK), and the GastroVir strip (Coris Bioconcept, Belgium). Since vaccination started in 2009, rotavirus-positive cases have decreased from 48% in 2009 to 19% in 2012 but the number of rotavirus-positive cases increased to 28% in 2013 (Page *et al.*, 2014; Tshangela *et al.*, 2012). The surveillance programme has also reported a decrease of 52% in the number of diarrhoeal cases from 2009-2013 (Page *et al.*, 2014). This leaves a large number of cases which are caused by other pathogens, these may include bacteria, parasites and other viruses, or are of unknown aetiology. The other viruses may include enteroviruses, such as coxsackie virus groups A and B, and NoV.

NoV was first reported in South Africa in 1993, with the identification of GI.1 and GII.1 strains in various outbreaks, followed by the identification of GII.3 in 1995 (Wolfaardt, 1997). Since their first identification, noroviruses have been isolated from various stool samples and water sources in South Africa. A recent study has shown a detection rate of 14.3% from hospitalised patients in the Pretoria region, with a detection of 11 strains, some of which circulated during the same period. Of these 43% of the cases were strain GII.4 (Mans *et al.*, 2010). This study showed that NoV has a high prevalence in South Africa, but there is still limited data on this virus as routine testing is not performed.

While known causative agents such as rotavirus and NoV have been isolated in South Africa, other known causative agents such as AiV have not been found. Other viruses, newly associated with gastroenteritis, such as SAFV have yet to be isolated in South Africa. The next section describes the techniques commonly used for the isolation and detection of viruses.

### ***1.5 Methods of Virus Detection***

Several methods have been developed for the detection and analysis of viruses (Finkbeiner *et al.*, 2008; Storch, 2000). These methods include cell culture, TEM, antigen detection and molecular methods.

Cell culture was first used for the isolation and study of viruses in 1948 by Weller and Enders, where they cultivated mumps in suspended cell culture (Storch, 2000). The presence of viruses is detected in cell lines by morphological changes in the cell, known as cytopathic effect (CPE), which is typically viewed using a light microscope. Cell culture techniques are still used today for the identification and study of viruses because this technique allows for the cultivation of viable isolates. Using a variety of cell lines, different viruses and unexpected viruses can be identified from many samples allowing for the identification of new viruses and the treatment of disease. Often TEM and other techniques are used in conjunction with tissue culture.

TEM has been used in the detection and identification of viruses since 1938, where the poxvirus was first identified (Storch, 2000). This technique has been used to identify many viruses over the years, including NoV and SAFV (Jones, 2007; Kapikain *et al.*, 1972). Due to the size and morphology of viruses, and the development of negative and positive stains, rapid detection and identification of viruses from many samples, including cell culture lysates, stool samples, urine and water samples, can be performed (Storch, 2000). New viruses have also been identified using TEM analysis alongside other techniques, including genome analysis.

Identification of viruses can also be achieved by antigen-detection techniques, such as immunofluorescence (IF) and enzyme linked immunosorbent assays (Odell and Cook, 2013). These techniques involve the detection of a viral antigen using monoclonal antibodies. In the case of IF, the antigen is detected directly, where a fluorophore is chemically linked to the antibody, or indirectly, where a secondary antibody linked to a fluorophore is used to detect the primary antibody, with the use of a fluorescent microscope (Odell and Cook, 2013). The ELISA technique identifies the presence of the viral antigen through a colour change or fluorescent reaction (Gan and Patel, 2013). The virus is detected by the binding of the antigen to an antibody. An enzyme is then linked to the antibody and a substrate is added to the enzyme which results in a colour change. There are 4 types of ELISAs which can be used, direct, indirect, sandwich and competitive (Gan and Patel, 2013). Direct ELISA involve the adhesion of the antigen directly to a microtitre plate followed by the binding of a primary antibody to the antigen. The enzyme which reacts with the substrate is bound directly to the

primary antibody. Indirect ELISAs also rely on the adhesion of the antigen directly to a microtitre plate and a primary antibody is then bound to the antigen (Gan and Patel, 2013). An enzyme-conjugated secondary antibody is then added to the reaction and binds to the primary antibody. The substrate is introduced to the reaction and a colour change occurs. In the case of the sandwich ELISA, the microtitre plate is coated with a known quantity of an antibody which will capture the antigen when added to the well (Gan and Patel, 2013). The primary antibody, specific to that of the antigen, is added to the reaction and binds to the antigen, sandwiching the antigen between the bound and primary antibodies. Once again the secondary antibody, linked to the enzyme, is added to the reaction and binds to the primary antibody and the substrate is added resulting in the colour change. The last type of ELISA is the competitive ELISA (Gan and Patel, 2013). This reaction works by incubating the primary antibody with the antigen, creating an antibody-antigen complex. The wells of the microtitre plate are coated with a known quantity of the same antigen. The antibody-antigen complex solution is then added to the microtitre plate and any free primary antibody in the sample will bind to the antigen which is adhered to the well. Once again, a secondary antibody, linked to the enzyme is added to the reaction followed by the substrate. However, unlike the other ELISAs, a lack of colour change in the reaction indicates the presence of the antigen in the sample (Gan and Patel, 2013). These techniques are useful for viruses which do not grow particularly well in tissue culture, and are also able to yield rapid results (Gan and Patel, 2013). There are many commercially-available monoclonal antibodies (IF) and ELISA kits for different viruses, allowing for the screening of large number of samples (Gan and Patel, 2013; Odell and Cook, 2013). These two techniques do not require viral viability, allowing for less stringent handling methods.

Molecular methods are commonly used for the identification and detection of viruses (Storch, 2000). These methods include polymerase chain reactions (PCR) and nucleotide sequencing. For the identification of viruses using these techniques, nucleic acids are required. Viruses can have one of five types of genomes (Ball, 2007). The genomes can either be double-stranded DNA, single-stranded DNA, positive-stranded RNA, negative-stranded RNA or double-stranded RNA (Ball, 2007). These can be extracted from the viruses by using techniques such as a phenol chloroform extraction or one of the many commercial DNA or RNA extraction kits (Tan and Yaip, 2009). The extracted DNA or RNA can then be used as a template for identification techniques such as PCR.

PCR analysis, which was first developed in 1985, allows for the amplification of specific nucleotide sequences, including viral sequences, from many samples (reviewed by Garibyan and Avashia, 2013; Storch, 2000). PCR assays use a DNA polymerase, such as *Taq* polymerase, for the amplification of selected regions from a template DNA. The region of DNA to be amplified is specified by primers which the DNA polymerase attaches to (reviewed by Garibyan and Avashia, 2013). Primers are short DNA fragments which are complimentary to part of the region of the DNA template to be amplified. The DNA polymerase links nucleotides, complimentary to that of the DNA template, together to create the amplicon. In order for this to take place the temperature needs to be correct for each component to perform as required. As DNA is double stranded, the first step is to separate the strands so the polymerase can access the single strands (reviewed by Garibyan and Avashia, 2013). This is performed at high temperatures. The second stage is the annealing of the primers which occurs at a temperature dictated by the best annealing of the primers to the template. The third step is the extension of the primers to form PCR products. This is performed at the optimum temperature for the polymerase. A PCR assay is exponential and can be used to detect a sequence from small amounts of DNA and the results are observed through agarose gel electrophoresis (reviewed by Garibyan and Avashia, 2013).

Since the development of PCR assays, technology has advanced allowing for quantification of results as shown through real-time PCR (qPCR) (Staggemeier *et al.*, 2012). This technique involves the addition of either a fluorescent probe which hybridises with a complimentary sequence on the PCR product or the incorporation of fluorescent dyes into the double-stranded DNA product (reviewed by Garibyan and Avashia, 2013; Staggemeier *et al.*, 2012). qPCR detects and quantifies the amount of PCR product while the reaction is still running by detecting the level of fluorescence present in the reaction (Staggemeier *et al.*, 2012).

While PCR and qPCR assays are great techniques for detecting sequences they require a DNA template. For DNA viruses standard PCR and qPCR assays can be performed but viruses which have an RNA genome require a different type of PCR assay, the reverse transcription-PCR (RT-PCR) assay (Ozoemena *et al.*, 2004). RT-PCR assays use a RNA-dependent DNA polymerase (reverse transcriptase) to synthesise a copy DNA (cDNA) of the viral RNA genome which is used as the template for a PCR reaction (reviewed by Garibyan

and Avashia, 2013; Ozoemena *et al.*, 2004). This cDNA synthesis step can either be performed in a separate reaction prior to the PCR assay (two-step RT-PCR assay) or it can become part of the PCR reaction by the addition of the reverse transcriptase enzyme and the RNA, instead of DNA, to the PCR mixture and the reverse transcription becomes the first step prior to the PCR cycle (one-step RT-PCR assay) (Wacker and Godard, 2005). RT-PCR assays are used to detect RNA viruses and RNA expression. Quantitative RT-PCR (qRT-PCR) assays can be used to quantify the RNA present in a sample. To increase the detection rate of sequences, nested PCR/RT-PCR assays can be performed. These involve the amplification of a PCR product using two sets of primers (Staggemeier *et al.*, 2012). The first PCR reaction is prepared as a standard reaction. The PCR product then becomes the template for a second PCR reaction which uses a second set of primers to amplify a region within the template (Staggemeier *et al.*, 2012). For the detection of multiple sequences, such as more than one virus, a multiplex PCR/RT-PCR can be used (Staggemeier *et al.*, 2012; Elnifro *et al.*, 2000). This technique uses a number of primer sets, where each set will amplify a different nucleotide sequence from either one virus or multiple viruses, within a PCR assay. This technique is useful when the sample is limited as fewer reactions will need to be performed (Elnifro *et al.*, 2000). It is also cost effective and time saving.

PCR assays are used to detect a wide variety of viruses including NoV, adenovirus and SAFV and the advantages include rapid detection of the viruses as the samples can be screened in hours and viruses do not need to be propagated (reviewed by Garibyan and Avashia, 2013; Magwalivha *et al.*, 2012; da Silva *et al.*, 2007; Jones, 2007). PCR assays can, however, only detect viruses which are presumed to be present (reviewed by Garibyan and Avashia, 2013). Where an unknown virus is suspected nucleotide sequencing can be used (reviewed by Stranneheim and Lundeberg, 2012). This technique usually involves the extraction of viral DNA or RNA followed by cloning into a vector, followed by sequencing. This technique has been used in the identification of many viruses including SAFV, though newer, molecular methods are being used for virus identification including metagenomics.

In recent years, metagenomics has become an important tool in the identification and study of micro-organisms, including viruses (Finkbeiner *et al.*, 2008; Storch, 2000). Metagenomics utilises sequencing techniques, such as Sanger-sequencing and, more recently, next-

generation sequencing. Many studies use Sanger-sequencing alongside the development of clone libraries to study the viral communities present in a given environment. This is achieved as follows: viral particles are isolated from a given sample, viral DNA or RNA is extracted from the virus particles. In the case of RNA, cDNA is synthesised by reverse-transcription, the DNA or cDNA is then cloned into the chosen vector (Finkbeiner *et al.*, 2008, Edwards and Rohwer, 2005). Bacterial cells are then transformed, the plasmid DNA is extracted and sequenced. Some studies have included a PCR amplification step using random primers to increase the amount of viral DNA or cDNA present in the sample as well as providing restriction sites which allow for better ligation of the viral DNA to the vector (Finkbeiner *et al.*, 2008; Edwards and Rohwer, 2005). This approach has been used for the detection of viruses associated with diarrhoeal disease and has identified known and novel viruses from the stool samples, but this method is very time- and labour-intensive as hundreds, if not thousands, of clones have to be sequenced (Finkbeiner *et al.*, 2008).

While both clone libraries and PCR assays are both useful techniques for the identification of viruses, these techniques vary in a variety of ways. Firstly, PCR assays only require nanograms of DNA while clone libraries require milligrams of DNA to successfully amplify and screen for viruses (Hoseini and Sauer, 2015; Finkbeiner *et al.*, 2008; Edwards and Rohwer, 2005). Secondly, Clone libraries amplify the DNA *in vivo* inside a bacterium while PCR amplifies it *in vitro*. Thirdly, clones have to be screened after isolation to ensure the correct one is being sequenced, PCR amplicons do not necessarily have to be screened if the DNA was pure (Hoseini and Sauer, 2015). Lastly, clone libraries are very labour-intensive and can take several days to perform these experiments from DNA extraction all the way to sequencing. PCR amplification of viral DNA and sequencing is less labour-intensive than that of clone libraries and can be completed in a matter of hours.

Since the development of parallel, high-throughput sequencing technologies, such as the 454-Life Sciences (Roche), Illumina (Solexa) and SOLiD (Applied Bioscience), next-generation sequencing methods have been used in metagenomic studies. Next generation sequencing is used for the detection of known and unknown viruses as follows: viral particles are isolated from a given sample (Bibby, 2013). The DNA or RNA viral genome is extracted from the viral particles, cDNA is synthesised from the RNA genome by reverse transcription. The

nucleic acids are then fragmented and sequenced (Bibby, 2013). If short fragments are present, they can be assembled to create longer sequences. The raw and assembled sequences are then identified through the use of a local or global alignment to known viral sequences. These technologies allow for sequencing of the DNA or RNA extracted from a given sample without needing to clone into a vector, decreasing the time and labour required for these studies (Petrosino *et al.*, 2009; Finkbeiner *et al.*, 2008). These technologies can be used for both deep sequencing, where all the viruses in a given environment can be detected and identified, and full genome sequencing, where a single, or select few, viral genomes can be fully sequenced. More than one sample can be sequenced at once to compare the viral community in many samples, however the depth of these samples will be limited compared to the sequencing of a single sample (Petrosino *et al.*, 2009; Finkbeiner *et al.*, 2008). Metagenomics has been used in a wide range of studies. It has been used for the identification of viruses in many environments, including within the human digestive system, allowing for a greater understanding of the virome of humans (Petrosino *et al.*, 2009; Finkbeiner *et al.*, 2008). A variety of viruses have been identified using this technique including saffold virus, cosavirus, klassevirus/salivirus, polymavirus, bufavirus, tusavirus and recovirus, all of which have been associated with gastroenteritis (Bibby, 2013; Kapoor *et al.*, 2008; Jones *et al.*, 2007).

## **1.6 Motivation**

Acute infantile gastroenteritis is a serious disease worldwide and in South Africa it is responsible for 20% of all deaths in children under the age of five years (reviewed by Lanata *et al.*, 2013). Rotavirus is the leading cause of this disease in South Africa. Since the start of the rotavirus vaccination in 2009, the number of rotavirus-positive cases has decreased, leaving a large number of cases that are caused by other pathogens, such as NoV, or are of unknown aetiology (Page *et al.*, 2014; Tshangela *et al.*, 2012).

While NoV is the second leading cause of infantile gastroenteritis there is no surveillance program to monitor the prevalence of this virus in South Africa and no vaccine currently in circulation (Mans *et al.*, 2010). There are studies which have reported the identification of NoV strains in clinical samples, but these were limited to a specific region in the Gauteng province of South Africa (Mans *et al.*, 2013; Mans *et al.*, 2010).

The number of gastroenteritis cases of unknown aetiology is estimated to be 40% in South Africa (Cohen *et al.*, 2010). While novel viruses, such as SAFV, have been identified worldwide, they have not been isolated in South Africa. These viruses may be the cause of some of these cases. Other viruses which have a high prevalence of disease, such as AiV, in many other countries have also not been identified in South Africa. The inability to identify these viruses may be due to the techniques which are currently used for surveillance of gastroenteritis. These techniques, such as ELISA, are often virus specific therefore would not identify unknown viruses present in the samples (Gan and Patel, 2013). In order to identify SAFV, AiV and other viruses which may be the cause of the disease, techniques such as metagenomics need to be employed. The identification of these and other viruses from stool samples from symptomatic patients where rotavirus is not present may aid in the surveillance and treatment of this disease in South Africa.

### ***1.7 Primary Aim and Objectives***

The primary aim of the project is to develop techniques for the identification of NoV and selected picornaviruses associated with acute infantile gastroenteritis.

The specific objectives of the project are: 1) To prepare and screen rotavirus-negative stool samples and environmental samples by transmission electron microscopy examination for the presence of viral particles. 2) To extract viral RNA from selected environmental and stool samples which show the presence of virus particles following TEM analysis. 3) To develop positive controls and RT-PCR assays for the identification of NoV, AiV and SAFV from the selected stool and environmental samples. 4) To apply RT-PCR amplification of specific viral sequences to identify specific viruses including SAFV, AiV and NoV from the stool and environmental samples.

The following paragraphs describe the content of the remaining chapters.

The next chapter, Chapter 2, describes the development of the sample preparation techniques, which include filter sterilisation, PEG 6000 precipitation and TEM analysis. As well as the development of two-step RT-PCR assays to be used during this study. These techniques were

developed using a known picornavirus, namely TMEV, as this virus can be replicated in tissue culture and so is a renewable source of virus particles, unlike the samples to be screened for selected viruses.

Chapter 3 describes the development of the positive controls and the RT-PCR assays to be used in the identification of NoV, AiV and SAFV from the samples used in this study. The positive controls were developed by cloning the NoV GII N/S domain and the AiV 5'UTR and 3CD regions of the genomes into pGEM®-T Easy. RNA was transcribed *in vitro* from pNoVGII, pAiV5'UTR, pAiV3CD and pSAFV (donated by Jan Drexler). This RNA was then used to develop the RT-PCR assays. The two-step RT-PCR assays involve the synthesis of cDNA from the *in vitro* RNA followed by the amplification of selected viral sequences of NoV GII, AiV and SAFV. These viral sequences include the N/S domain of NoV GII, the 5'UTR and 3CD of AiV and the 2C sequence of SAFV. The positive controls were synthesised to aid in the development of the RT-PCR assays and to be used as positive controls in the screening of selected samples for NoV, AiV and SAFV. The RT-PCR assays were developed to allow for the screening of samples for these viruses. Screening for NoV will allow us to determine that the techniques used in this study can be applied to the real-world samples as AiV and SAFV have yet to be identified in South Africa.

In Chapter 4 the wastewater, oyster and clinical samples to be used in this study are described. It also describes the filter concentration, PEG 6000 precipitation methods and screening for the presence of viral particles using TEM. The sample preparation was performed to concentrate virus particles and to remove any contaminants, such as bacteria, which may interfere with downstream applications. The TEM analyses were performed to confirm the presence and concentration of virus particles in the wastewater, oyster and clinical samples.

Chapter 5 describes the RNA extraction and screening of the wastewater, oyster and clinical samples for the presence of NoV using the RT-PCR assay developed in Chapter 3. This was done to ensure NoV GII, which was expected to be present in some of the samples, could be detected using these techniques so that these techniques could be applied to the other viruses.

The final chapter, Chapter 6, discusses the conclusions made from the results obtained during the study. An indication of future work than can be performed to further the study is also discussed.

A flow diagram of the study design is shown in Figure 1.8 and Figure 1.9 below.

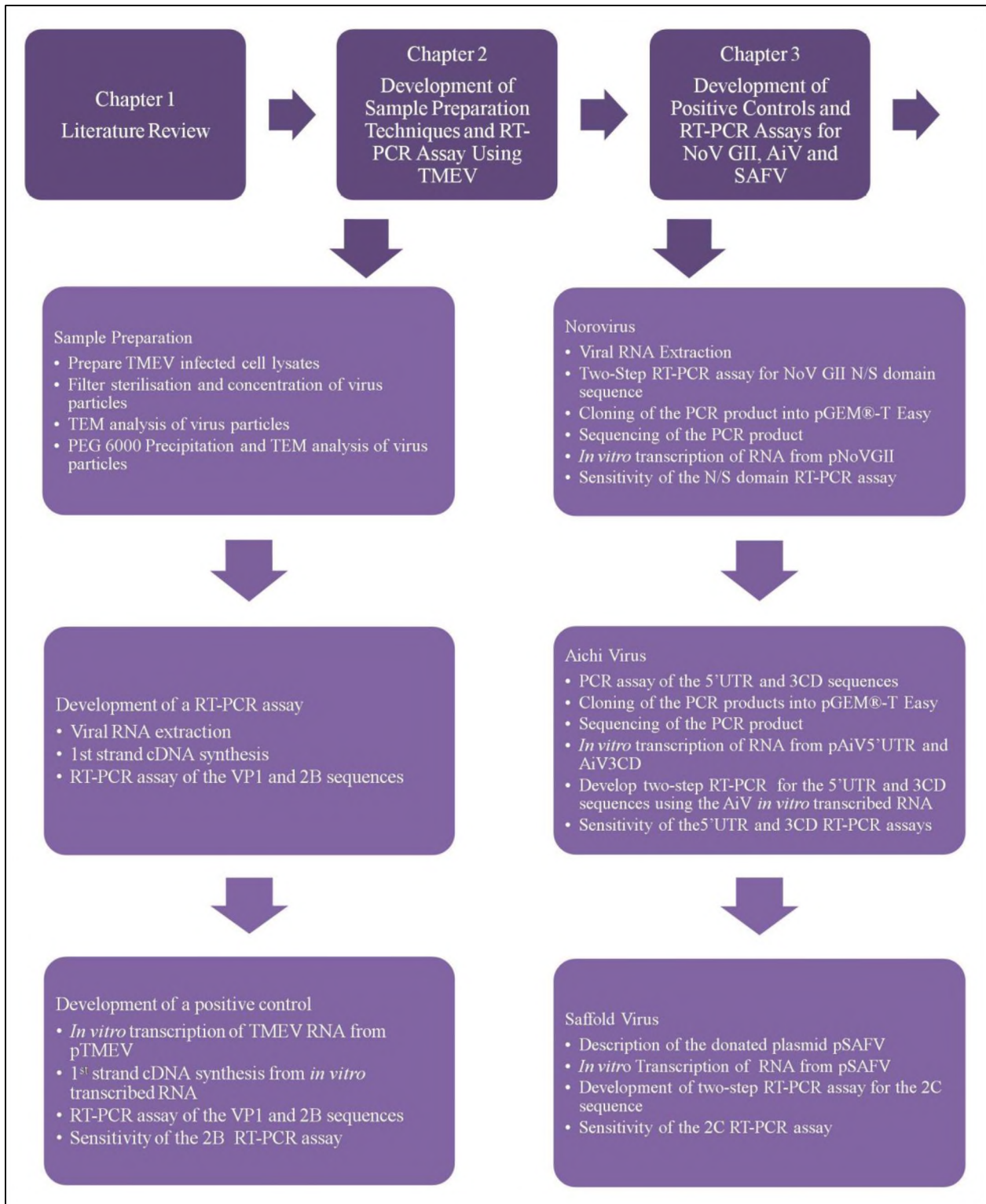


**Figure 1.8: Flow diagram of the study design (Chapters 1-3).**

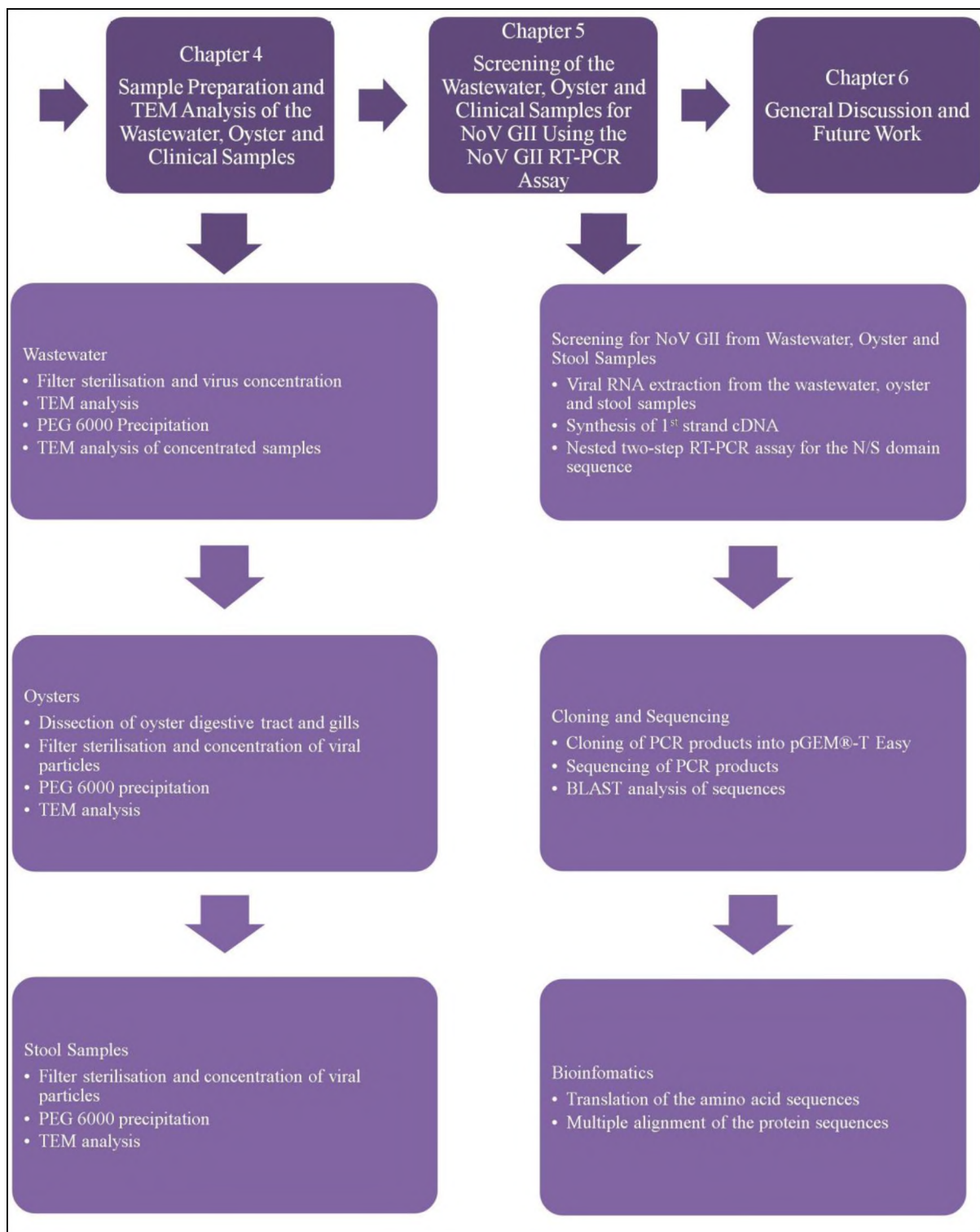


**Figure 1.9: Flow diagram of the study design (Chapters 4-6).**

## ***Chapter 2: The Development of Sample Preparation Techniques and RT-PCR Assays Using Theiler's Murine Encephalomyelitis Virus***

### ***2.1 Introduction***

This chapter describes the development of methods which can be used in the identification of selected positive-strand RNA viruses in a variety of samples, including wastewater, oyster and clinical samples. Before conducting RT-PCR assays, it is necessary to develop methods for sample filtration and concentration by polyethylene glycol (PEG) 6000 precipitation. Samples then undergo screening by transmission electron microscopy before RNA extraction, first-strand cDNA synthesis and RT-PCR using virus-specific oligonucleotides.

Due to the limited supply of samples being analysed, the methods were developed using Theiler's Murine Encephalomyelitis virus GDVII which can be replicated to high levels in a Baby Hamster Kidney cell line (BHK-21) in the laboratory. TMEV belongs to the *Picornaviridae* (genus: *Cardiovirus*) and is an appropriate model for development and optimisation of virus isolation and identification techniques as it shares a similar genome organisation and morphology to that of AiV and SAFV, as well as to members of the *Caliciviridae*.

RT-PCR assays are sensitive, specific and commonly used to detect the presence of positive strand viruses in a variety of samples. The primary aim of this study is to develop RT-PCR assays for the detection of AiV and SAFV which have not been found in South Africa. As NoV is a leading cause of viral gastroenteritis, and has been detected in wastewater and clinical samples in South Africa, it was decided to develop RT-PCR assays to verify its presence in the samples acquired. In order to carry out RT-PCR assays, it is necessary to obtain viral RNA from the samples. Prior to RNA extraction samples require filter-sterilisation to remove cell debris and other contaminants. Following filter-sterilisation, it is important to concentrate the viral particles in the samples as, unlike viruses grown in cell culture, they are likely to be present in low concentrations in environmental and clinical samples.

PEG 6000 precipitation can be used to concentrate viruses from environmental samples as well as samples grown in cell culture. In 1963, Herbert used PEG and NaCl to precipitate both rod-shaped small and round virus particles from plant matter (Herbert, 1963). Since this development, many studies have isolated a variety of viruses from a wide range of environments, including Lewis and Metcalf (1988), who developed a method using PEG 6000 to precipitate out viruses from shellfish, fresh estuarine water and water sediment seeded with rotavirus, poliovirus and hepatitis A virus (Lewis and Metcalf, 1988). Their results showed that PEG precipitation was able to precipitate selected samples from a variety of sources and, when compared to a commonly-used organic flocculation method, PEG precipitation yielded a higher percentage of virus recoveries than that of organic flocculation. Lewis *et al.* (2010) then adapted this method for the recovery of human indicator viruses from oysters and mussels (Lewis *et al.*, 2010).

The remainder of this chapter describes the development of the sample preparation techniques using TMEV GDVII as a model. These include filter concentration and PEG 6000 precipitation, the screening of infected cell lysates by TEM, viral RNA extraction and the development of an RT-PCR assay protocol using TMEV GDVII genome-specific oligonucleotides. The cell lysates were prepared by filter-sterilisation to remove debris and to increase the concentration of potential viruses present in the samples. The samples were screened by TEM before and after concentration to determine the presence of virus particles along with their morphology. Finally a two-step RT-PCR assay, where the cDNA is synthesised first and added to a PCR reaction, was developed for the identification of TMEV GDVII VP1 and 2B sequences in the cell lysates. This assay is applied to other samples for the detection of specific viruses in Chapter 3.

The specific objectives for this chapter are to:

- Infect BHK-21 cells with TMEV and prepare cell lysates.
- Develop a filter-sterilisation and concentration technique using TMEV-infected cell lysates.
- Screen the cell lysates by TEM to determine the presence of virus particles and their morphology.
- Develop a PEG precipitation protocol in combination with sodium chloride.

- Develop a two-step RT-PCR assay for the detection of TMEV GDVII sequences, with *in vitro* transcribed TMEV RNA serving as a positive control.
- Determine the minimum amount of RNA required for the two-step RT-PCR assays using RNA transcribed *in vitro* from TMEV GDVII cDNA and viral RNA from infected lysates.

## ***2.2 Materials and Methods***

### ***2.2.1 TMEV Sample Preparation***

BHK-21 cells were kindly supplied by Martin Ryan (University of St Andrews, UK). The cells were maintained in complete medium, Dulbecco's modified Eagle's medium (DMEM, Lonza Group Ltd, Basel Switzerland) supplemented with 5% Foetal Bovine Serum (FBS, Lonza Group Ltd, Basel Switzerland) and 1% Penicillin, Streptomycin and Fungizone (PSF, Sigma-Aldrich, USA) in 25 cm<sup>2</sup> flasks at 37°C with 10% CO<sub>2</sub>.

For the preparation of TMEV GDVII stocks, an 80% confluent monolayer of cells was infected with a 1 ml TMEV stock (previously prepared in the laboratory). The media was poured off and the cells rinsed with Phosphate-Buffered Saline (PBS) [137 mM NaCl, 2.7 mM KCL, 10 mM Na<sub>2</sub>HPO<sub>4</sub>, 2 mM KH<sub>2</sub>PO<sub>4</sub> (pH 7.4)]. The virus stock was poured onto the cells and incubated at room temperature with shaking for 1 hr to allow for virus adsorption. Using serum-free DMEM, the medium in the flask was made up to 10 ml and the flask was incubated overnight at 37°C with 10% CO<sub>2</sub>. The viral stocks were then stored in 1 ml aliquots at -80°C.

### ***2.2.2 Filter Sterilisation and Concentration of TMEV Infected Lysates***

The TMEV infected lysates were prepared by infecting BHK-21 cells with a multiplicity of infection of 3, as determined previously in the laboratory by Lindsay Murray (Murray, 2007). NP-40 (Sigma-Aldrich, USA) was added to the supernatant, to a final concentration of 1%, and the supernatant was incubated with shaking at room temperature for 1 hr and centrifuged at 4000 xg for 20 min to remove debris. The supernatant was passed through 0.25 µm syringe filters (GVS Filtering Technology, USA) and concentrated to 2 ml using 4 ml Vivaspin columns (Sartorius Stedim Biotech, Germany), by centrifugation at 4000 xg for approximately 10 min; as per manufacturer's protocol.

### ***2.2.3 Transmission Electron Microscopy Analysis of the TMEV Sample***

Forvar carbon coated grids (Wirsam Scientific, South Africa) were prepared for TEM analysis by placing approximately 20 µl of the TMEV sample on the grid for 1 min followed by staining with 1% uranyl acetate for 1 min. The grids were viewed under the JOEL JEM 2100 transmission electron microscope (Physics Department, Nelson Mandela Municipality University), images were captured with the 1000SC TEM digital camera (Gatan Inc, USA) and analysed using Gatan Digital Micrograph imaging software version 2.1 (Gatan Inc, USA) or the Zeiss Libra 120 transmission electron microscope (Electron Microscopy Unit, Rhodes University). Images were captured with the Mega View G2 camera (Olympus, Germany) and analysed with the i10 Soft Imaging System (Olympus, Germany).

### ***2.2.4 PEG 6000 Precipitation of Virus Particles***

For PEG precipitation a 50% (w/v) solution of PEG 6000 was prepared in double-distilled water (ddH<sub>2</sub>O). A second TMEV sample was prepared. This sample was used to determine the correct sodium chloride (NaCl) concentration for PEG precipitation. The concentrated sample was divided into two 1 ml samples and PEG 6000 was added to a final concentration of 8% and NaCl to final concentrations of 0.15 M and 0.25 M respectively. The samples were incubated at 4°C overnight and centrifuged at 10 000 *xg* for 30 min at 4°C. The pellet was resuspended in 200 µl ddH<sub>2</sub>O. The two samples were screened by TEM as described above, Chapter 2, section 2.2.3.

### ***2.2.5 Viral RNA Extraction***

Viral RNA was extracted from the cell lysate using the QIAamp® Viral RNA Mini Kit (Qiagen, USA), according to manufacturer's instructions as follows: 140 µl of the TMEV sample was lysed by adding to 560 µl of buffer AVL containing carrier RNA and incubating at room temperature for 10 min. The RNA was precipitated out by adding 560 µl 100% ethanol to the solution which was then centrifuged through the QIAamp Mini column at 6000 *xg* for 1 min, allowing the RNA to bind to the column. The column was washed by adding 500 µl buffer AW1 and centrifuging at 6000 *xg* for 1 min. A second wash was performed by adding 500 µl buffer AW2 and centrifuging at 12 000 *xg* for 3 min. The RNA was eluted by adding 40 µl buffer AVE, incubating at room temperature for 1 min and centrifuging at 6000 *xg* for 1 min. The extracted RNA was stored at -80°C until used.

The RNA was analysed by 1% agarose gel electrophoresis in 1x Tris Acetate EDTA (TAE) buffer [40 mM Tris (pH8.0), 0.1% glacial acetic acid, 1 mM EDTA], in the presence of 0.5 µg/ml ethidium bromide. The KAPA Universal DNA Ladder (KAPA Biosystems, USA) was used as molecular weight marker throughout the study and the DNA was mixed with 1x loading dye (Fermentas, USA) before loading and electrophoresis was performed in 1x TAE buffer for 30 min at 90 V. Bands were visualised using the Uvipro Chemi with the Uvipro software (Uvitech, Cambridge, UK). The RNA concentration was measured using a Nanodrop 2000 Spectrophotometer (Thermo Scientific, USA).

### 2.2.6 First-Strand cDNA Synthesis and RT-PCR Assay

First-strand cDNA was synthesised from the extracted viral RNA using the RevertAid™ Premium first-strand cDNA synthesis kit (Fermentas, USA) according to the manufacturer's protocol. In brief, the reaction was prepared as follows: 25 ng/µl to 50 ng/µl final concentration RNA, 5 µM random hexamer primers, 0.5 mM dNTP mix, 1x reaction buffer, 1 µl RevertAid™ Premium enzyme mix and to 20 µl nuclease-free water. The reaction was incubated at 25°C for 10 min, 50°C for 30 min and 85°C for 5 min to terminate the reaction.

Forward (F) and reverse (R) oligonucleotides, as shown in Figure 2.1 and Table 2.1 below, were designed to amplify the full length coding sequence of TMEV 2B (412 bp) and VP1 (828 bp).

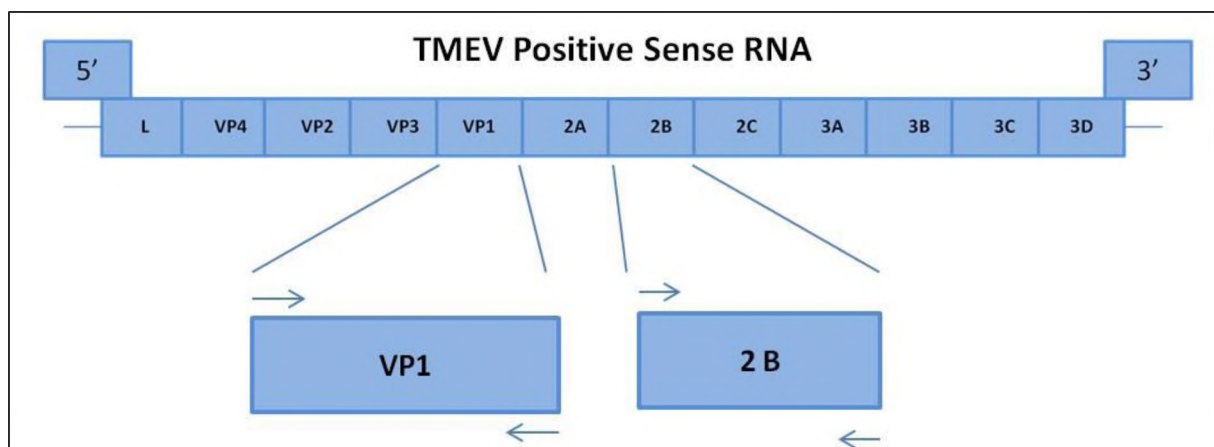


**Figure 2.1:** Schematic diagram of the VP1 and 2B forward (→) and reverse (←) oligonucleotides and the position of binding to the VP1 and 2B coding sequences.

**Table 2.1: Forward and Reverse Oligonucleotide Sequences for TMEV 2B and VP1.**

Primer	Nucleotide Sequence	Binding Site	Size
2B-F	5'- GGATCCCCTGTGCAGTCGGTTTTTCA -3'	4234 – 4255 bp	412 bp
2B-R	5'- GTCGACTCAGTCAGGTTGCATCACAT -3'	4626 – 6448 bp	
VP1-F	5'- GGATCCGGAATTGACAATGCTGAGAAG -3'	3008 – 3029 bp	828 bp
VP1-R	5'- GTCGACTCACTCGAACTC -3'	3823 – 3835 bp	

RT-PCR assays were performed to amplify the full length TMEV 2B and VP1 sequences, using a MJ Mini™ Personal Thermal Cycler (Bio-Rad, USA). In brief, 1x ready mix with Mg<sup>2+</sup> (KAPA Biosystems, USA), 0.4 μM forward and reverse primers, ~4 ng/μl final concentration first-strand cDNA template and 9.5 μl ddH<sub>2</sub>O were mixed. Negative control reactions were set up in the same manner except that ddH<sub>2</sub>O was used instead of the first-strand cDNA template. The cycling parameters used for the RT-PCR reactions were as follows: 95°C for 1 min 30s, 30 cycles of 95°C for 30s, 55°C for 45s, 72°C for 2 min and a final elongation of 72°C for 5 min. The RT-PCR products were analysed by 1% agarose gel electrophoresis.

### ***2.2.7 In Vitro Transcription***

In order to produce RNA for use as a positive control in RT-PCR assays, TMEV cDNA was transcribed *in vitro* from pTMEV (Kindly supplied by Martin Ryan University of St. Andrews, UK). The plasmid map is shown in Figure 2.2 below.

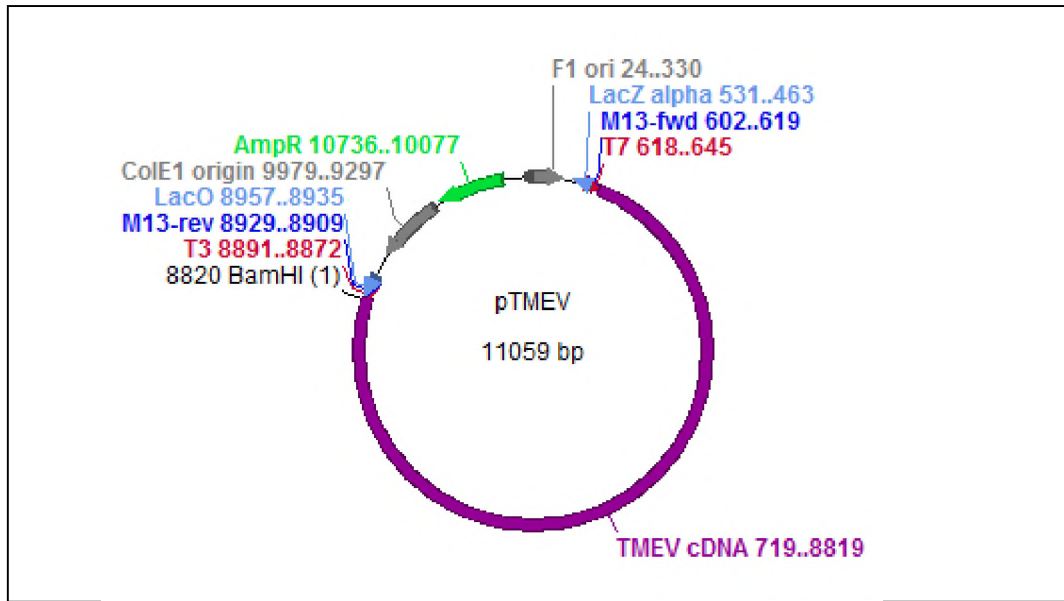


**Figure 2.2: Schematic diagram of pTMEV. Essential features include the TMEV GDVII cDNA, *lacZα* and *lacO* promoter encoding sequence, T3 and T7 RNA polymerase promoter.**

pTMEV (Figure 2.2) is made up of the vector pBluescript SK(-) and the full genome of TMEV GDVII. pBluescript SK(-) encodes the  $\beta$ -galactosidase alpha (*lacZα*) gene as well as the lactose operator (*lacO*) promoter for which allows for blue/white screening when selecting for the colony containing the plasmid with the insert (Agilent Technologies Inc., 2008). The vector also encodes for ampicillin resistance allowing for the selection of colonies containing the plasmid. Two RNA transcription promoters are present in the vector, T3 and T7, allowing for *in vitro* transcription of RNA from this plasmid. A multiple cloning site is also present, allowing for digestion of the plasmid with restriction enzymes, including *Bam* HI.

pTMEV was linearised by digestion with the restriction enzyme *Bam* HI as follows: the reaction was set up using  $\sim 70$  ng/ $\mu$ l final concentration of plasmid DNA, 0.7x buffer, 3 U/ $\mu$ l *Bam* HI restriction enzyme and sterile ddH<sub>2</sub>O to 15  $\mu$ l. The reaction was incubated at 37°C for 30 min. The digested plasmid was analysed by 1% agarose gel electrophoresis. The linear plasmid was cleaned using the Wizard® SV gel and PCR clean-up system (Promega, USA). In brief, the digested band was excised out of the 1% agarose gel and weighed. Membrane Binding Solution was added at 10  $\mu$ l for every 10 mg of agarose gel and the gel was dissolved by incubating at 50°C for 10 min. The solution was transferred to an SV Minicolumn and incubated at room temperature for 1 min. The solution was centrifuged at

16000  $g$  for 1 min after which the flow through was discarded and the column was washed with 700  $\mu$ l Membrane Wash Solution. The column was centrifuged at 16000  $g$  for 1 min after which the flow through was, once again, discarded. The column was washed again with 500  $\mu$ l of the Membrane Wash Solution and centrifuged at 16000  $g$  for 5 min and the flow through was again discarded. To elute the plasmid DNA, 50  $\mu$ l of nuclease-free water was added to the column and incubated for 1 min at room temperature followed by centrifugation at 16000  $g$  for 1 min. RNA was then transcribed from the linearised plasmid using the TranscriptAid™ T7 High Yield Transcription kit (Fermentas, USA). The *in vitro* RNA transcription reaction was set up as follows: 1x transcription buffer, 1 U/ $\mu$ l RiboLock™ RNase inhibitor, ATP/CTP/GTP/UTP to a final concentration of 2mM, 0.02  $\mu$ g/ $\mu$ l linearised template DNA, 30 U/ $\mu$ l T7 RNA polymerase and to 50  $\mu$ l ddH<sub>2</sub>O. The reaction was incubated at 37°C for 2 hrs. The RNA was treated with DNase I (Fermentas, USA) to remove the plasmid template. This was done by adding DNase I (final concentration 0.04 U/ $\mu$ l) to the reaction mixture and incubating at 37°C for 15 min and, to inhibit the reaction, EDTA (final concentration 0.01 M) was added and the reaction was incubated at 65°C for 10 min. The RNA was analysed using 1% agarose gel electrophoresis.

### ***2.2.8 First-Strand cDNA Synthesis and RT-PCR Assay from In Vitro Transcribed RNA***

First-strand cDNA was synthesised from the *in vitro* transcribed RNA using the RevertAid™ Premium first-strand cDNA synthesis kit according to the manufacturer's protocol as described above, Chapter 2, section 2.2.6. The RT-PCR assay for TMEV 2B and VP1 was carried out as described above, Chapter 2, section 2.2.6 and the RT-PCR products were analysed by 1% agarose gel electrophoresis.

### ***2.2.9 Sensitivity of the RT-PCR Assay***

Five, 5-fold serial dilutions were prepared using the TMEV *in vitro* transcribed RNA and the concentrations were measured using the Nanodrop 2000 Spectrophotometer (Thermo Scientific, USA). First-strand cDNA was synthesised using 1  $\mu$ l of RNA (with the following concentrations: 607.9 ng/ $\mu$ l, 131.8 ng/ $\mu$ l, 26.7 ng/ $\mu$ l, 6 ng/ $\mu$ l and 2 ng/ $\mu$ l) using the RevertAid™ Premium first-strand cDNA synthesis kit. RT-PCR assays were performed for the amplification of the coding sequences of TMEV 2B as described above, Chapter 2, section 2.2.6, and analysed by 1% agarose gel electrophoresis.

## ***2.3 Results***

### ***2.3.1 Transmission Electron Microscopy***

BKH-21 cells were infected with TMEV GDVII after which the cell lysates were filter sterilised and concentrated and virus particles were precipitated with and without PEG 6000 at a NaCl concentration of 0.15 M or 0.25 M before TEM analysis. Figure 2.3 below shows the result of the transmission electron microscopy of the TMEV sample without PEG (panels A and B), the sample with PEG 6000 and a NaCl concentration of 0.15 M (panels C and D) and the samples precipitated with PEG 6000 and NaCl concentration of 0.25 M (panels E and F).

Viral particles can be seen in panels A-F in Figure 2.3. The particles are approximately 30 nm in diameter and are icosahedral in shape. Panels A and B in Figure 2.3 show the presence of virus particles which are bound to cellular debris, but panels C-F show minimal amounts of cellular debris. Low numbers of virus particles were observed in the sample which was not treated with PEG 6000, panels A and B. In panels C and D, the sample treated with PEG 6000 and 0.15 M NaCl showed a larger number of virus particles than panels A and B. In panels E and F, the sample treated with PEG 6000 and 0.25 M NaCl, the highest number of viral particles was observed, and many of the viral particles formed clusters.

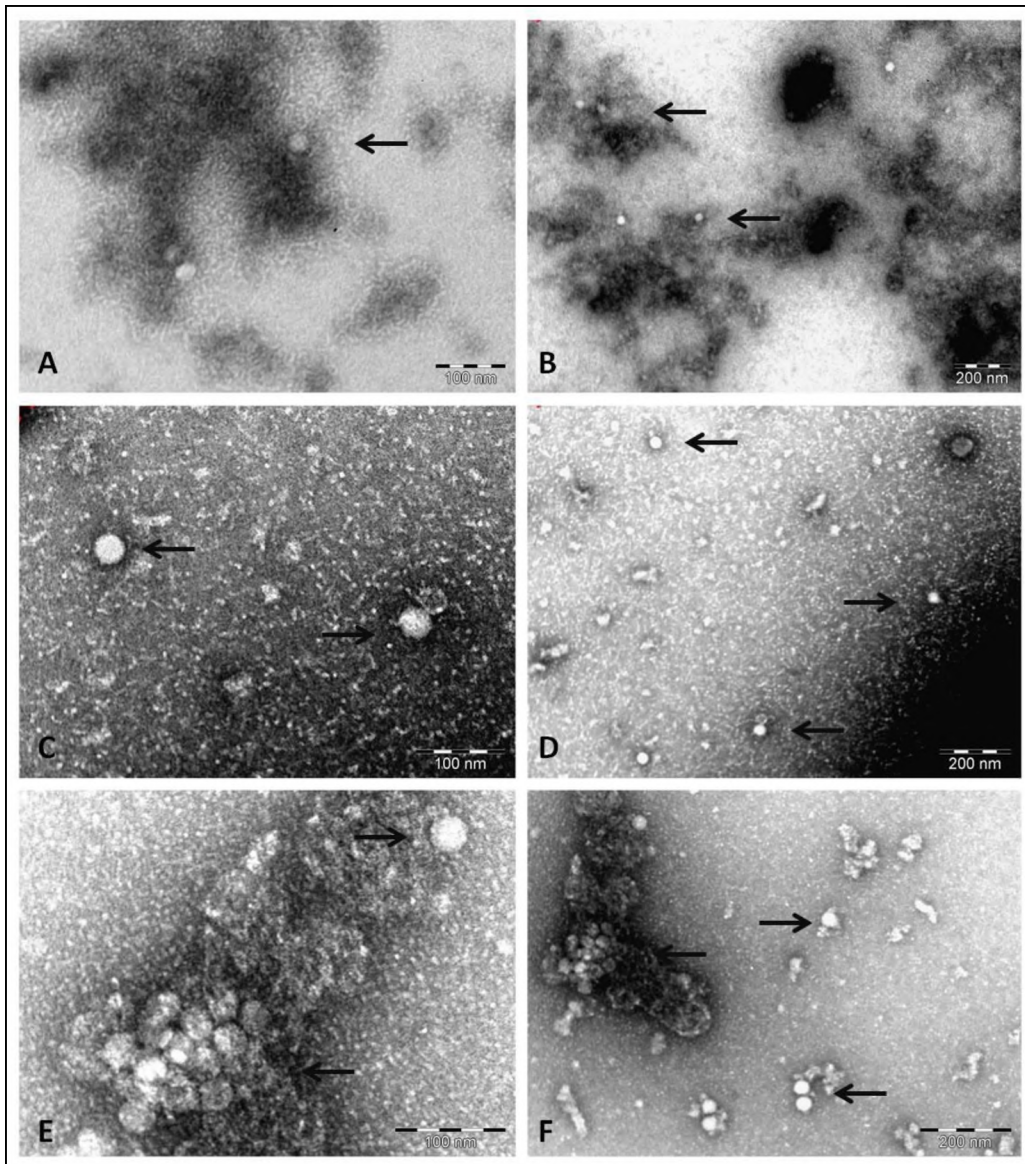


**Figure 2.3: TEM images of the TMEV samples before and after PEG precipitation. Panel A-B:** Transmission electron micrographs of the TMEV sample without PEG 6000. **Panel C-D:** Transmission electron micrographs of the TMEV sample treated with 8% PEG 6000 and 0.15 M NaCl. **Panel E-F:** Transmission electron micrographs of the TMEV sample treated with 8% PEG 6000 and 0.25 M NaCl. Arrows point towards single or clusters of viral particles.

### ***2.3.2 RNA Extraction from TMEV Particles***

The next objective was to extract RNA from the TMEV particles, treated with 8% PEG 6000 and 0.25 M NaCl. Figure 2.4 below shows the results of the RNA extraction. Two faint bands were observed at approximately 10 000 and 4000 bp (as indicated by the upper two arrows). The majority of the RNA was observed as a smear ranging between approximately 1200 – 500 bp in size (as indicated by the bottom-most arrow).

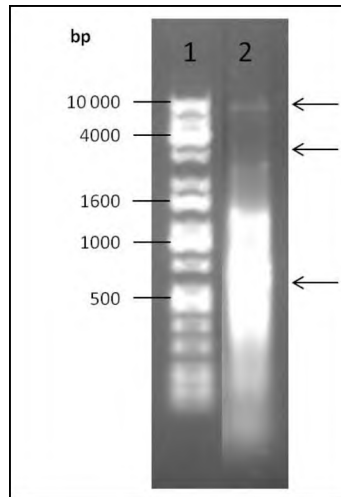


**Figure 2.4:** Agarose gel electrophoresis of the RNA extracted from the TMEV cell lysate. Lane 1: Kapa Universal marker; lane 2: TMEV infected cell lysate treated with 8% PEG 6000 in the presence of 0.25 M NaCl.

### 2.3.3 RT-PCR Assays for the Detection of TMEV 2B and VP1 Sequences

A protocol for the two-step RT-PCR assay involved the synthesis of first-strand cDNA from viral RNA followed by RT-PCR using TMEV GDVII-specific oligonucleotides. The results of the RT-PCR assay are shown in Figure 2.5 below.

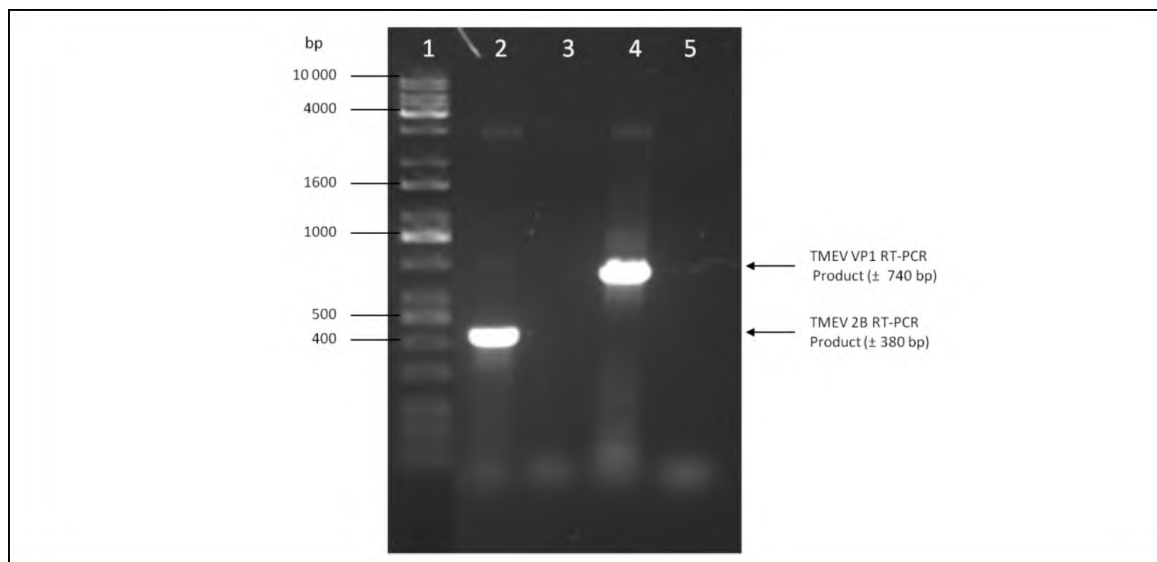


**Figure 2.5:** Agarose gel electrophoresis of the RT-PCR assays for TMEV 2B and VP1 performed on the RNA extracted from the TMEV sample treated with 8% PEG 6000 and 0.25M NaCl. Lane 1: Kapa Universal marker; lane 2: TMEV 2B RT-PCR; lane 3: TMEV 2B RT-PCR negative control; lane 4: TMEV VP1 RT-PCR; lane 5: TMEV VP1 RT-PCR negative control.

Figure 2.5 shows the results from the two-step RT-PCR assays for 2B and VP1 coding sequence performed on the RNA extracted from the TMEV virus particles. Lanes 3 and 5 show the results of the negative controls where the template was replaced with water. As expected, no bands were present. In lane 4 a single band was present at 828 bp which corresponds to the TMEV VP1 coding sequence. In lane 2 a single band 412 bp in size was present and corresponds to that of the TMEV 2B coding sequence.

### 2.3.4 *In Vitro* Transcription of RNA from pTMEV

This experiment aimed to perform an *in vitro* transcription of TMEV RNA from pTMEV. This was done to allow for the development of techniques using a known virus with high RNA concentrations. The RNA could also act as a positive control in future experiments. To achieve this pTMEV was linearised with *Bam* HI followed by *in vitro* transcription of RNA. The results are shown in Figure 2.6 below.

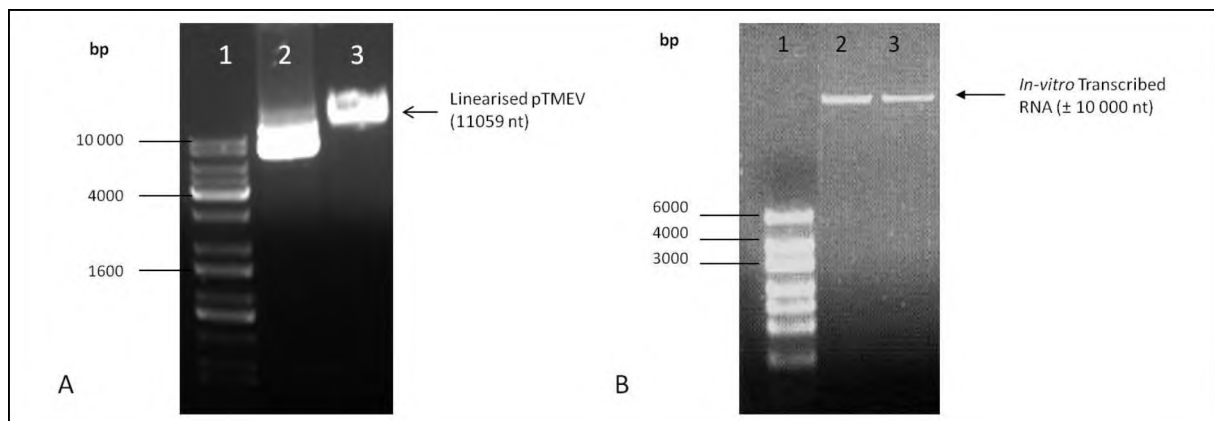


**Figure 2.6:** (A) Agarose gel electrophoresis of pTMEV before and after linearization with *Bam* HI. Lane 1: Kapa Universal Marker; lane 2: pTMEV before digestion with *Bam* HI; lane 3: pTMEV after digestion with *Bam* HI. (B) Agarose gel electrophoresis of the *in vitro* transcribed RNA from the linearised pTMEV. Lane 1: RNA marker; lane 2: TMEV *in vitro* transcribed RNA; lane 3: TMEV *in vitro* transcribed RNA treated with DNase I.

Figure 2.6 (A), lane 2 shows pTMEV, 11 059 bp in size, before linearising with *Bam* HI. Lane 3 shows a single band of 11 059 bp, indicating the complete digestion pTMEV with *Bam* HI. The linear plasmid was then used as a template for *in vitro* transcription [Figure 2.6 (B)]. A single band, approximately 10 000 bp in size, is present in lane 2. The RNA was then treated with DNase I and, once again, a single band approximately 10 000 bp in size was present in lane 3, although fainter than that in lane 2.

### 2.3.5 Development of a Two-Step RT-PCR Assay from *In Vitro* Transcribed RNA

The RT-PCR assay used to amplify TMEV 2B and VP1 sequences from first strand cDNA synthesised using *in vitro* transcribed RNA from linearised template is shown below in Figure 2.7.

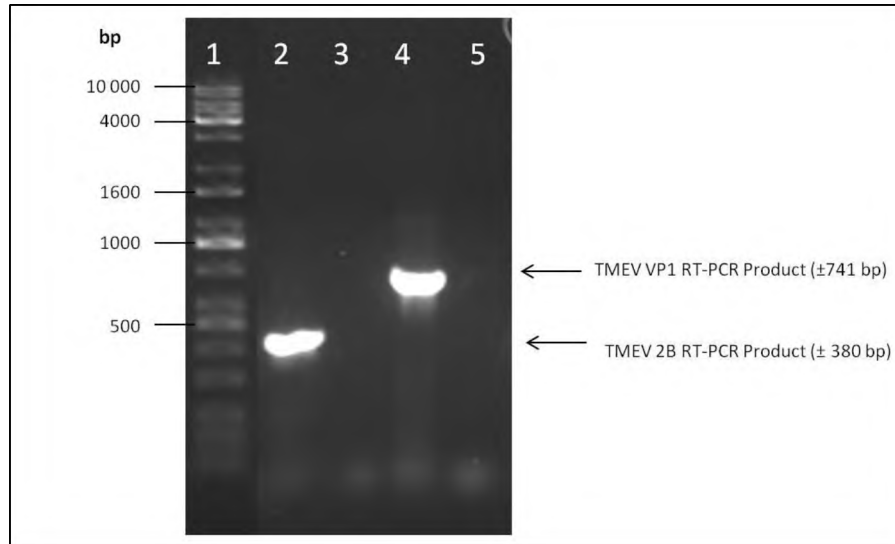


**Figure 2.7:** Agarose gel electrophoresis of the two-step RT-PCR assay for the TMEV 2B and VP1 coding sequences from the TMEV *in vitro* transcribed RNA. Lane 1: Kapa Universal marker; lane 2: TMEV 2B RT-PCR; lane 3: TMEV 2B RT-PCR negative control; lane 4: TMEV VP1 RT-PCR; lane 5: TMEV VP1 RT-PCR negative control.

In Figure 2.7, lane 2 shows a band 412 bp in size, which corresponds to the TMEV 2B coding sequence. Lane 4 also shows the presence of a band 828 bp in size for the TMEV VP1 coding sequence. Lanes 3 and 5 are negative controls where the template was replaced with water and no bands are observed.

### 2.3.6 Sensitivity of the Two-Step RT-PCR Assay

As virus particles (and therefore RNA) are expected to be present in low concentrations in the samples to be analysed, an assay was developed to determine the minimum amount of RNA necessary to yield RT-PCR products. This was achieved by dilution of the *in vitro* transcribed RNA and the two-step RT-PCR assay for TMEV 2B was performed. The results are shown in Figure 2.8 below.

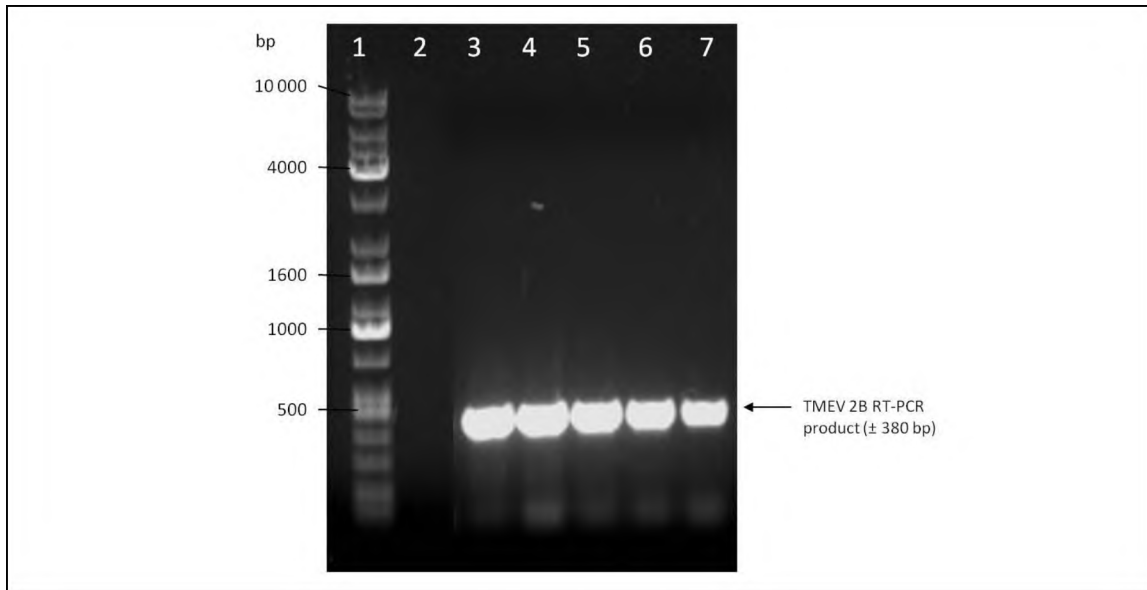


**Figure 2.8:** Agarose gel electrophoresis of the dilution series RT-PCR assay for TMEV 2B from the *in vitro* transcribed RNA. Lane 1: Kapa Universal marker; lane 2: negative control; lane 3: 607.9 ng/ $\mu$ l of TMEV RNA; lane 4: 131.8 ng/ $\mu$ l of TMEV RNA; lane 5: 26.7 ng/ $\mu$ l TMEV RNA; lane 6: 6 ng/ $\mu$ l TMEV RNA; lane 7: 2 ng/ $\mu$ l TMEV RNA.

Lane 2 in Figure 2.8 shows the results of the negative control for the two-step RT-PCR assay for the amplification of the TMEV 2B coding sequence. No bands were present in this lane (as expected) as the first-strand cDNA was replaced with water. A band of 412 bp in size and corresponding to the TMEV 2B coding sequence is observed in lanes 3-7. The band decreased in intensity as the RNA concentration decreased, and it was determined that an amount of 2 ng/ $\mu$ l of RNA was sufficient for detection.

## 2.4 Discussion

This chapter describes the use of TMEV as a model for the development of sample preparation techniques and the optimisation of RT-PCR assays to detect specific TMEV sequences.

Cell lysates were filter sterilised and concentrated by centrifugation. To confirm that the viruses were still present in the sample after initial preparation, TEM analysis was performed and particles similar in size and morphology to those previously published were observed (Lipton and Friedmann, 1980). The absence of bacteria and other large debris in the electron micrographs showed that the filter sterilisation technique was successful. Since the viruses were present in low concentrations, PEG 6000 precipitation was performed with 0.15 M and

0.25 M NaCl. Polyethylene glycol is widely used to precipitate viruses from a wide variety of samples, including stool samples, shellfish and wastewater. Lewis and Metcalf (1988) successfully used PEG precipitation for the concentration of pathogenic human viruses, namely hepatitis A virus, rotavirus and poliovirus, from environmental samples. This was achieved by treating the elution's from oysters, water and sediment samples with a final concentration of 8% (wt/vol) PEG 6000 and the effectiveness of the PEG precipitation was determined by the percent of virus recoveries achieved. These results were also compared to that of organic flocculation, a commonly-used method for virus recovery, and PEG precipitation was shown to have a higher recovery rate. A later study by Lewis *et al.* (2010) adapted this PEG precipitation method for the recovery of enteric viruses from oysters and muscles (Lewis *et al.*, 2010). In this study they compared the virus recovery rate of whole shellfish tissue and digestive tract tissue as well as the virus recovery rate of a second PEG precipitation step. The study found that the modifications to the method increased the effectiveness of PEG precipitation methods; however, the second PEG precipitation step had no effect on the virus recovery rate. In this study, PEG precipitation increased the number of virus particles present in the TEM micrographs with the highest number of particles seen in the TMEV infected cell lysate treated with 0.25 M NaCl.

RT-PCR assays are commonly used for the identification of specific RNA viruses in a wide variety of samples, including stool samples, infected shellfish and wastewater. Examples of studies which have utilised RT-PCR assays for the identification of SAFV and AiV include Drexler *et al.* (2011), Blinkova *et al.* (2009), Drexler *et al.* (2008) and Pham *et al.* (2007). Blinkova *et al.* (2009) and Drexler *et al.* (2008) used nested RT-PCR assays, where two sets of oligonucleotides were used to amplify the 2C (helicase) and VP1 sequences, respectively, for the identification of SAFV in clinical samples. Pham *et al.* (2007) also used a nested RT-PCR assay to identify AiV in clinical samples from Japan, Bangladesh, Thailand and Vietnam. Drexler *et al.* (2011) used a mixture of nested RT-PCR assays and real-time RT-PCR assays for the identification of AiV and the concentrations of shedding in northern Germany. Using RNA extracted from TMEV infected cell lysates and *in vitro* transcribed, a two-step RT-PCR assay protocol was successfully developed for the amplification of 2B and VP1 coding sequences of TMEV GDVII.

Because the viruses are expected to be in low concentration in the samples to be analysed it is important to estimate the minimum amount of RNA required for RT-PCR assays. The concentrations of RNA extracted from TMEV particles and produced *in vitro* were 262.6 ng/μl and approximately 3000 ng/μl respectively. To determine the minimum amount of RNA required to produce an RT-PCR product, RT-PCR assays for TMEV 2B were performed with varying amounts of extracted and *in vitro* RNA and the minimum amount of RNA determined to be as low as 25ng of viral RNA and 2 ng/μl of *in vitro* RNA.

In conclusion, sample preparation techniques were successfully developed using TMEV infected cell lysates. It was possible to amplify specific viral sequences in a two-step RT-PCR assay using RNA extracted from virus particles and produced *in vitro*. These techniques will be applied for the detection of viruses in stool samples, wastewater and oysters suspected to be infected with viruses samples as described in subsequent chapters. In Chapter 3 the construction of plasmids containing AiV, SAFV and NoV sequences for use as positive controls for RT-PCR assays is described along with the development of the relevant RT-PCR assays.

## ***Chapter 3: The Development of Positive Controls for the Detection of Norovirus GII, Aichi Virus and Saffold Virus Sequences in RT-PCR Assays***

### ***3.1 Introduction***

In order to validate RT-PCR assays for the detection of specific viruses in any given sample, positive controls consisting of partial genome sequences are required. In the case of positive strand RNA viruses cDNA representing target regions can be inserted into appropriate vectors. These controls are necessary to show that the oligonucleotides bind to the selected region of the genome producing an amplicon of the expected size. The use of positive controls in the assay will also confirm the presence or absence of viruses in the samples being analysed.

NoV is one of the leading causes of gastroenteritis worldwide and many studies have identified it in a variety of samples including wastewater, shellfish and clinical samples, through the use of RT-PCR assays (Mans *et al.* 2013; Mans *et al.* 2010; Kageyama *et al.*, 2003). Using both conventional and real-time RT-PCR assays NoV was detected in stool samples collected from 1997-2000 in Japan (Kojima *et al.*, 2002). Kojima *et al.* (2002) reported that NoV was present in stool samples using genogroup-specific primers, which allowed for the differentiation between GI and GII strains. Using RT-PCR assays with genotype-specific oligonucleotides, noroviruses have been detected in sewage-polluted river water and stool samples of hospitalised paediatric patients in South Africa (Mans *et al.*, 2013; Mans *et al.*, 2010). The positive identification of NoV in the wastewater, oysters and stool samples in this study will indicate that the sample preparation methods and the RT-PCR assays utilised are effective for the identification of viruses, and can thus be used for the identification of novel viruses, such as AiV and SAFV.

AiV was first isolated from stool samples of patients with oyster-associated non-bacterial gastroenteritis in Japan. Since 1991, AiV has been detected in many countries, including China, Pakistan, Germany, Brazil and Thailand, and is now considered an important human pathogen (Chuchaona *et al.*, 2016; Drexler *et al.*, 2011; Pham *et al.*, 2007; Oh *et al.*, 2006; Yamashita *et al.*, 1995). Two regions of the genome have been targeted for the detection of

AiV; the first is a 1008 bp region of the 5'UTR, the second is the 3CD junction. Both the 5'UTR and 3CD sequences were PCR amplified and ligated into pGEM®-T Easy for *in vitro* transcription. *In vitro* RNA can be used as a positive control for the development of RT-PCR assays of the 5'UTR and 3CD regions. These RT-PCR assays will be used for the identification AiV in the wastewater, oysters and stool samples. The development of these RT-PCR assays may assist in the identification of AiV in South Africa, as it has not been identified here as of yet.

SAFV is a novel picornavirus that was first identified in 2007 in a stool sample collected from a patient with a fever of unknown origin (Jones *et al.*, 2007). Since then, several strains have been characterised, and the full genome sequence of SAFV-3 has been obtained (Zoll *et al.*, 2009). Drexler *et al.* (2008) reported three lineages of SAFV using RT-PCR from three cohorts of stool samples collected in Germany and Brazil. A study performed by Blinkova *et al.* (2009) detected SAFV by RT-PCR from clinical samples collected from children in Pakistan and Afghanistan from 2006-2008. Although SAFV has been identified and characterised in many countries around the world, there are no reports of SAFV in South Africa.

The overall aim of this chapter was to create a set of positive controls for use in RT-PCR assays for the detection of NoV, AiV and SAFV. To develop the positive control for NoV detection, viral RNA was extracted from a NoV positive stool sample and amplified by RT-PCR and cloned into pGEM®-T Easy. The approach for AiV positive control required amplification of the 5'UTR and 3CD sequences from AiV cDNA, followed by cloning into pGEM®-T Easy. The full length cDNA of SAFV cloned into pSP72+ was used directly for *in vitro* transcription.

The specific objectives of this chapter were as follows:

- Extract RNA from NoV particles and amplify the GII N/S domain sequence for cloning into pGEM®-T Easy and *in vitro* transcription of RNA.
- Amplification of the AiV 5'UTR and AiV 3CD regions for cloning into pGEM®-T Easy and *in vitro* transcription of RNA.

- *In vitro* transcription of SAFV RNA.
- Development of two-step RT-PCR assays for the amplification of specific viral sequences using *in vitro* transcribed RNA and determining the sensitivity of the RT-PCR assays.

## **3.2 Materials and Methods**

### **3.2.1 Norovirus**

#### **3.2.1.1 Viral RNA Extraction**

A NoV GII positive stool sample was kindly provided by Maureen Taylor (University of Pretoria, South Africa). Viral RNA was extracted from the NoV GII positive stool sample using the QIAamp® Viral RNA Mini Kit (Qiagen, USA), according to manufacturer's instructions as described in Chapter 2, section 2.2.5. The extracted RNA was stored at -80°C until required. The RNA was analysed by 1% agarose gel electrophoresis and the concentration was estimated using a Nanodrop 2000 Spectrophotometer (ThermoScientific, USA).

#### **3.2.1.2 Development of a Two-Step RT-PCR Assay for the Amplification of the N/S Domain of the VP1 Sequence**

To develop a two-step RT-PCR assay for NoV, first-strand cDNA was synthesised using approximately 500 ng of viral RNA using the RevertAid™ Premium first-strand cDNA synthesis kit (Fermentas, USA) according to the manufacturer's protocol as described in Chapter 2, section 2.2.6. Forward and reverse oligonucleotides for the coding region for the N/S domain of the VP1 for NoV GII, described by Kojima *et al.* (2002), were used in the RT-PCR assay. Figure 3.1 below, shows a schematic diagram of the NoV GII genome with the oligonucleotide binding sites indicated by arrows, while the oligonucleotide sequence and binding site are described in Table 3.1 below.

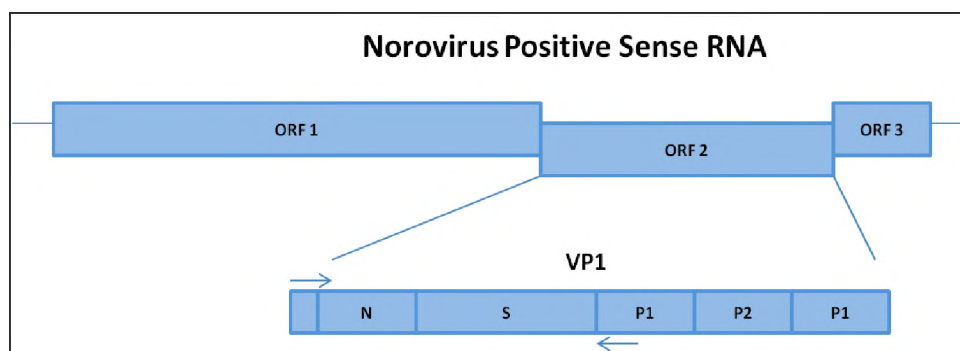


**Figure 3.1:** A schematic diagram of the forward (→) and reverse (←) primer binding sites for the NoV GII VP1 N/S domain coding region.

**Table: 3.1:** The Forward and Reverse Oligonucleotides for the NoV GII VP1 N/S Domain Coding Region as Described by Kojima *et al.* (2002).

Primer	Nucleotide Sequence	Binding Site	Size
N/S GII F	5'-CNTGGGAGGGCGATCGCAA-3'	5046 – 5064 bp	342 nt
N/S GII R	5'-CCRCCNGCATRHCCRTTRTACAT-3'	5366 – 5388 bp	

A nested RT-PCR assay was performed to amplify the VP1 N/S domain coding sequence, using the MJ Mini™ Personal Thermal Cycler (Bio-Rad, USA) as follows: 1x ready mix with Mg<sup>2+</sup> (KAPA Biosystems, USA), 0.4 μM of the forward and reverse oligonucleotides, ~4 ng/μl final concentration first-strand cDNA template and 9.5 μl ddH<sub>2</sub>O. A negative control reaction was set up in the same manner except that ddH<sub>2</sub>O was used instead of the first-strand cDNA template. The cycling parameters used for the first round RT-PCR reaction were as follows: 95°C for 1 min 30s, 35 cycles of 95°C for 30s, 55°C for 45s, 72°C for 1 min and a final elongation of 72°C for 5 min.

The second round of PCR amplification was performed as follows: 1x ready mix with Mg<sup>2+</sup> (KAPA Biosystems, USA), 0.4 μM of the forward and reverse oligonucleotides, 5 μl first round RT-PCR product and 9.5 μl ddH<sub>2</sub>O. A negative control reaction was set up in the same manner except that ddH<sub>2</sub>O was used instead of the first round RT-PCR product. The 2nd round RT-PCR assay used the same cycling parameters as described for the first round RT-PCR assay. The nested RT-PCR products were analysed by 1% agarose gel electrophoresis.

### **3.2.1.3 Cloning and Sequencing of the RT-PCR Product**

The growth media used in this study were Luria Bertani broth (LB: 0.5% NaCl, 0.5% yeast extract and 1% tryptone powder) and Luria Bertani agar (LA: 0.5% NaCl, 0.5% yeast extract, 1% tryptone powder and 3% bacteriological agar). Bacterial cultures were grown in LB or LA supplemented with ampicillin (Amp, final concentration 100 µg/ml).

The VP1 N/S domain coding sequence (342 bp) amplicon was ligated into pGEM®-T Easy (Promega, USA) as follows: 0.3 U/µl T4 DNA ligase, 0.2x rapid ligation buffer, ~100 ng/µl final concentration DNA, ~5 ng/µl pGEM®-T Easy and 5 µl ddH<sub>2</sub>O; total volume 10 µl. Ligation was carried out overnight at 4°C to create pNoVGII. The ligation was transformed into competent DH5α *E. coli* cells (Lucigen® Corporation, USA), according to the manufacturer's protocol. Briefly: 5µl of the ligation reaction was added to 40 µl *E. coli* cells, the cells were incubated on ice for 30 minutes. The cells were heat shocked at 42 °C for 45s then returned to ice for 2 min, 960 µl of LB was added to the cells and the cells were incubated at 37 °C for 1 hour with shaking at 250 rpm, 100 µl of the transformed cells were grown overnight on LA/Amp plates supplemented with IPTG (final concentration 0.5µM) and X-gal (final concentration 80 µg/ml) allowing for blue/white screening. Six white colonies were incubated overnight at 37°C in 5 ml LB/Amp. The plasmids were extracted using the Zippy plasmid miniprep kit (ZymoResearch, USA) according to the manufacturer's protocol and analysed by 1% agarose gel electrophoresis. To confirm the presence of inserts, plasmids were digested with *Eco* RI as follows: the reaction was set up using ~70 ng/µl final concentration of plasmid DNA, 1x reaction buffer, 0.3 U/µl *Eco* RI restriction enzyme and sterile ddH<sub>2</sub>O to 15 µl. The reaction was incubated at 37°C for 30 min and analysed by 1% agarose gel electrophoresis. One plasmid named pNoVGII, containing an insert of the 342 bp, was sent to Inqaba Biotechnical Industries (Pty) Ltd for sequencing. The sequence was analysed using NCBI BLAST

([Blast.ncbi.nlm.nih.gov/Blast.cgi](http://Blast.ncbi.nlm.nih.gov/Blast.cgi)).

### **3.2.1.4 In Vitro Transcription of RNA from pNoVGII**

pNoVGII was linearised by digestion with the restriction enzyme *Pst* I as follows: the reaction was set up using ~70 ng/µl final concentration of plasmid DNA, 1x reaction buffer,

0.3 U/ $\mu$ l *Pst* I restriction enzyme and sterile ddH<sub>2</sub>O to 15  $\mu$ l. The reaction was incubated at 37°C for 30 min and analysed by 1% agarose gel electrophoresis.

The linear plasmid was cleaned using the Wizard® SV gel and PCR clean-up system as described in Chapter 2, section 2.2.7 and RNA was transcribed from the linearised plasmid using the TranscriptAid™ T7 High Yield Transcription kit, treated with DNase I and analysed by 1% agarose gel electrophoresis as described in Chapter 2, section 2.2.7. First-strand cDNA was synthesised using *in vitro* transcribed RNA using the RevertAid™ Premium first-strand cDNA synthesis kit (Fermentas, USA) as per the manufacturer's protocol as described in Chapter 2, section 2.2.6. RT-PCR assay was performed for the coding sequence of NoV GII VP1 N/S domain as described in Chapter 3, section 3.2.1.2 above, however, ~2 ng/ $\mu$ l of pNoVGII was used as a positive control for the RT-PCR assay and the RT-PCR assay was analysed by 1% agarose gel electrophoresis

### ***3.2.1.5 Sensitivity of the Norovirus GII RT-PCR Assay***

Five-fold, serial dilutions of the *in vitro* transcribed RNA were prepared and the RNA concentrations were estimated as described in Chapter 2, section 2.2.5. First-strand cDNA was synthesised using 1  $\mu$ l of RNA (with the following concentrations: 481.2 ng/ $\mu$ l, 98.9 ng/ $\mu$ l, 19.7 ng/ $\mu$ l, 3.4 ng/ $\mu$ l and 0.9 ng/ $\mu$ l) using the RevertAid™ Premium first-strand cDNA synthesis kit (Fermentas, USA) as per the manufacturer's protocol as described in Chapter 2, section 2.2.6. RT-PCR assays were performed for the amplification of the coding sequences of NoV GII VP1 N/S domain as described in Chapter 3, section 3.2.1.2 above and ~2 ng/ $\mu$ l of pNoVGII was used as a positive control. The RT-PCR assay was analysed by 1% agarose gel electrophoresis.

## ***3.2.2 Aichi Virus***

### ***3.2.2.1 PCR Assays for the 5'UTR and 3CD Coding Sequence***

Jan F. Drexler (University of Bonn Medical Centre, Germany) kindly provided a plasmid which contained a 1008 bp nucleotide sequence of the 5'UTR region of AiV. The 5'UTR coding sequence insert was amplified using the primer set described by Drexler *et al.* (2011). Figure 3.2 shows a schematic diagram of the AiV genome and the binding sites of the

forward and reverse oligonucleotides are indicated by arrows. The sequences and binding sites are shown in Table 3.2 below.

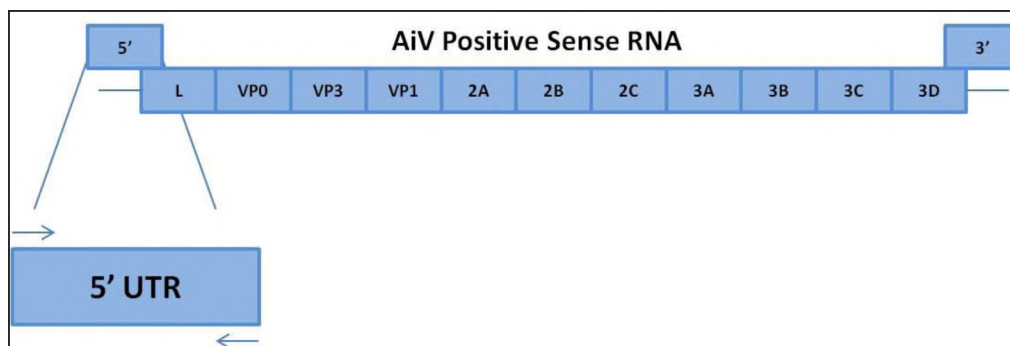


**Figure 3.2:** Schematic diagram of the forward (→) and reverse (←) primer binding sites for 5'UTR.

**Table 3.2:** Forward and Reverse Oligonucleotides for AiV 5'UTR as Described by Drexler *et al.* (2011).

Primer	Nucleotide Sequence	Binding Site	Size
5'UTR-F	5'- GTTACTCCATTCAGCTTCTTCGGAAC -3'	69 – 94 bp	1008
5'UTR-R	5'- CAGGATTGGACATCAGAATCATAGAG -3'	1039 – 1064 bp	bp

The PCR reaction for the AiV 5'UTR coding sequence was carried out as follows: 1x ready mix with  $Mg^{2+}$  (KAPA Biosystems, USA),  $0.4\mu M$  of the forward and reverse oligonucleotides,  $\sim 2$  ng/ $\mu l$  of the 5'UTR plasmid and  $9.5 \mu l$  ddH<sub>2</sub>O. Negative control reactions were set up in the same manner except ddH<sub>2</sub>O was used instead of the 5'UTR plasmid. The cycling parameters were as follows:  $95^{\circ}C$  for 1 min 30s, 35 cycles of  $95^{\circ}C$  for 30s,  $55^{\circ}C$  for 45s,  $72^{\circ}C$  for 1 min and a final elongation of  $72^{\circ}C$  for 5 min. This was performed using the MJ Mini™ Personal Thermal Cycler (Bio-Rad, USA) and analysis of the amplicon was performed using 1% agarose gel electrophoresis.

For the development of the two-step RT-PCR assay for the AiV partial 3CD coding sequence, a 266 bp PCR amplicon of the coding sequence of the partial 3CD region for AiV was kindly provided by Hiroshi Ushijima (University of Tokyo, Japan). The coding sequence

for the partial 3CD amplicon was amplified using the primer set described by Pham *et al.* (2007). Figure 3.3 is a schematic diagram of the AiV genome and the binding site of the oligonucleotides are indicated by arrows. The sequence and binding sites are described in Table 3.3 below.

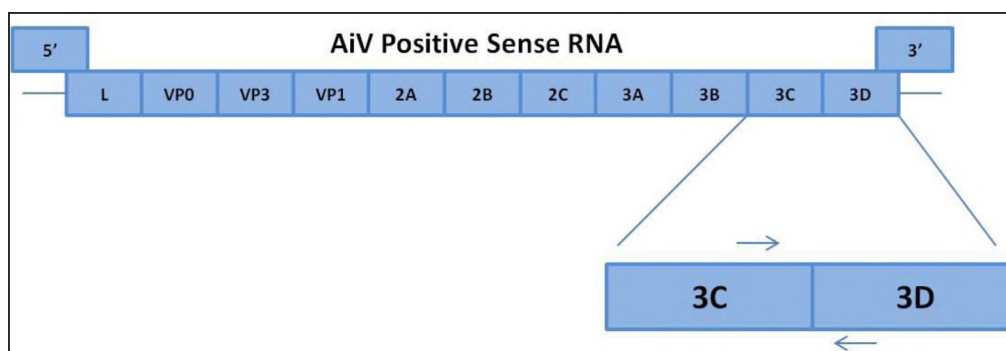


**Figure 3.3:** Schematic diagram of the forward (→) and reverse (←) primer binding sites for 3CD.

**Table 3.3:** Forward and Reverse Oligonucleotides for AiV Partial 3CD Coding Sequence Described by Pham *et al.* (2007).

Primer	Nucleotide Sequence	Binding Site	Size
3CD-F	5'- GACTTCCCCGGAGTCGTCGTCT -3'	6426 – 6448 bp	266 bp
3CD-R	5'- GACATCCGGTTCGACGTTGAC -3'	6672 – 6692 bp	

The PCR reaction for the partial 3CD coding sequence was carried out as follows: 1x ready mix with  $Mg^{2+}$  (KAPA Biosystems, USA), 0.4  $\mu M$  of the forward and reverse oligonucleotides,  $\sim 2ng/\mu l$  of the 3CD PCR product and 9.5  $\mu l$  ddH<sub>2</sub>O. Negative control reactions were set up in the same manner except ddH<sub>2</sub>O was used instead of the 3CD PCR product. The cycling parameters used were as follows: 95°C for 1 min 30s, 35 cycles of 95°C for 30s, 55°C for 45s, 72°C for 1 min and a final elongation of 72°C for 5 min. This was performed using the MJ Mini™ Personal Thermal Cycler (Bio-Rad, USA) and analysis of the amplicon was performed using 1% agarose gel electrophoresis.

### ***3.2.2.2 Cloning of the Aichi Virus 5'UTR and 3CD PCR Products***

The AiV 5' UTR (1008 nt) and 3CD (266 nt) amplicons were ligated into pGEM®-T Easy as per the manufacturer's protocol, as described in Chapter 3, section 3.2.1.2 above. The Zippy plasmid miniprep kit (ZymoResearch, USA) was used to extract the plasmids which were analysed by 1% agarose gel electrophoresis. The plasmids were digested with *Eco* RI, as described above in Chapter 3, section 3.2.1.3 above, and analysed by 1% agarose gel electrophoresis. One plasmid containing each insert was sent to Inqaba Biotechnical Industries (Pty) Ltd for sequencing. The sequences were analysed using NCBI BLAST ([Blast.ncbi.nlm.nih.gov/Blast.cgi](http://Blast.ncbi.nlm.nih.gov/Blast.cgi)).

### ***3.2.2.3 In Vitro Transcription of RNA from pAiV5'UTR and pAiV3CD***

pAiV3CD was linearised by digestion with *Pst* I, as per the manufacturer's protocol, described in Chapter 3, section 3.2.1.4, and analysed by 1% agarose gel electrophoresis. The linear plasmid was cleaned using the Wizard® SV gel and PCR clean-up system (Promega, USA) as described in Chapter 2, section 2.2.7. RNA was transcribed from the cleaned pAiV3CD and the uncut pAiV5'UTR in an *in vitro* transcription reaction using RevertAid™ T7- *in vitro* RNA Transcriptase kit (Fermentas, USA), according to the manufacturer's protocol, as described in Chapter 2, section 2.2.7. The *in vitro* transcribed RNA for AiV 5'UTR and partial 3CD was treated with DNase I and was analysed using 1% agarose gel electrophoresis.

### ***3.2.2.4 Two-Step RT-PCR Assay from the Aichi Virus 5'UTR and 3CD In Vitro Transcribed RNA***

First-strand cDNA was synthesised using *in vitro* transcribed RNA from pAiV5'UTR and pAiV3CD using the RevertAid™ Premium first-strand cDNA synthesis kit (Fermentas, USA), as described in Chapter 2, section 2.2.8. RT-PCR assays were performed for the coding sequences of AiV 5'UTR and partial 3CD, using the oligonucleotides described in Tables 3.2 and 3.3, respectively, and the protocols as described in Chapter 3, section 3.2.2.1 above. The RT-PCR reactions were analysed by 1% agarose gel electrophoresis.

### 3.2.2.5 Sensitivity of the Two-Step RT-PCR Assays for the Aichi Virus 5'UTR and 3CD Coding Region

Five-fold, serial dilutions of the AiV 5'UTR and 3CD *in vitro* transcribed RNA were made and the concentrations of each dilution were measured. First-strand cDNA was synthesised using 1 µl of RNA (with the following concentrations: 5'UTR: 452.7 ng/µl, 102.5 ng/µl, 24.7 ng/µl, 3.5 ng/µl and 0.7 ng/µl; 3CD 429.6 ng/µl, 97.2 ng/µl, 13.8 ng/µl, 0.2 ng/µl and 0 > ng/µl) for each of the dilution using the RevertAid™ Premium first-strand cDNA synthesis kit (Fermentas, USA) as per the manufacturer's protocol. RT-PCR assays were then performed for the amplification of the coding sequences of AiV 5'UTR and partial 3CD as described in Chapter 3, section 3.2.2.1, and analysed by 1% agarose gel electrophoresis

## 3.2.3 Saffold Virus

### 3.2.3.1 pSAFV

Figure 3.4 shows a schematic diagram of the pSAFV plasmid kindly provided by Christian Drosten (University of Bonn Medical Centre, Germany). The pSP72+ vector contains both the SP6 and T7 RNA polymerase promoter sites for RNA transcription, the  $\beta$ -lactamase coding region for ampicillin resistance (allowing for selection of the plasmid), and a multiple cloning site which includes *Xho I*, which allows for the linearisation of pSAFV for *in vitro* transcription of RNA of the full length SAFV genome that is inserted in this plasmid (Promega, 2006).

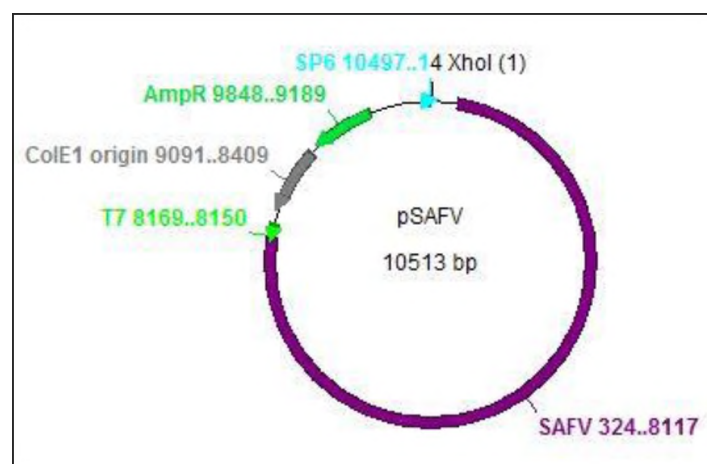


**Figure 3.4: Schematic diagram of the plasmid map of pSAFV.** pSAFV contains an Amp resistance gene (Amp<sup>r</sup>), the T7 and SP6 promoters, a multiple cloning site which includes the restriction site for *Xho I* and the full length genome of SAFV.

### 3.2.3.2 *In Vitro* Transcription of RNA from pSAFV

pSAFV was linearised by digestion with *Xho* I as follows: the reaction was set up using ~70 ng/μl of plasmid DNA, 1x buffer, 0.3 U/μl *Xho* I restriction enzyme and sterile ddH<sub>2</sub>O to 15 μl. The reaction was incubated at 37°C for 30 min and the digested plasmid was analysed by 1% agarose gel electrophoresis. The linear plasmid was cleaned using the Wizard® SV gel and PCR clean-up system (Promega, USA) and RNA was transcribed from the linearised plasmid using the RevertAid T7- *in vitro* RNA Transcriptase kit (Fermentas, USA) as per the manufacturer's protocol. The RNA was treated with DNase I as described in Chapter 2, section 2.2.7 and was analysed using 1% agarose gel electrophoresis.

### 3.2.3.3 Developing a Two-Step RT-PCR Assay for the Detection of Saffold Virus 2C Coding Region

First-strand cDNA was synthesised from the *in vitro* transcribed RNA using the RevertAid™ Premium first-strand cDNA synthesis kit (Fermentas, USA) according to the manufacturer's protocol. Forward and reverse oligonucleotides were designed to amplify the full length coding sequence of SAFV 2C (975 nt) and an internal region of the SAFV 2C coding sequence (540 nt). The 2C sequence was chosen as the target region for RT-PCR assays as it is highly conserved within the picornavirus family. This may allow for an increase in the detection of all SAFV genotypes. Figure 3.5 below shows a schematic diagram of SAFV genome with the binding sites of the oligonucleotides indicated by arrows. Table 3.4 below describes the sequences and binding sites for the full length and partial 2C oligonucleotides.

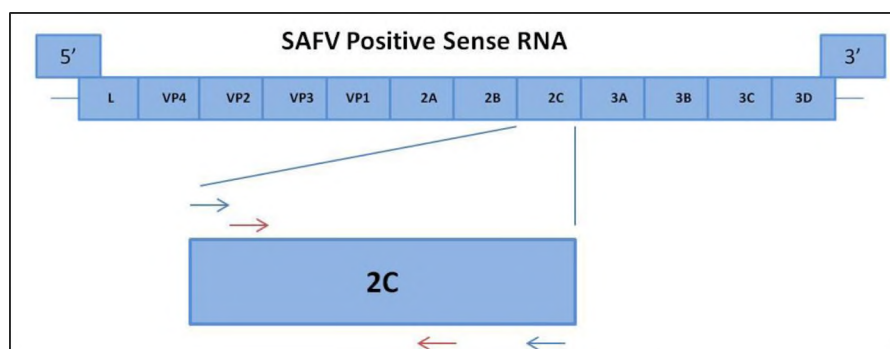


**Figure 3.5: Schematic diagram of the forward and reverse primer binding site for SAFV 2C.** The Blue arrows indicate the forward (→) and reverse (←) primers for the full 2C RT-PCR product. The red arrows indicate the forward (→) and reverse (←) primers for the internal 2C RT-PCR product.

**Table 3.4: Forward and Reverse Oligonucleotide Sequences for SAFV Full Length 2C and Internal Region of 2C.**

Primer	Nucleotide Sequence	Binding Site	Size
<b>2C-F</b>	5'- AAAGGATCCTCTCCTATTAGAGAAG -3'	4600 - 4616 bp	975 bp
<b>2C-R</b>	5'- AAAGTCGACTTGAGCGACTAATGTGTTC -3'	5565 - 5575 bp	
<b>2CI- F</b>	5'- AAAGGATCCACTTCATGGTTCAAA -3'	4690 – 4706 bp	540 bp
<b>2CI- R</b>	5'- AAAGTCGACGTTAGAAGTGAAG -3'	5217 - 5230 bp	

RT-PCR assays were then performed to amplify the SAFV full and partial 2C coding sequences as follows: 1x ready mix with Mg<sup>2+</sup> (KAPA Biosystems, USA), 0.4 µM final concentration of the forward and reverse oligonucleotides, 4 ng/µl first-strand cDNA template and 9.5 µl ddH<sub>2</sub>O. Negative control reactions were set up in the same manner except ddH<sub>2</sub>O was used instead of the first-strand cDNA template. The cycling parameters used for the RT-PCR reactions were as follows: 95°C for 1 min 30s, 30 cycles of 95°C for 30s, 55°C for 45s, 72°C for 2 min and a final elongation of 72°C for 5 min. The RT-PCR products were analysed by 1% agarose gel electrophoresis.

#### **3.2.3.4 Sensitivity of the Saffold Virus 2C RT-PCR Assay**

Five-fold, serial dilutions were prepared using the SAFV *in vitro* transcribed RNA and the concentrations were estimated. First-strand cDNA was synthesised using 1 µl of RNA (with the following concentrations: 556.9 ng/µl, 115.3 ng/µl, 23.5 ng/µl, 4.8 ng/µl and 1 ng/µl) the RevertAid Premium first-strand cDNA synthesis kit (Fermentas, USA) as described in Chapter 2, section 2.2.6. RT-PCR assays were then performed for the amplification of the coding sequences of SAFV full length 2C as described in Chapter 3, section 3.2.4.2 and analysed by 1% agarose gel electrophoresis.

#### **3.2.4 Plasmids**

Table 3.5 provides a summary of the plasmids synthesised in this chapter, including the vector, insert size and product, and the reference from where the insert was obtained.

**Table 3.5: The Vector, Insert Size, Insert Product and Reference of the Plasmids used to Synthesis *In Vitro* Transcribed RNA.**

Plasmid	Vector	Insert Size	Insert Product	Reference
pNoVGII	pGEM®-T Easy	342 nt	Partial VP1 N/S Domain region	Kojima <i>et al.</i> (2002)
pAiV5'UTR	pGEM®-T Easy	1008 nt	5' UTR region	Drexler <i>et al.</i> (2011)
pAiV3CD	pGEM®-T Easy	266 nt	Partial 3CD region	Pham <i>et al.</i> (2007)
pSAFV	pSP72+	9000 nt	Full Genome	Drexler <i>et al.</i> (2008)

### 3.3 Results

#### 3.3.1 Norovirus

##### 3.3.1.1 The Development of a Two-Step RT-PCR Assay for the Detection of NoV GII

Using the RNA extracted from the NoV GII positive stool sample, a nested two-step RT-PCR was developed for the detection of NoV GII. The first step was the synthesis of first-strand cDNA from the NoV GII RNA, followed by the amplification of the NoV GII VP1 N/S domain coding sequence. The first-strand cDNA was used as a template for the first round of the nested RT-PCR. The second round RT-PCR was performed using the first round RT-PCR product as a template. The results for the first and the second round of the nested RT-PCR assay are shown in Figure 3.6 below.

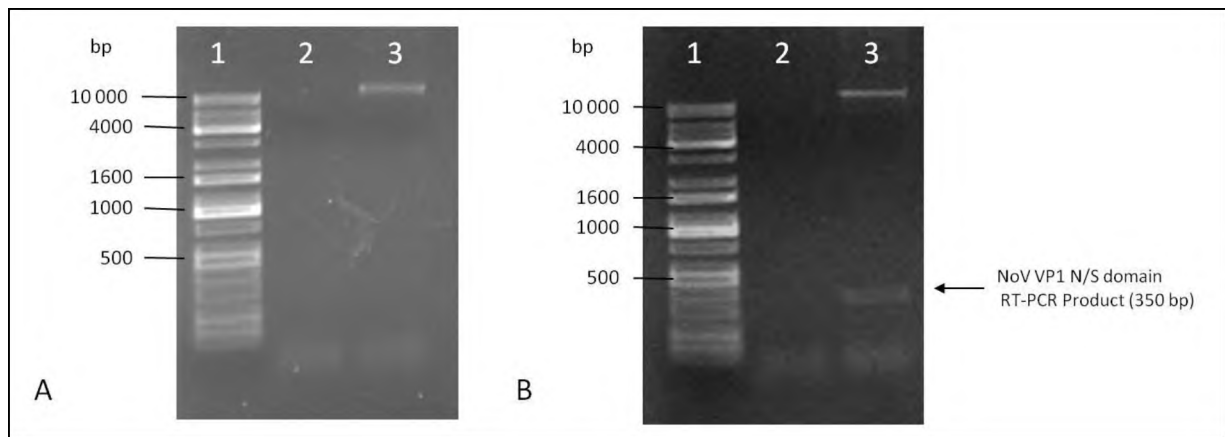
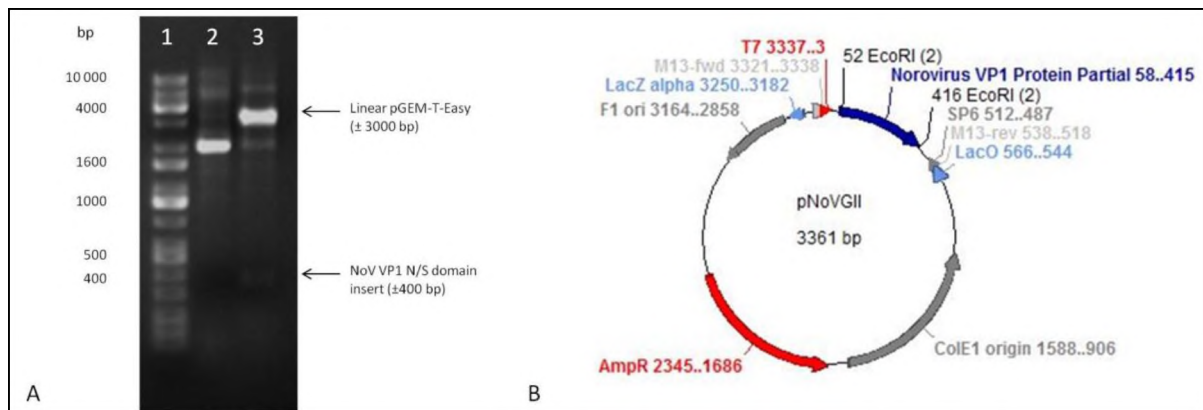


**Figure 3.6: (A) Agarose gel electrophoresis of the first round of the RT-PCR assay performed on the NoV GII RNA. Lane 1: Kapa Universal marker; lane 2: negative control; lane 3: NoV GII positive stool sample. (B) Agarose gel electrophoresis of the second round of the RT-PCR assay performed on the NoV GII RNA. Lane 1: Kapa Universal marker; lane 2: negative control; lane 3: NoV GII positive stool sample.**

Figure 3.6 shows the results from the nested two-step RT-PCR assay performed on the RNA extracted from the NoV GII positive stool sample. No bands were present in lane 2, figure 3.6 (A) [as expected] as water was used as the template rather than the first-strand cDNA. In lane 3, the first round of the RT-PCR assay showed only one band of approximately 10 000 bp in size. No band corresponding to the NoV GII VP1 N/S domain coding region was amplified in this reaction. Figure 3.6 (B), lane 3 shows the second round of the RT-PCR assay and two bands can be seen. The first is the 10 000 bp band seen in the first round of the RT-PCR assay and the second band is 342 bp which corresponds to the NoV GII VP1 N/S domain coding region amplified in this reaction. Lane 2 shows the results of the negative control from the second round of the RT-PCR assay and once again no bands were present as expected. The RT-PCR product was cloned into pGEM®-T Easy.

### ***3.3.1.2 Cloning of the PCR Amplicon from NoV GII into pGEM®-T Easy***

The NoV GII RT-PCR product was cloned into pGEM®-T Easy and the integrity of the plasmid was determined by the digestion of pNoVGII with *Eco* RI and sequencing using the T7 primer. The results of the digestion and the plasmid map are shown in Figure 3.7 below. In Appendix II, the nucleotide sequence of the NoV GII RT-PCR product insert in pNoVGII is shown in Figure 5S and the multiple alignment of pNoVGII to the reference strain of NoV GII (Accession no. HQ008055.1) published by published by Mans *et al.* (2010) is shown in Figure 19S (Appendix II).



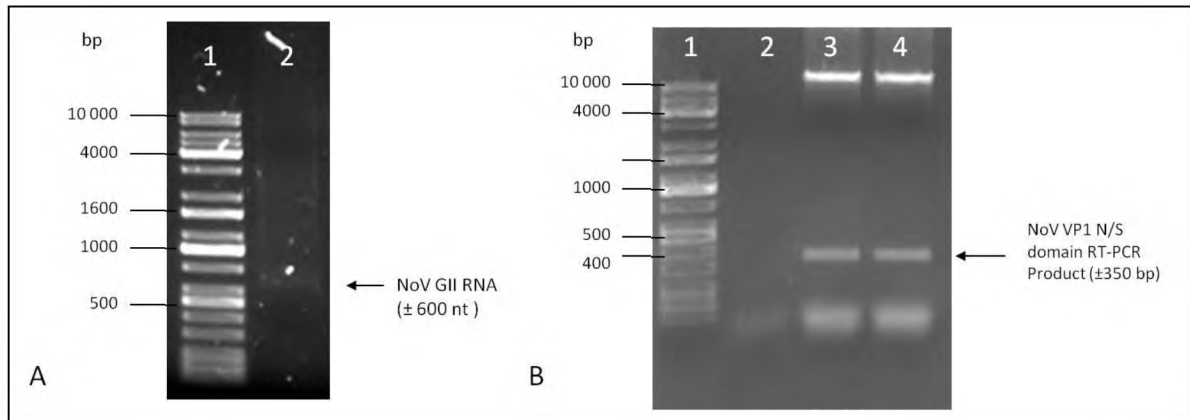
**Figure 3.7: (A) Agarose gel electrophoresis of pNoVGII before and after digestion with the restriction enzyme *Eco RI*. Lane 1: Kapa Universal marker; lane 2: Undigested plasmid; lane 3: plasmid digested with the restriction enzyme *Eco RI*. (B) A schematic diagram of the plasmid map of pNoVGII.**

Figure 3.7 (A) shows that when the pNoVGII was digested with *Eco RI*, in lane 3, a band was present at 3000 bp and at approximately 342 bp, these correspond to those of the linear pGEM®-T-Easy vector (3015 bp) and the NoV GII insert (342 bp). Figure 3.7 (B) shows a plasmid map for pNoVGII, which is 3361 bp in size. The pGEM®-T Easy vector is a linear vector 3015 bp in size with a single thymidine at the 3' on each end, these T-overhangs allow for easy insertion of PCR products amplified using a polymerase which created 5' A-overhangs. This vector contains both the T7 and SP6 RNA polymerase promoters which flank the multiple cloning site. For selection purposes, an ampicillin resistance gene is present, and to screen for plasmids containing the insert, the plasmid contains the  $\alpha$ -peptide coding region of the enzyme  $\beta$ -galactosidase in which the multiple cloning site is found. The  $\alpha$ -peptide is inactivated on insertion of a DNA fragment allowing for Blue/White screening (Promega, 2010). *E. coli* DH5 $\alpha$  cells are used for cloning as they support the Blue/ White screening, as they contain the *lacZ* $\Delta$ M15 gene.

Sanger sequencing of the NoV GII N/S domain insert from pNoVGII showed the correct insertion of the NoV GII RT-PCR product into pGEM®-T Easy (Figure 5S, Appendix II) and BLAST analysis of the sequence showed it to be 99 % identical to the NoV sequence (Accession no. HQ008055.1) published by Mans *et al.* (2010) (Figure 19S, Appendix II).

### 3.3.1.3 *In Vitro* Transcription of NoV GII RNA from pNoVGII and RT-PCR Assay

pNoVGII was linearised with *Pst* I and *in vitro* RNA transcription was performed. First-strand cDNA was synthesised and the first round of the RT-PCR assay for the NoV GII VP1 N/S domain coding region was performed. The results for the *in vitro* transcription of NoV GII RNA and the RT-PCR assay are shown in Figure 3.8 below.



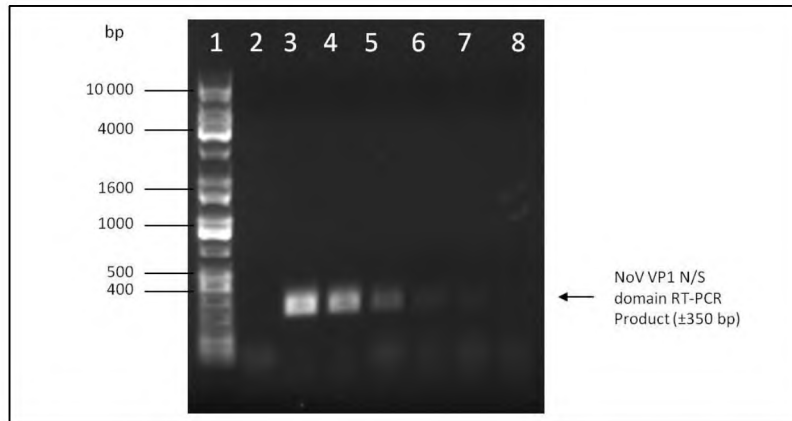
**Figure 3.8:** (A) Agarose gel electrophoresis of the *in vitro* transcribed RNA from pNoVGII. Lane 1: Kapa Universal marker; lane 2: NoV GII *in vitro* transcribed RNA. (B) Agarose gel electrophoresis of the RT-PCR assay from the NoV GII *in vitro* transcribed RNA. Lane 1: Kapa Universal marker; lane 2: negative control; lane 3: positive control; lane 4: *in vitro* transcribed RNA.

Figure 3.8 (A), lane 2 shows a band 600 bp in size, corresponding to the *in vitro* transcribed RNA from the pNoVGII. This RNA was used in a two-step RT-PCR assay for amplification of the NoV GII N/S domain coding region. Figure 3.8 (B), shows the results from the RT-PCR assay. Lane 2 shows no bands as expected as the first-strand cDNA used as a template was replaced with ddH<sub>2</sub>O; however a band was present in lane 3 at 342 bp as expected as the positive control used pNoVGII as the template. Lane 4 shows the results from the RT-PCR assay from the first-strand cDNA synthesised from the *in vitro* transcribed RNA from pNoVGII. A band was present at 342 bp which corresponds to that of the NoV GII N/S domain coding sequence.

### 3.3.1.4 Sensitivity of the Two-Step RT-PCR Assay for NoV GII

The minimum RNA required for the two-step RT-PCR assay was determined using the *in vitro* transcribed RNA from pNoVGII. This was achieved by diluting the *in vitro* transcribed

RNA, followed by performing a two-step RT-PCR assay for the NoV VP1 N/S domain coding region. The results are shown in Figure 3.9 below.



**Figure 3.9: Agarose gel electrophoresis of the dilution series RT-PCR assay from the *in vitro* transcribed RNA from NoV GII.** Lane 1: Kapa Universal marker; lane 2: negative control; lane 3: positive control; lane 4: 481.2 ng/μl *in vitro* transcribed RNA; lane 5: 98.9 ng/μl *in vitro* transcribed RNA; lane 6: 19.7 ng/μl *in vitro* transcribed RNA; lane 7: 3.4 ng/μl *in vitro* transcribed RNA; lane 8: 0.9 ng/μl *in vitro* transcribed RNA.

In Figure 3.9, the negative control from the NoV GII two-step RT-PCR, lane 2, showed no bands, as expected, as ddH<sub>2</sub>O was used as the template. A band was present at 342 bp in the positive control, lane 3, as expected as pNoVGII was used as the template. A band was also present in lanes 4-7 which decreased in intensity with decreasing concentrations of RNA template. At a concentration of 0.9 ng/μl, the RT-PCR product was no longer visible, lane 8, and the minimum concentration to produce an amplified product was 3.4 ng/μl.

### 3.3.2 Aichi Virus

#### 3.3.2.1 PCR Amplification of the AiV 5'UTR Coding Region

The amplification of the 5'UTR coding region was performed using the primer set 5'UTR F/R and using the protocol based on that described by Drexler *et al.* (2011). The results of the PCR assay are shown in Figure 3.10 below.

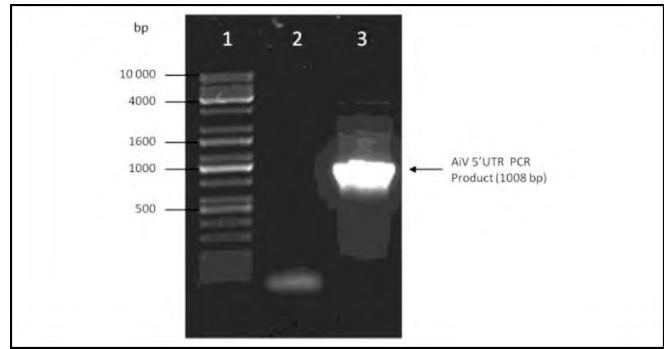


**Figure 3.10: Agarose gel electrophoresis of the PCR assay from the AiV 5' UTR plasmid provided by Jan Drexler.** Lane 1: Kapa Universal marker; lane 2: negative control; lane 3: AiV 5'UTR plasmid.

The negative control from AiV 5'UTR PCR, lane 2 in Figure 3.10 showed no bands as expected. The amplicon of approximately 1008 bp, as seen in lane 3, was ligated into pGEM®-T Easy.

### 3.3.2.2 PCR Amplification of the AiV partial 3CD Coding Region

The cDNA encoding the AiV partial 3CD coding region was amplified using the primer set 3CD F/R and the protocol described by Pham *et al.* (2007). The results are shown in Figure 3.11 below.

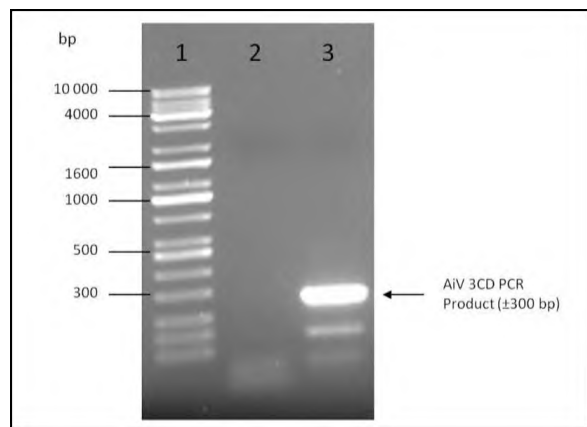


**Figure 3.11: Agarose gel electrophoresis of the PCR assay performed on the 3CD cDNA.** Lane 1: Kapa Universal marker; lane 2: negative control; lane 3: 3CD cDNA.

In Figure 3.11, no band was present in the negative control, lane 2. Two bands were present in lane 3. The upper band of 266 bp corresponds to that of the AiV partial 3CD coding region which was ligated into pGEM®-T Easy.

### 3.3.2.3 Cloning of the PCR Amplicons into pGEM®-T Easy to create pAiV5'UTR and pAiV3CD

The AiV 5' UTR and partial 3CD amplicons were ligated into pGEM®-T Easy to create pAiV5'UTR and pAiV3CD, respectively. The plasmids were digested with *Eco* RI to confirm the presence of the correct inserts (data not shown) and sequenced. Figure 1S and Figure 2S in Appendix I shows the nucleotide sequences of the inserts of pAiV5'UTR and pAiV3CD, respectively. Figure 3S and Figure 4S shows a multiple alignment of pAiV5'UTR and pAiV3CD to the reference strain of AiV (Accession number AB010145), respectively. Figure 3.12 below shows the plasmid maps of pAiV5'UTR and pAiV3CD.

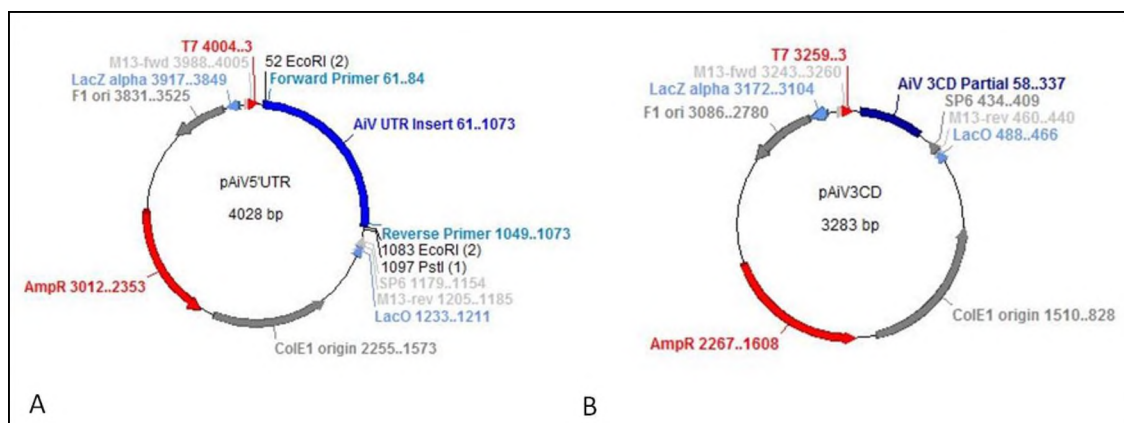


**Figure 3.12: A schematic diagram of the plasmid maps of: (A) pAiV5'UTR and (B) pAiV3CD.** Both plasmids contain the T7 and SP6 promoters, the *LacZ* $\alpha$  and *LacO* genes, the *Amp*<sup>r</sup> gene and a multiple cloning site which contains two *Eco* RI restriction sites. pAiV5'UTR contains the coding sequence of the 5'UTR amplicon while pAiV3CD contains the amplicon of the 3CD coding sequence.

The inserts of the pAiV5'UTR and pAiV3CD plasmids were sequenced; Figure 1S and Figure 2S (Appendix I) show that the RT-PCR products of AiV 5'UTR and AiV 3CD were correctly inserted into pGEM®-T Easy, respectively. BLAST analysis of pAiV5'UTR and pAiV3CD showed a 97 % identity to the AiV reference strain (Accession number AB010145), Figure 3S and Figure 4S (Appendix I), respectively.

Figure 3.12 (A) shows a schematic diagram of the plasmid map of pAiV5'UTR which is 4028 bp in size and Figure 3.12 (B) shows the schematic plasmid map of pAiV3CD which is 3283 bp in size.

#### 3.3.2.4 Development of a Two-Step RT-PCR Assay for AiV 5'UTR

RNA was transcribed from pAiV5'UTR followed by synthesis of first-strand cDNA. The cDNA was used as the template for the RT-PCR assay for the 5'UTR coding sequence. The results of the two-step RT-PCR assay are shown in Figure 3.13 below.

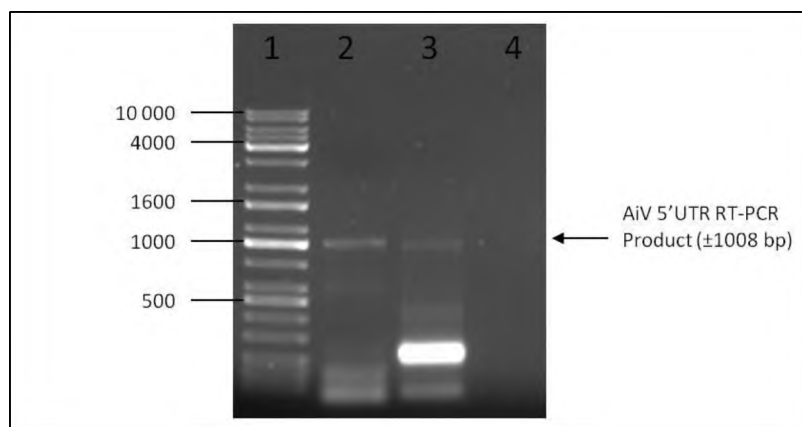


**Figure 3.13: Agarose gel electrophoresis of the two-step RT-PCR assays from the *in vitro* transcribed RNA from pAiV5'UTR.** Lane 1: Kapa Universal marker; lane 2: positive control; lane 3: first-strand cDNA from the *in vitro* transcribed RNA; lane 4: negative control.

A band of approximately 1008 bp corresponding to the AiV 5'UTR coding sequence is present in the positive control, lane 2, as expected, as the positive control template is pAiV5'UTR. Lane 3 contains two clear bands, the first is approximately 1008 bp in size and corresponds to that of the AiV 5'UTR amplicon. The second, smaller band was determined to be a second oligonucleotide binding site within the AiV 5'UTR region. Lane 4 shows no bands present in the negative control as expected as water was used as the template rather than the AiV 5'UTR first-strand cDNA.

### 3.3.2.5 Development of a Two-Step RT-PCR Assay for AiV 3CD

pAiV3CD was linearised with *Pst* I prior to *in vitro* transcription of RNA. First-strand cDNA was then synthesised followed by RT-PCR amplification of the partial 3CD coding region. Figure 3.14 below shows the results of the two-step RT-PCR assay.

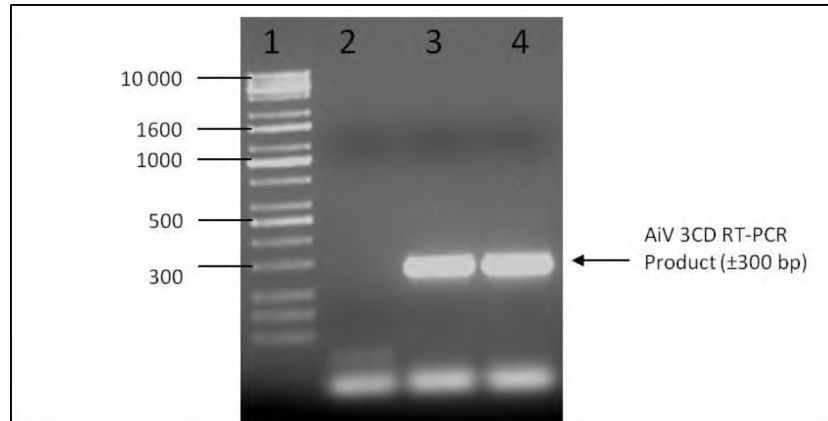


**Figure 3.14: Agarose gel electrophoresis of the two-step RT-PCR assays from the *in vitro* transcribed RNA from pAiV3CD.** Lane 1: Kapa Universal marker; lane 2: negative control; lane 3: positive control; lane 4: *in vitro* transcribed RNA.

The negative control, lane 2, showed no bands as expected as ddH<sub>2</sub>O was used as the template in the RT-PCR assay. The positive control, lane 3, shows the presence of a 266 bp band as expected as pAiV3CD was used as the template for the RT-PCR assay. The RT-PCR assay performed on the first-strand cDNA showed a single band at 266 bp which corresponds to that of the AiV partial 3CD coding region.

### 3.3.2.6 Sensitivity of the Two-Step RT-PCR Assay for AiV 5'UTR and AiV3CD

Five-fold, serial dilutions of the RNA were performed followed by the synthesis of strand-strand cDNA for each dilution of RNA. RT-PCR amplification of the AiV 5'UTR and partial 3CD coding regions was performed using the first-strand cDNA for each dilution. The results are shown in Figure 3.15 below.

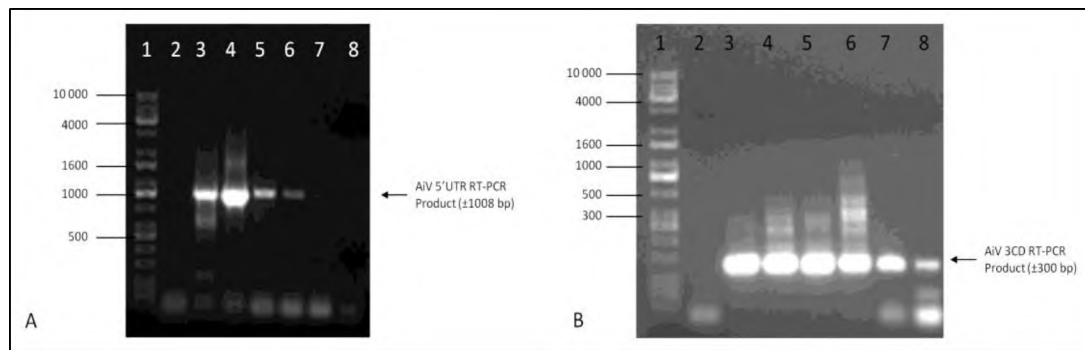


**Figure 3.15: Agarose gel electrophoresis of the dilution series RT-PCR assay from the *in vitro* transcribed RNA from: (A) pAiV5'UTR.** Lane 1: Kapa Universal marker; lane 2: negative control; lane 3: positive control; lane 4: 452.7 ng/μl *in vitro* transcribed RNA; lane 5: 102.5 ng/μl *in vitro* transcribed RNA; lane 6: 24.7 ng/μl *in vitro* transcribed RNA; lane 7: 3.5 ng/μl *in vitro* transcribed RNA; lane 8: 0.7 ng/μl *in vitro* transcribed RNA. **(B) pAiV3CD.** Lane 1: Kapa Universal marker; lane 2: negative control; lane 3: positive control; lane 4: 429.6 ng/μl *in vitro* transcribed RNA; lane 5: 97.2 ng/μl *in vitro* transcribed RNA; lane 6: 13.8 ng/μl *in vitro* transcribed RNA; lane 7: 0.2 ng/μl *in vitro* transcribed RNA; lane 8: 0 ng/μl *in vitro* transcribed RNA.

In Figure 3.15 (A) the negative control from the AiV 5'UTR RT-PCR, lane 2, showed no bands, as expected, as ddH<sub>2</sub>O was used as the template. A band was present at 1008 bp in the positive control, lane 3, as expected, as pAiV5'UTR was used as the template. Lanes 4-7 also showed the presence of this 1008 bp band however it decreased in intensity with decreasing concentrations of RNA template. At a concentration of 0.7 ng/μl, the RT-PCR product was no longer visible, lane 8, and the minimum concentration to produce an amplified product was 3.5 ng/μl. In Figure 3.15 (B), once again the negative control from the AiV 3CD RT-PCR, lane 2, showed no bands as ddH<sub>2</sub>O was used as the template. The positive control, lane 3, showed the presence of a 266 bp band, as expected, as pAiV3CD was used as the template. A band was also present in lanes 4-8 at 266 bp which, decreases in intensity with the decrease in RNA concentration. The minimum concentration to produce an amplicon for AiV 3CD is 0.2 ng/μl.

### 3.3.3 Saffold Virus

#### 3.3.3.1 *In Vitro* Transcription of SAFV RNA from pSAFV

pSAFV was linearised with the restriction enzyme *Xho* I followed by the *in vitro* transcription of RNA. The results are shown in Figure 3.16 below.

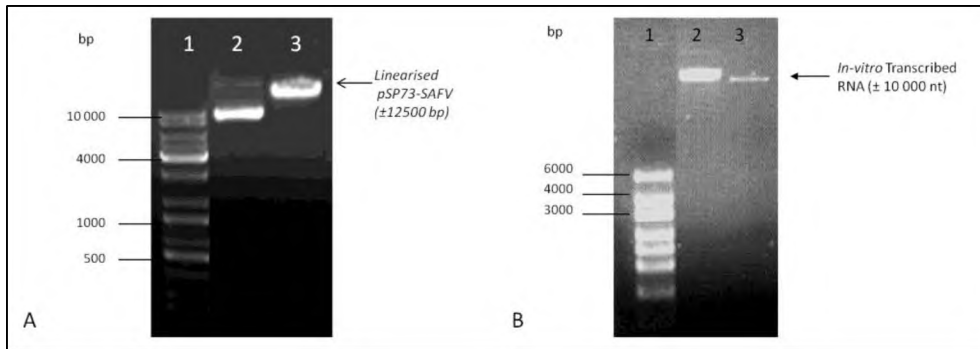


**Figure 3.16: (A) Agarose gel electrophoresis of pSAFV before and after linearization.** Lane 1: Kapa Universal Marker; lane 2: pSAFV plasmid before digestion with *Xho* I; lane 3: pSAFV plasmid after digestion with *Xho* I. **(B) Agarose gel electrophoresis of the *in vitro* transcribed RNA from the linearised pSAFV.** Lane 1: RNA marker; lane 2: SAFV *in vitro* transcribed RNA; lane 3: SAFV *in vitro* transcribed RNA treated with DNase I.

Figure 3.16 (A), lane 2, shows pSAFV before linearising with *Xho* I. Lane 3 shows pSAFV after linearising with *Xho* I, and a single band of over 10 000 bp in size can be seen, indicating that complete digestion occurred. Figure 3.16 (B), shows the *in vitro* transcribed RNA from pSAFV. In both lanes 2 and 3, a clear band can be seen at over 10 000 bp, however, the band of RNA before treating with DNase I, lane 2, is brighter than that of the one after treating with DNase I, lane 3. This RNA was used to develop a two-step RT-PCR assay for SAFV.

### 3.3.3.2 Development of a Two-Step RT-PCR Assay for SAFV

From the *in vitro* transcribed RNA, first-strand cDNA was synthesised. The RT-PCR assay was then performed in the first-strand cDNA for the amplification of the SAFV full length 2C region (975 bp) as well as an internal region of 2C (540 bp). The results are shown in Figure 3.17 below.

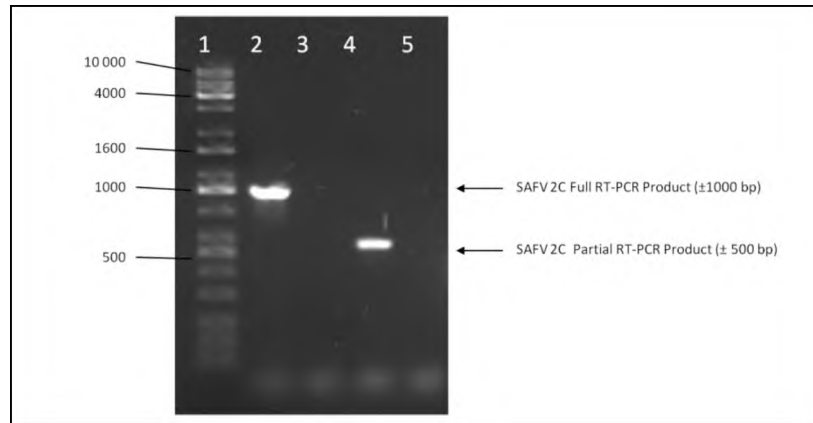


**Figure 3.17: Agarose gel electrophoresis of the two-step RT-PCR assay for the SAFV 2C, full and partial, coding sequences from the SAFV *in vitro* transcribed RNA.** Lane 1: Kapa Universal marker; lane 2: SAFV Full length 2C RT-PCR; lane 3: negative control for the SAFV full length 2C RT-PCR; lane 4: SAFV partial 2C RT-PCR; lane 5: SAFV partial 2C RT-PCR negative control.

Figure 3.17 shows the results from the RT-PCR assay for SAFV full length and internal 2C. In lane 2, a single band of approximately 975 bp in size can be seen corresponding to that of the SAFV full length 2C coding region. Lane 4 shows the presence of a single band 540 bp in size which corresponds to the SAFV internal coding region of 2C. Both lanes 3 and 5 do not show the presence of any band as they are the negative controls. This was expected as the template used in these reactions was ddH<sub>2</sub>O rather than the first-strand cDNA synthesised from the SAFV *in vitro* transcribed RNA.

### ***3.3.3.3 Sensitivity of the Two-Step RT-PCR Assay for SAFV***

First-strand cDNA was synthesised from serial dilutions of the SAFV *in vitro* transcribed RNA and the RT-PCR assay was performed on each dilution. The results of are shown in Figure 3.18 below.

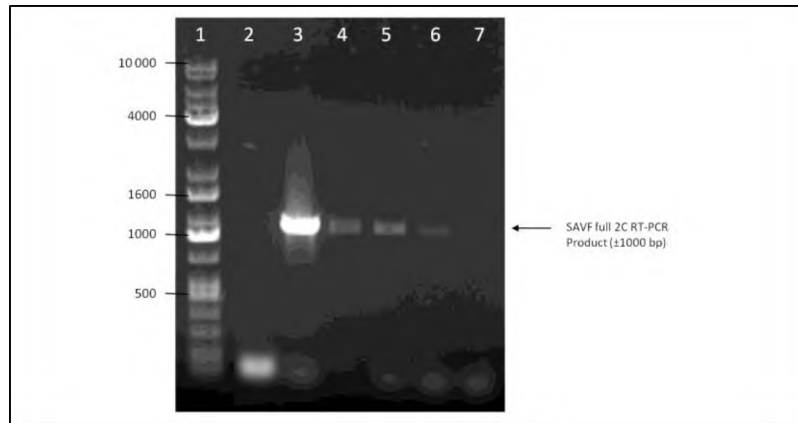


**Figure 3.18: Agarose gel electrophoresis of the dilution series RT-PCR assay for SAFV full 2C from the *in vitro* transcribed RNA.** Lane 1: Kapa Universal marker; lane 2: negative control; lane 3: 556.9 ng/ $\mu$ l of SAFV RNA; lane 4: 115.3 ng/ $\mu$ l of SAFV RNA; lane 5: 23.4 ng/ $\mu$ l SAFV RNA; lane 6: 4.8 ng/ $\mu$ l SAFV RNA; lane 7: 1 ng/ $\mu$ l SAFV RNA.

The negative control, lane 2 of Figure 3.18, shows no bands, as expected, as ddH<sub>2</sub>O was used as the template. Lanes 3-6 all show the presence of a single band approximately 975 bp in size which decreases in intensity as the RNA concentration decreases. No bands were present when the RNA concentration was 1 ng/ $\mu$ l, lane 7, and the minimum RNA concentration required to produce an amplicon was 4.8 ng/ $\mu$ l.

### 3.4 Discussion

The aim of this chapter was to develop positive controls for RT-PCR assays for the detection of specific sequences for NoV GII, AiV and SAFV. Plasmids containing selected sequences for NoV GII and AiV were successfully created by cloning specific sequences, selected based on literature, into pGEM®-T Easy. For SAFV, a plasmid containing the full length genome was obtained. From these plasmids, RNA was successfully transcribed *in vitro* and was used in two-step RT-PCR assays.

For the creation of a positive control for the NoV RT-PCR, RNA was extracted from a NoV GII infected stool sample and an RT-PCR assay was performed. The 342 bp fragment of the partial VP1 N/S domain coding sequence was successfully amplified and cloned into pGEM®-T Easy. RNA was successfully transcribed from the pNoVGII plasmid and a RT-PCR assay using the *in vitro* transcribed RNA produced the same 342 bp fragment. It was determined that the minimum amount of RNA required for this RT-PCR assay was 0.9 ng/ $\mu$ l.

A positive control for both the AiV 5'UTR and partial 3CD RT-PCR assays were successfully developed through the amplification of the AiV 5'UTR 1008 bp insert and the partial 3CD cDNA fragment (266 bp) followed by cloning of the amplicons into pGEM®-T Easy. Using pAiV5'UTR and pAiV3CD as templates, RNA was successfully transcribed and the 1008 bp 5'UTR and the 266 bp partial 3CD coding sequences were successfully amplified from the *in vitro* transcribed RNA using the RT-PCR assays. The minimum amount of RNA for the 5'UTR RT-PCR assay was determined to be 0.7 ng/μl and <0 ng/μl for the 3CD RT-PCR assay. As pSAFV contains the T7 promoter and RNA was directly transcribed from this plasmid to be used as a positive control for the RT-PCR assays. From the *in vitro* transcribed RNA, both the full length 2C (975 bp) and partial 2C (540 bp) coding sequences were successfully amplified using RT-PCR assays and the minimum amount of RNA for the full length 2C RT-PCR assay was determined to be 1 ng/μl.

The RT-PCR assay chosen for detection of NoV was described by Kojima *et al.* (2002), where genogroup-specific primers were used in the detection of NoV GI and GII from stool samples which showed Norwalk-like virus particles. The G2SKF/G2SKR primer set, designed by Kojima and colleagues, was chosen for this study as these primers identified NoV GII in 100% of the stool samples screened with a single RT-PCR assay (Kojima *et al.*, 2002). However, in our study, a nested RT-PCR assay had to be performed with the G2SKF/G2SKR primer set in order to amplify the 342 bp fragment from RNA extracted from stool samples. This may be due to low concentrations of RNA resulting in a lower cDNA concentration, leading to poor amplification of the PCR product in the first round or the RT-PCR assay may require adjustments for the correct amplification conditions. Kojima *et al.* (2002) also designed primers (G1SKF/G1SKR) for NoV GI, however, this study did not perform this RT-PCR assay as a NoV GI positive control was not available.

The G1SKF/G1SKR and G2SKF/G2SKR primer sets have since been used in other studies for the identification of NoV in the GI and GII genogroups. Loisy *et al.* (2005) used the primer set for the identification of NoV GI and GII from both natural and artificially-infected oysters. In this study, RNA from Norwalk virus strain (8FIIa) and RNA extracted from a NoV GII positive stool sample were used as positive controls in the RT-PCR and real-time

RT-PCR assays which they performed. A similar positive control was used to the one chosen in our study for the NoV GII RT-PCR assay.

For the detection of AiV in the wastewater, oyster and stool samples, two RT-PCR assays were chosen based on literature. The first RT-PCR assay detects of the 5'UTR coding region and the second detects a partial region of the 3CD coding region. The 5'UTR RT-PCR assay was performed based on the work of Drexler *et al.* (2011), where a nested RT-PCR assay and a real-time RT-PCR assay were developed for the detection of AiV in stool samples. Jan Drexler kindly supplied a plasmid containing one of the 5'UTR PCR product from the study of Drexler *et al.* (2011). The backbone of this plasmid was unknown and so it could not be used directly in this study. A single round PCR was therefore performed on the plasmid, using the 5'UTR F/R primers, for the development of the positive control resulting in the amplification of the 1008 bp fragment.

Yamashita *et al.* (2000) developed a RT-PCR assay for the detection of AiV using three primer sets, the third of which amplified a 519 bp region of the 3CD junction. AiV isolates (grown in Vero cells) and stool samples were then screened for the presence of AiV using the three primer sets (Yamashita *et al.*, 2000). The AiV standard strain (A846/88) RNA was used as a template in the RT-PCR assays and positive results were seen for all three primer sets. The primer set designed to amplify the 3CD junction was shown to be most sensitive. Pham *et al.* (2007) developed a nested RT-PCR using the 3CD junction primer set from Yamashita *et al.* (2000) as well as an internal primer set. Using the nested RT-PCR assay, it was possible to successfully identify AiV from 28 stool samples collected from Japan, Bangladesh and Vietnam (Pham *et al.*, 2007). The 266 bp fragment of the AiV 3CD from Pham *et al.* (2007) was used for the development of a positive control for the AiV 3CD RT-PCR assay in this study. For this reason only the second round RT-PCR primers from Pham *et al.* (2007) were chosen for the development of a positive control in this study.

Blinkova *et al.* (2009) identified SAFV RNA fragments from stool samples collected from children under the age of 15, who suffered from non-polio acute flaccid paralysis, from South Asia during 2008. The SAFV RNA fragments were identified through shotgun sequencing and RT-PCR assays of the 2C (helicase) and VP1 regions. The 2C nested RT-PCR assay was

used for the identification of SAFV sequences while the VP1 RT-PCR assay was used for classification of the genotypes (Blinkova *et al.*, 2009). From the 107 samples screened, 11 tested positive for SAFV and so a similar method was used in this study. Two sets of new primers for the 2C region were designed as those described by Blinkova *et al.* (2009) were degenerate primers. The first set of primers (external primers) amplify a 975 bp region of the 2C sequence while the second set of primers (internal primers) amplify a 540 bp region within the 2C external primers potentially allowing for a nested RT-PCR assay. In this study only RT-PCR assays, not nested RT-PCR assays were performed with each primer set unlike Blinkova *et al.* (2009) who used a nested RT-PCR assay. The 975 bp region was used to determine the sensitivity of the assays in this study as the focus was the development of techniques. If this RT-PCR assay was used for diagnostic detection the 540 bp region would be used as the viral RNA in samples may be degraded and a higher detection rate may occur with this RT-PCR assay. The 2C (helicase) sequence was chosen as it is highly conserved throughout the picornavirus family, increasing the efficiency of the primers as there is less sequence variation which may occur in other regions of the genome (Blinkova *et al.*, 2009; Racaniello, 2007).

Using the RT-PCR assays and primer sets designed by Kojima *et al.* (2002), Drexler *et al.* (2011) and Pham *et al.* (2007), positive controls were successfully developed for the detection of NoV GII, AiV 5'UTR coding region and a partial region of the 3CD junction of AiV, respectfully. Two RT-PCR assay positive controls were also successfully developed for the 2C coding region of SAFV based on the work published by Blinkova *et al.* (2009). The next chapter describes the samples used in this study, namely wastewater, oyster and clinical samples as well as their preparation by filter concentration and PEG precipitation. Screening of filter concentrated samples by TEM for the presence of viral particles is also performed.

## ***Chapter 4: Preparation of Samples and Morphological Analysis of Virus Particles***

### ***4.1 Introduction***

In Chapter 3, the development of RT-PCR assays and positive controls for the identification of NoV, AiV and SAFV using either viral RNA (NoV) or *in vitro* transcribed RNA were described. This chapter describes the samples to be used in this study which include clinical samples, wastewater and oysters. In addition, the method of preparation of the samples for TEM screening is also presented.

Viruses associated with gastroenteritis, such as NoV and AiV have previously been isolated from wastewater and water sources contaminated with sewage in many studies worldwide (di Martino *et al.*, 2013; Lodder *et al.*, 2013; Mans *et al.*, 2013; La Rosa *et al.*, 2008; da Silva *et al.*, 2007). Wastewater was thus chosen as a sample type in this study. Shellfish, such as oysters, are often associated with gastroenteritis and many of these cases are as a result of the viruses, including enteroviruses, NoV and AiV (Reuter *et al.*, 2011; Formiga-Cruz *et al.*, 2005; Loisy *et al.*, 2005; Le Guyader *et al.*, 2000; Atmar *et al.*, 1995; Yamashita *et al.*, 1991). Previous studies have isolated these viruses from oysters therefore, as oysters suspected to contain viruses were available, they were also used in this study. Many studies have isolated viruses associated with gastroenteritis from stool samples, including enteroviruses, NoV, AiV and SAFV (Mans *et al.*, 2014; Nielsen *et al.*, 2013; Chau *et al.*, 2011; Eden *et al.*, 2010; Pham *et al.*, 2010; Drexler *et al.*, 2008; Oh *et al.*, 2006). Stool samples were thus chosen as the third sample type for use in this study for the identification NoV, AiV and SAFV.

While the virus particles may be present in high concentrations ( $10^9$ - $10^{13}$ ) in nature, these concentrations often occur in large sample sizes, such as a litre of water (reviewed by Staggemeir *et al.*, 2012). As PCR assays use small volumes of sample in the reactions it is therefore important to concentrate the samples to increase the sensitivity of the PCR assay. Filtering the sample allows for the removal of inorganic and organic contaminants, such as soil particles and bacteria, which may have adverse effects on downstream processing (Casas and Sunén, 2001). During the handling of the sample, virus particles are unavoidably lost, increasing the need to concentrate the samples. This can be performed after filtering of the

sample. Concentrating techniques such as PEG precipitation are also able to remove other amplification inhibitors (Casas and Sunén, 2001). The wastewater, oysters and stool samples were filtered and concentrated to remove debris and contaminants, and to increase the virus concentrations in the samples. Syringe filters and concentrator columns can be used to remove debris and contaminants and initially concentrate the samples. PEG precipitation can then be used to further concentrate the virus particles present in the samples, and may help in removing any smaller debris which passes through the filtering step. PEG precipitation has been used in a wide variety of studies, including that of Lewis and Metcalf (1988) and Lewis *et al.* (2010), to concentrate virus particles in a given sample.

Once the samples have been filtered and concentrated, the viruses can then be detected and identified (reviewed by Staggemeier *et al.*, 2012). While RT-PCR assays are used for the identification of viruses in a variety of samples, it is important to ensure virus particles are present in the samples first. This can be achieved through screening of filter concentrated samples by TEM to examine the morphological characteristics and approximate the number of particles present (reviewed by Staggemeier *et al.*, 2012).

The specific objectives were:

- To filter sterilise the wastewater, oysters and clinical samples, in order to remove bacteria and cell debris.
- To screen samples for virus particles and determine morphological characteristics.

## ***4.2 Materials and Methods***

The three samples types chosen in this study include wastewater, oysters suspected to be infected with viruses and 30 rotavirus-negative stool samples collected from symptomatic patients. These samples are discussed below.

### ***4.2.1 Wastewater Sample***

#### ***4.2.1.1 Sample Preparation and Transmission Electron Microscopy***

A 200 ml sewage sample was collected from the Belmont Valley Wastewater Treatment Plant (Grahamstown, Eastern Cape South Africa). The sample was filtered through 0.20  $\mu\text{m}$

sterile syringe filters (Lasec, South Africa) and concentrated to 6 ml using 20 ml and 4 ml Vivaspin columns (Sartorius Stedim Biotech, Germany) according to the manufacturer's protocol. Samples were prepared for TEM analysis and imaged as described in Chapter 2, section 2.2.3.

#### ***4.2.1.2 Precipitation with PEG 6000***

The wastewater supernatant collected above, Chapter 4, section 4.2.1.1, was assumed to have a NaCl of 0.15 M. As Chapter 2 showed an increase of virus particle recovery using PEG 6000 with a NaCl concentration of 0.25 M, the NaCl concentration of the wastewater supernatant was increased to a final concentration of 0.25 M. PEG precipitation was performed on the sample as described in Chapter 2, section 2.2.4. In brief, PEG 6000 was added to a final concentration of 8% and incubated overnight at 4°C. After incubation the samples were centrifuged at 10 000 *xg* for 30 min at 4°C and the pellets were resuspended in 300 µl ddH<sub>2</sub>O. The sample was prepared for TEM analysis and imaged as described in Chapter 2, section 2.2.3.

### ***4.2.2 Oyster Samples***

#### ***4.2.2.1 Sample Preparation and Transmission Electron Microscopy***

Oysters suspected to be infected with viruses were donated by Oribi Haven, Kasouga, Eastern Cape, South Africa. The oysters were originally collected from Port Elizabeth, Eastern Cape, South Africa. The digestive tract, stomach and gills, as shown in Figure 4.1, were removed from five oysters by dissection, amalgamated and homogenised in 10 ml ddH<sub>2</sub>O with a final concentration of 0.25 M NaCl, using a stick blender (Sunbeam, USA). The sample was treated with a final concentration of 1% NP-40 (Sigma-Aldrich, USA) for 1 hr with shaking at room temperature and centrifuged at 4000 *xg* for 20 min. The supernatant was filtered through 0.20 µm sterile syringe filters (Lasec, South Africa) and concentrated to 2 ml using 4 ml Vivaspin columns (Sartorius Stedim Biotech, Germany) according to the manufacturer's protocol. PEG precipitation was performed on the sample and TEM analysis was performed as described above in Chapter 2, section 2.2.4.

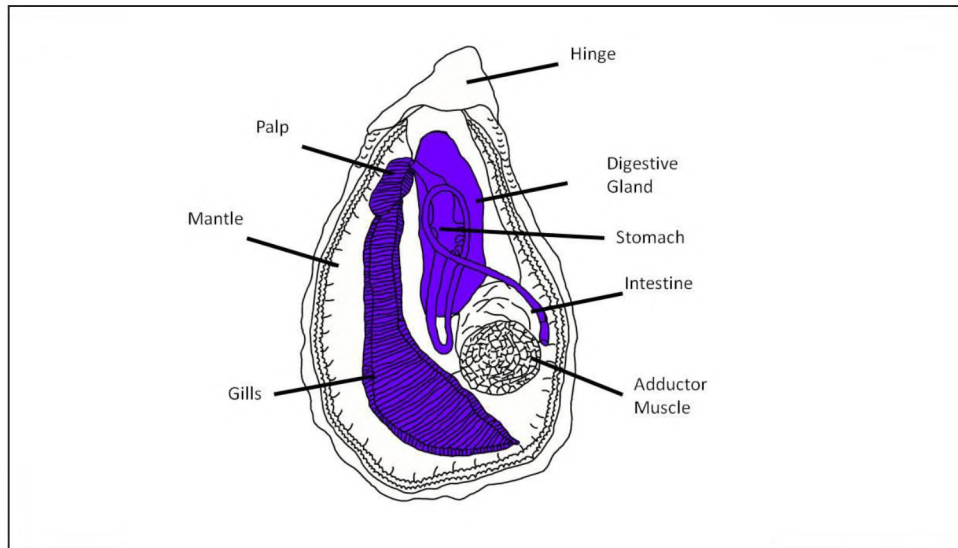


**Figure 4.1:** A schematic diagram of the internal organs of an oyster (adapted from <http://lanwebs.lander.edu/faculty/rsfox/invertebrates/crassostrea.html>; drawn by Kate Bryan [Rhodes University, South Africa]). The digestive tract, stomach and gills, which were dissected out of the oyster, are shown in purple.

### ***4.2.3 Stool Samples***

#### ***4.2.3.1 Sample Preparation and Transmission Electron Microscopy***

Thirty rotavirus negative stool samples were donated by the Diarrhoeal Pathogens Research Unit (MEDUNSA, Limpopo University). The samples were initially screened, by the staff at the Diarrhoeal Pathogens Research Unit, for the presence of rotavirus using the ProSpecT Rotavirus ELISA kit (Oxoid, UK). The sample number, date of collection, age and gender of the patients from which the stool samples were collected, were recorded and are shown in Table 4.1 below.

**Table 4.1: Data Pertaining to the Patients from which the Stool Samples were Collected.**

Rhodes sample no	Sample no	Collection Date	Patient Gender	Patient Age
P1	5666	11/6/2011	Female	1 Year
P2	5667	14/6/2011	Male	5 Months
P3	5673	16/6/2011	Male	1 Year
P4	5675	17/6/2011	Male	2 Years
P5	5677	14/6/2011	Female	3 Years
P6	5679	14/6/2011	Male	2 Years
P7	5681	13/6/2011	Female	1 Year
P8	5687	17/6/2011	Male	4 Months
P9	5689	17/6/2011	Male	1 Year
P10	5693	18/6/2011	Male	3 Years
P11	5702	20/6/2011	Female	4 Years
P12	5706	21/6/2011	Male	2 Years
P13	5707	24/6/2011	Male	3 Years
P14	5719	21/6/2011	Female	3 Months
P15	5723	25/6/2011	Male	2 Years
P16	5729	9/5/2011	Male	4 Years
P17	5730	9/5/2011	Female	1 Year
P18	5759	5/5/2011	Female	0 Months
P19	5763	15/5/2011	Female	3 Years
P20	5770	13/5/2011	Male	4 Years
P21	5776	17/5/2011	Male	1 Year
P22	5783	30/5/2011	Female	10 Months
P23	5785	31/5/2011	Female	1 Year
P24	5788	3/6/2011	Female	4 Months
P25	5789	6/6/2011	Male	1 Year
P26	5803	8/6/2011	Female	2 Years
P27	5805	9/6/2011	Female	2 Years
P28	5807	8/6/2011	Female	2 Years
P29	5809	10/6/2011	Female	0 Months
P30	5811	10/6/2011	Female	11 Months

Approximately 500 µl of each stool sample was suspended in 5 ml of 0.15 M NaCl and briefly vortexed (adapted from the Isolation of viral RNA from stool using the QIAamp® Viral RNA Mini Kit User-Developed Protocol, Qiagen®, 2010). The samples were then clarified by centrifugation at 4000 *xg* for 20 minutes. The supernatant was filtered through 0.20 µm sterile syringe filters (Lasec, South Africa) and concentrated, by centrifugation at 4000 *xg* for 10 min or until the sample was concentrated to approximately 500 µl, using 4 ml Vivaspin columns (Sartorius Stedim Biotech, Germany) as per the manufacturer's protocol. The NaCl concentration was increased to a final concentration of 0.25 M and PEG precipitation was performed as described above, in Chapter 2, section 2.2.1.4. Each sample was then prepared for TEM analysis and imaged as described in Chapter 2, section 2.2.3.

### ***4.3 Results***

#### ***4.3.1 Transmission Electron Microscopy Wastewater Sample***

The wastewater sample was analysed for the presence of viral particle by TEM. To increase the concentration of potential virus particles, PEG precipitation was performed with 0.25 M NaCl. Figure 4.2 shows the TEM micrographs for the wastewater sample after PEG precipitation.

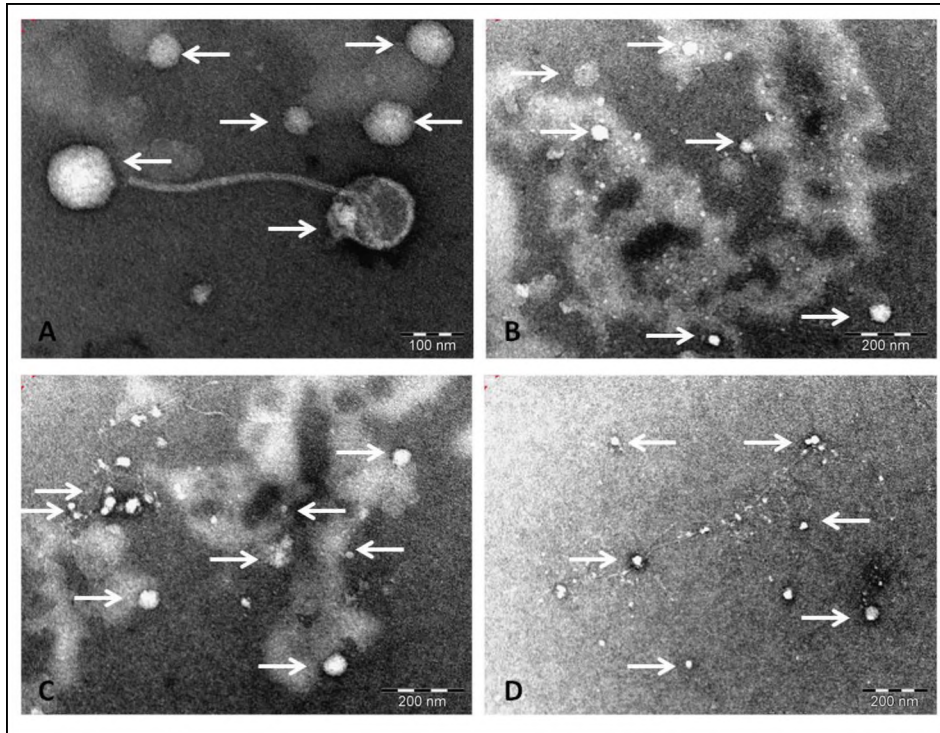


**Figure 4.2: TEM images of the wastewater sample after PEG precipitation. Panel A-D:** TEM images from the wastewater sample treated with 8% PEG 6000 and 0.25 M NaCl concentration. Arrows point towards single or clumps of viral particles.

The TEM images in Figure 4.2 show a wide variety of virus particles isolated from the wastewater sample. These particles were icosahedral in shape, of which some showed the presence of a tail. The diameter of the viral particles ranged from 30 nm to 100 nm.

#### ***4.3.2 Transmission Electron Microscopy of Oyster Extracts***

The oyster extracts were analysed for the presence of viral particles by TEM. To increase the concentration of potential viral particles, PEG precipitation was performed with 8% PEG and 0.25 M NaCl. Figure 4.3 shows the TEM micrographs for the oyster samples after PEG precipitation.

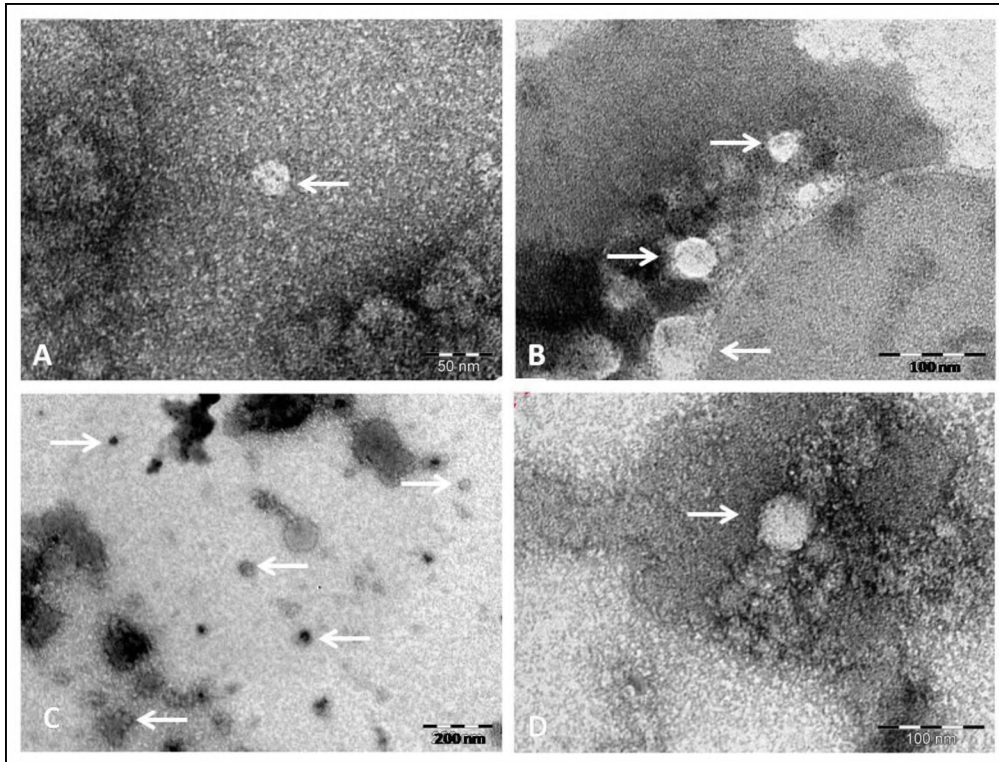


**Figure 4.3: TEM images of the oyster samples after PEG precipitation. Panel A-D:** TEM images from the oyster sample treated with 8% PEG 6000 and 0.25 M NaCl. Arrows point towards single or clumps of viral particles.

In the oyster samples, only one type of virus particle was present. These were small (30-40 nm in diameter), round virus particles as can be seen in panels A-D of Figure 4.3. Single viral particles can be seen in panels A and D, while panels B and C show multiple particles, including some which are forming clumps.

#### ***4.3.3 Transmission Electron Microscopy of Stool Samples***

To determine if there were viral particles present in the stool samples PEG precipitation was performed with 8% PEG and 0.25 M NaCl after which TEM analysis was performed. Figure 4.4 below shows the TEM images from after PEG precipitation and Figure 4.5 below shows transmission electron micrographs of the variety of viral particles seen in the stool samples.

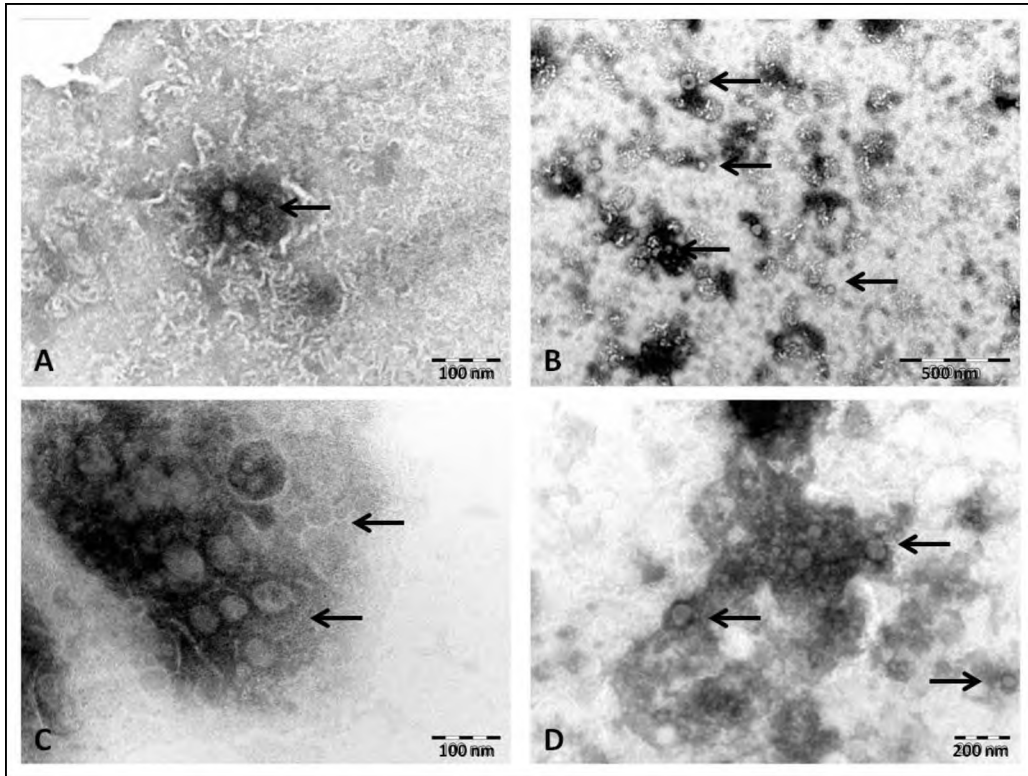


**Figure 4.4: TEM images of selected stool samples after PEG precipitation. Panel A-B:** TEM images from stool samples P10 and P19 respectively after PEG precipitation with 0.25 M NaCl and 8% PEG 6000. **Panel C-D:** TEM images from stool sample P2 after PEG precipitation with 0.25 M NaCl and 8% PEG 6000. Arrows point towards single or clumps of viral particles.

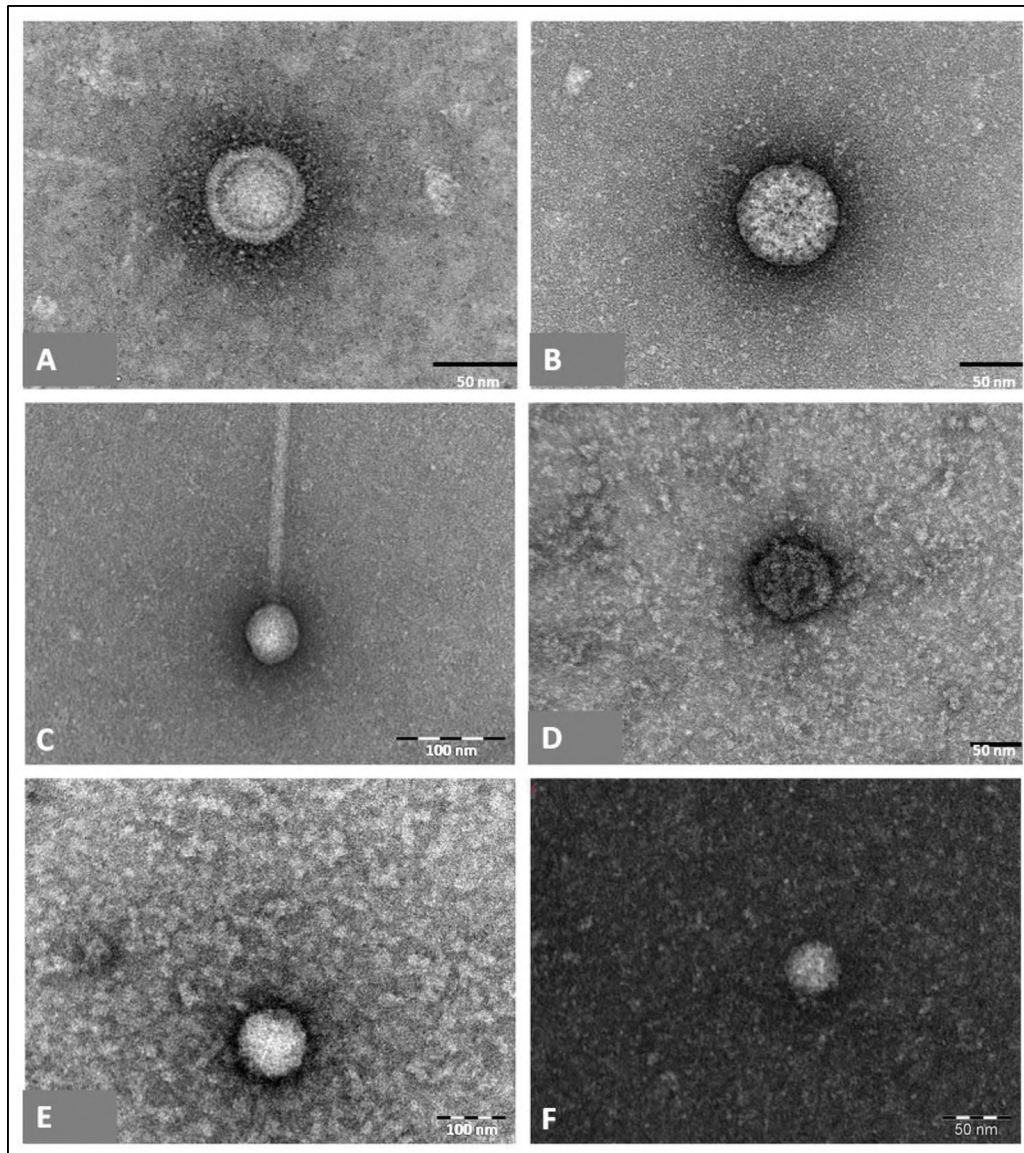


**Figure 4.5: TEM images of selected stool samples showing the variety of virus particles present. Panel A-F:** Transmission electron micrographs from stool samples P17, P25, P23, P9, P10 and P24 respectively showing single virus particles.

All 30 stool samples showed the presence of viral particles. The TEM images in Figures 4.4 and 4.5 showed viral particles ranging from 30 nm to 100 nm in diameter and are icosahedral in shape, some of which have tails. Viral particles present in Figure 4.4 panels A-D show clustering of the virus particles and a large number of virus particles could be seen.

Figure 4.5 panels A-F show a variety of virus particles found in the stool samples. Panels A, D, E and F show virus particles which are icosahedral in shape, with no protruding surface proteins and are 30 – 50 nm in diameter. Panel B shows a virus particle approximately 80 nm

in diameter with protruding surface proteins. Panel C shows a virus with a tail and the capsid of the virus is approximately 50 nm in diameter.

#### **4.4 Discussion**

Three samples were chosen for screening in this study, these were wastewater, oysters suspected to be infected with viruses and rotavirus-negative stool samples collected from symptomatic paediatric patients in South Africa.

Wastewater was chosen as a sample as viruses are expected to be found in this sample, including enteroviruses, NoV and AiV, which have been found in sewage samples in many studies including that of Formiga-Cruz *et al.* (2005), da Silver *et al.* (2007) and di Martino *et al.* (2013). In Formiga-Cruz *et al.* (2005) sewage was screened by multiplex RT-PCR and the sample was found to contain adenovirus, enteroviruses (including poliovirus and coxsackie viruses) and hepatitis A virus. Da Silver *et al.* (2007) performed a study to determine the removal of NoV GI and GII during wastewater treatment. The detected NoV GI in 43% and GII in 88% of their influent samples indicating that NoV is commonly found in sewage before treatment. AiV has been found in sewage samples around the world, including in Italy, as shown in the study by di Martino *et al.* (2013), where AiV was found in four wastewater treatment plants using RT-PCR assays.

The oysters were found to be associated with non-bacterial gastroenteritis, so viruses were thought to be present in them, and they were thus used as a sample in this study. Previous studies have found a wide variety of viruses associated with gastroenteritis in shellfish, including oysters, (Loisy *et al.*, 2005; Le Guyader *et al.*, 2000; Atmar *et al.*, 1995; Yamashita *et al.*, 1991). Loisy *et al.* (2005) showed the presence of NoV GII from 60 naturally contaminated oysters using RT-PCR assays. Le Guyader *et al.* (2000) collected 20 oysters and 30 mussels monthly, from five sites for three years to study human enteric viruses in shellfish (Le Guyader *et al.*, 2000). The study found Norwalk-like viruses, hepatitis A virus, rotavirus, enterovirus and astrovirus present in the shellfish throughout the study. Atmar *et al.* (1995) showed the presence of Norwalk-like viruses and hepatitis A virus in oysters and hard-shelled clams from Texas and South Carolina, USA, using PCR assays (Atmar *et*

*al.*, 1995). AiV was first identified in patients suffering from oyster associated gastroenteritis in three separate outbreaks in Japan, as shown by Yamashita *et al.* (1991).

Stool samples from patients with gastroenteritis contain a large variety of viruses associated with the disease, including enteroviruses, NoV, AiV and SAFV. Many studies look at the presence of selected viruses or their prevalence through detection of the viruses in stool samples. Pham *et al.* (2010) performed a multiplex RT-PCR assay on stool samples for the detection of AiV, human parechovirus, enteroviruses, and human bocavirus, many of which have been found in association with gastroenteritis in Japan. Drexler *et al.* (2011) detected the presence of AiV in stool samples collected from patients in northern Germany using RT-PCR assay and quantitative RT-PCR. NoV was identified in South Africa in stool samples from hospitalised patients in a study by Mans *et al.* (2010), which also focused on the genotyping of the strains detected by RT-PCR assays. Khamrin *et al.* (2011) identified SAFV from faecal samples taken from children with diarrhoea in Thailand using a RT-PCR assay which amplified the 5'UTR coding region.

TEM analysis of the wastewater sample showed the presence of a variety of virus particles while the oyster samples showed only one size of virus particles. This included small, round, non-enveloped viruses, 30-40 nm in diameter, as well as larger, round viruses, 80-100 nm in size. The stool samples showed a wide variety of viral particle sizes and morphologies, including small and large, round non-enveloped viral particles ranging in size from approximately 27-90 nm. The larger virus particles showed the presence of protruding surface proteins. The smaller virus particles present in the samples may belong to the *Caliciviridae* family as they exhibit a similar morphology to that of Norwalk-virus as shown by Green *et al.* (2000) and Wilhelmi (2003). They also show similar morphology to the TEM images of viruses present in the NoV stool sample (data not shown). They may, however, also belong to the *Picornaviridae* family as they also show a similar morphology to Poliovirus and AiV when compared to TEM images reported by the ICTV 9th report and Yamashita *et al.* (1998) (Knowles *et al.*, 2012; Yamashita *et al.*, 1998). The virus particles are also similar to that of the TEM images of TMEV (see Chapter 2), which is a known picornavirus. The larger viruses present in the wastewater and stool samples show the morphology of enteric adenoviruses as well as rotavirus, due to their size and the presence of

protruding surface proteins, when compared to TEM images (Berk, 2007; reviewed by Wilhelmi, 2003). As the rotavirus ELISA does not detect rotavirus group B and C, it is possible that the stool samples may contain rotaviruses belonging to these groups (Anderson and Weber, 2004). Adenoviruses are commonly found in wastewater samples (Berk, 2007). A virus with a head and a tail, 80 nm in diameter, can be seen in the wastewater sample. This morphology is indicative of a bacteriophage, which is expected in wastewater due to the presence of bacteria (Campbell, 2007).

The oysters, wastewater and clinical samples did not only show the presence of viral particles, but many of the viral particles present were similar in morphology to picornaviruses as well as caliciviruses. NoV was chosen as the first virus to be detected in this study as it is the second leading cause of viral gastroenteritis in South Africa and it has been shown to be present here in South Africa (Mans *et al.*, 2014, Mans *et al.*, 2010). Initial screening of AiV by RT-PCR assay was performed on the oysters and the wastewater sample but no results, either positive or negative, were obtained indicating that the RT-PCR assay required further optimisation. Due to time constraints, optimisation of the AiV RT-PCR assay and the screening of the wastewater, oysters and stool samples for SAFV by RT-PCR assay was not completed. The next chapter describes the screening of the wastewater, oyster and stool samples for NoV using an RT-PCR assay.

## ***Chapter 5: Detection of Norovirus GII in the Wastewater, Oyster and Stool Samples using an RT-PCR assay***

### ***5.1 Introduction***

Previous chapters describe the development of techniques for the isolation and detection of virus particles in TMEV-infected lysates, wastewater, oysters and stool samples. Significantly, screening of filter-sterilised samples by TEM showed the presence of picornavirus-like particles in all samples analysed. Although, the initial purpose of this study was to develop techniques for the identification of picornaviruses (specifically AiV and SAFV) which have not yet been described in South Africa, it was decided to first screen the samples for NoV given that it has been shown to be prevalent in this country. As described in Chapter 1, section 1.2.2, noroviruses are characterised into five different genogroups, of which GI and GII are major causative agents of gastroenteritis in humans (Zheng *et al.*, 2006). A previous study using real time qPCR assays have shown that several NoV genotypes including GI and GII are prevalent in water sources in Gauteng, South Africa (Mans *et al.*, 2013). In addition, NoV was detected in 14.3% of stool samples collected from hospitalised patients in Pretoria during 2008 (Mans *et al.*, 2010). Both of these studies reported that NoV strain GII.4 was the most common in South Africa. For this reason a RT-PCR assay was developed, as described in Chapter 3, for the detection of noroviruses in wastewater, oyster and stool samples.

The RT-PCR assay described in this chapter was performed based on a study by Kojima *et al.* (2002), where genogroup-specific primers targeting the capsid region of NoV GII were used to screen stool specimens during a gastroenteritis outbreak in Japan. The overall aim was to apply the RT-PCR assay developed in Chapter 3 to screen all samples for the presence of NoV GII and then perform a bioinformatics analysis of sequences obtained.

The specific objectives were as follows:

- To extract RNA from virus particles found in the wastewater, oyster and stool samples and to perform an RT-PCR assay for the detection of NoV GII.
- To sequence RT-PCR products and perform a bioinformatics analysis of the nucleotide and amino acid sequences.

## ***5.2 Materials and Methods***

### ***5.2.1 Viral RNA Extraction from the Wastewater, Oyster and Stool Samples***

Virus particles were obtained from wastewater, oyster and 30 stool samples as described in Chapter 4. Viral RNA was extracted using the QIAmp® Viral RNA Mini kit (Qiagen, USA) as described in Chapter 2, section 2.2.5, and analysed by 1% agarose gel electrophoresis as described in Chapter 2, section 2.2.5. The concentration was determined and RNA samples were stored at -80°C until required.

### ***5.2.2 Nested Two-Step Norovirus GII RT-PCR Assay Performed on the Wastewater, Oyster and Stool Samples First-Strand cDNA***

First-strand cDNA was synthesised from approximately 500 ng of viral RNA using the RevertAid™ Premium first-strand cDNA Synthesis kit (Fermentas, USA) according to the manufacturer's protocol as described in Chapter 2, section 2.2.6. The nested RT-PCR assay was performed using the N/S GII forward and reverse primers to amplify the NoV GII VP1 N/S domain coding sequence (described in Table 3.1) as follows: 1x ready mix with Mg<sup>2+</sup> (KAPA Biosystems, USA), 0.4 µM of the forward and reverse oligonucleotides, 4 ng/µl first-strand cDNA template and 9.5 µl ddH<sub>2</sub>O. A negative control reaction was set up in the same manner except that ddH<sub>2</sub>O was used instead of the first-strand cDNA template. The positive control was set up with ~2 ng/µl of pNoVGII. The cycling parameters used for the first round RT-PCR reaction were as follows: 95°C for 1 min 30s, 35 cycles of 95°C for 30s, 55°C for 45s, 72°C for 1 min and a final elongation of 72°C for 5 min.

The second round of PCR amplification was then performed as follows: 1x ready mix with Mg<sup>2+</sup> (KAPA Biosystems, USA), 0.4 µM of the forward and reverse oligonucleotides, 5 µl first round RT-PCR product and 9.5 µl ddH<sub>2</sub>O. A negative control reaction was set up in the same manner except that ddH<sub>2</sub>O was used instead of the first round RT-PCR product. The positive control was set up with ~2 ng/µl of pNoVGII. The second round RT-PCR assay used the same cycling parameters as described for the first round RT-PCR assay. The nested RT-PCR products were analysed by 1% agarose gel electrophoresis.

### ***5.2.3 Cloning, Sequencing and BLAST analysis of NoV RT-PCR Products***

RT-PCR amplicons representing a 342 bp region of the NoV GII genome were ligated into pGEM®-T Easy (Promega, USA) as per the manufacturer's protocol. Ligations were transformed and plasmids were extracted as described previously in Chapter 3 section 3.2.1.3. The plasmids were screened for the correct insert by restriction digestion with *Eco* RI as follows: as follows: the reaction was set up using ~70 ng/μl of plasmid DNA, 1x buffer, 3 U/μl *Eco* RI restriction enzyme and sterile ddH<sub>2</sub>O to 15 μl. The reaction was incubated at 37°C for 30 min and agarose gel electrophoresis. One plasmid from each sample (wastewater, oyster extracts and 11 stool samples) was sent to Inqaba Biotechnical Industries (Pty) Ltd for sequencing. This was performed using the T7 primer, in the forward direction only and the sequence was analysed using NCBI BLAST ([Blast.ncbi.nlm.nih.gov/Blast.cgi](http://Blast.ncbi.nlm.nih.gov/Blast.cgi)).

### ***5.2.4 Bioinformatics Analysis of the Sequences from the Wastewater, Oyster and Stool Samples***

Nucleotide sequences obtained from RT-PCR assays were translated using the XPasy translation tool (<http://web.expasy.org/translate>). A multiple alignment was performed on the nucleotide and amino acid sequences using ClustalW (<http://www.ebi.ac.uk/Tools/msa/clustalw2/>). A NoV GII sequence, described by Mans *et al.* (2010) [Accession no. HQ008055.1], was used as a reference strain to compare sequence identity and similarity.

## ***5.3 Results***

### ***5.3.1 Viral RNA Extraction from the Wastewater, Oyster and Stool Samples***

RNA extracted from the wastewater, oyster and stool samples was analysed by agarose gel electrophoresis (Figure 5.1 and Figure 5.2). The concentration of the RNA present in each sample was estimated and the results are shown in Table 5.1 below.

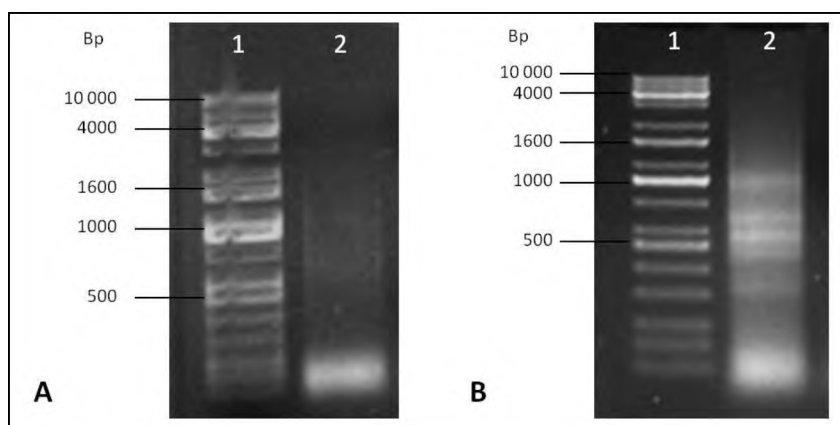


**Figure 5.1: Agarose gel electrophoresis of the viral RNA extracted from the (A) wastewater sample and (B) oyster sample. (A) Lane 1: Kapa Universal Molecular Marker and Lane 2: wastewater sample. (B) Lane 1: Kapa Universal Molecular Marker and lane 2: oyster sample.**

Lane 2 of Figure 5.1 (A) shows the presence of viral RNA, which was extracted from viral particles present in the wastewater sample. A smear of RNA can be seen from 10 000 bp to below 500 bp. Viral RNA was also successfully recovered from the viral particles present in the oyster extract as shown in lane 2, Figure 5.1 (B). A smear can be seen from 10 000 to below 500 bp and clear bands were present at approximately 1000 bp, 700 bp, 600 bp and 500 bp.

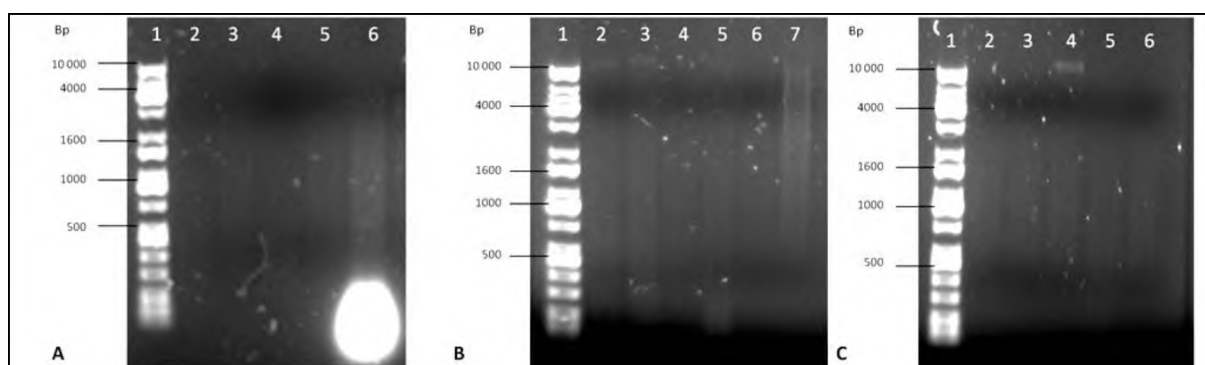


**Figure 5.2: Agarose gel electrophoresis of the viral RNA extracted from selected stool samples (A-C). (A) Lane 1: Kapa Universal Molecular Marker, lane 2: stool sample P14, lane 3: stool sample P25, lane 4: stool sample P22, lane 5: stool sample P4 and lane 6: stool sample P19. (B) Lane 1: Kapa Universal Molecular Marker, lane 2: stool sample P1, lane 3: stool sample P5, lane 4: stool sample P7, lane 5: stool sample P20, lane 6: stool sample P23 and lane 7: stool sample P30. (C) Lane 1: Kapa Universal Molecular Marker, lane 2: stool sample P12, lane 3: stool sample P13, lane 4: stool sample P15, lane 5: stool sample P24 and lane 6: stool sample P29.**

In Figure 5.2 (A), lanes 3, 5 and 6, RNA can be seen from 10 000 bp to below 500 bp with a high concentration of RNA below 500 bp, lane 6. No RNA can be seen in lanes 2 and 4.

Figure 5.2 (B) shows the presence of a clear band in lanes 2 and 3 at approximately 10 000 bp and the presence of RNA from 10 000 bp to below 500 bp, lanes 2, 3, 5 and 7. A clear band of RNA is present at 10 000 bp in lane 4 of Figure 5.2 (C) with the presence of RNA in lanes 2-6 from approximately 4000 bp to 500 bp. Table 5.1 Shows the RNA concentrations measured for all the samples.

**Table 5.1: RNA Concentrations Obtained for the Oyster, Wastewater and Stool Samples.**

Sample	RNA Concentration ng/μl	Sample	RNA Concentration ng/μl	Sample	RNA Concentration ng/μl
Oyster	110.4	P10	92.1	P21	85.3
Wastewater	137.0	P11	87.6	P22	105.2
P1	85.3	P12	126.1	P23	106.3
P2	35.4	P13	105.3	P24	110.0
P3	114.8	P14	101.3	P25	108.6
P4	127.0	P15	118.2	P26	62.0
P5	98.8	P16	73.7	P27	98.6
P6	133.5	P17	94.5	P28	102.4
P7	111.8	P18	91.7	P29	72.3
P8	86.2	P19	511.8	P30	109.4
P9	95.9	P20	105.8		

### ***5.3.2 Norovirus GII RT-PCR Assay Performed on the Wastewater and Oyster Samples***

To determine the presence of NoV GII in the wastewater and oyster samples, a nested RT-PCR was performed using the RNA extracted from the samples. This was achieved by synthesising first-strand cDNA from the RNA extracted from each sample, followed by the RT-PCR assay using primers for the N/S domain of VP1 region of the NoV genome. Figure

5.3 and Figure 5.4 show the results from the wastewater and oyster sample nested RT-PCR assays respectively.

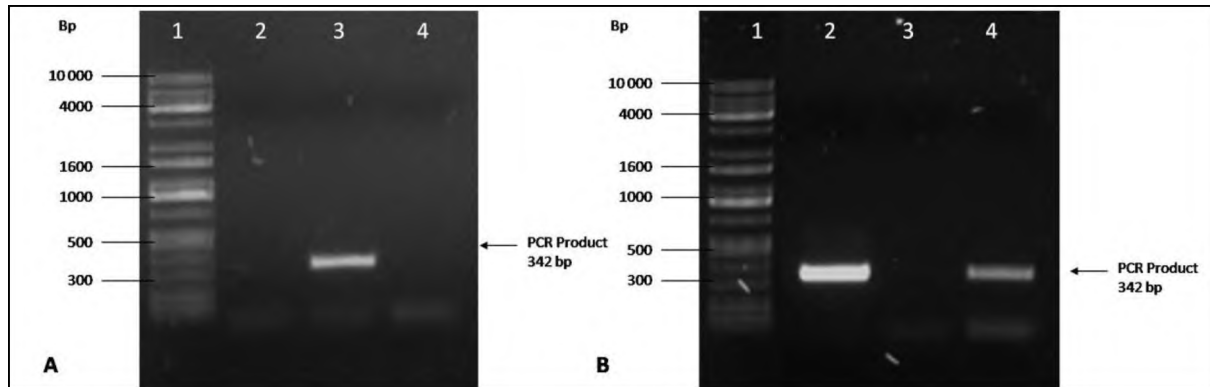


**Figure 5.3: Agarose gel electrophoresis of the wastewater NoV GII nested RT-PCR assay. (A) First round of the RT-PCR assay:** Lane 1: Kapa Universal Molecular Marker, lane 2: negative control, lane 3: positive control and lane 4: wastewater sample. **(B) Second round of the RT-PCR assay:** Lane 1: Kapa Universal Molecular Marker, lane 2: positive control, lane 3: negative control and lane 4: wastewater sample.

In the first round of the nested RT-PCR assay, Figure 5.3 (A), a clear band is present at 342 bp in the positive control, lane 3, as expected as pNoVGII was used as the template. No bands can be seen in the negative control, lane 2, or in the wastewater sample, lane 4. However, in the second round of the nested RT-PCR assay, Figure 5.3 (B), a clear band is present at 342 bp in the positive control, lane 2, and the wastewater sample, lane 4. Once again, there is no band in the negative control, lane 3.

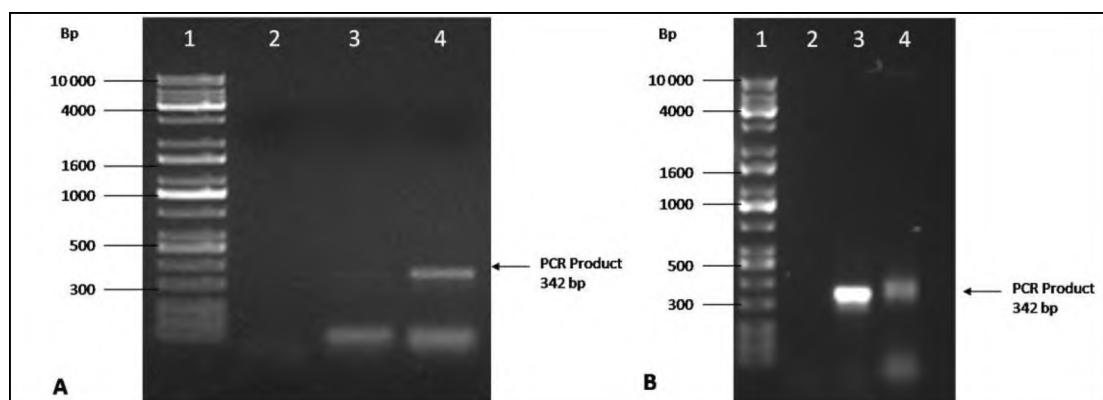


**Figure 5.4: Agarose gel electrophoresis of the oyster sample NoV GII nested RT-PCR assay. A) first round of the RT-PCR assay:** Lane 1: Kapa Universal Molecular Marker, lane 2: negative control, lane 3: oyster sample and lane 4: positive control. **B) second round of the RT-PCR assay:** Lane 1: Kapa Universal Molecular Marker, lane 2: negative control, lane 3: positive control and lane 4: oyster sample.

In Figure 5.4 (A), no bands are present in the negative control, lane 2, or the oyster sample, lane 3, but a clear band can be seen at 342 bp in the positive control, lane 4, as pNoVGII was used as the template. In the second round of the RT-PCR assay, Figure 5.4 (B), no bands were present in the negative control, lane 2, but a clear band was present at 342 bp in the positive control, lane 3, and the oyster sample, lane 4.

### 5.3.3 *Norovirus GII RT-PCR Assay Performed on the Stool Samples*

To determine the presence of NoV GII in the stool samples, a nested RT-PCR assay was performed. This was achieved by synthesising first-strand cDNA from the viral RNA extracted from the stool samples followed by a nested RT-PCR assay using the G2SKF/R primers which bind to the VP1 N/S domain region of the NoV GII genome. The results from selected samples are shown in Figure 5.5 below and Table 5.2 summarises the detection results for all stool samples.

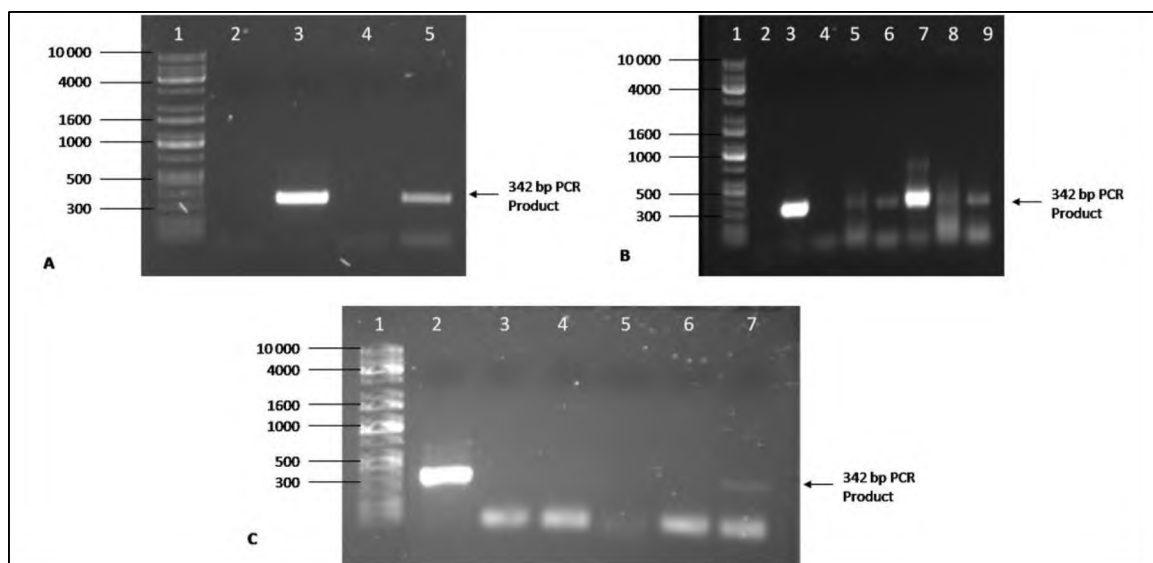


**Figure 5.5: Agarose gel electrophoresis of the NoV GII nested RT-PCR assay performed on selected stool samples. (A) Stool samples P1 and P2:** Lane 1: Kapa Universal Molecular Marker, lane 2: negative control, lane 3: positive control, lane 4: stool sample P2 and lane 5: stool sample P1. **(B) Stool samples P14 and P17- P21:** Lane 1: Kapa Universal Molecular Marker, lane 2: negative control, lane 3: positive control, lane 4: stool sample P14, lane 5: stool sample P17, lane 6: stool sample P18, lane 7: stool sample P19, lane 8: stool sample P20 and lane 9: stool sample P21. **(C) Stool samples P12, P13, P15 and P29:** Lane 1: Kapa Universal Molecular Marker, lane 2: positive control, lane 3: negative control, lane 4: stool sample P12, lane 5: stool sample P13, lane 6: stool sample P15 and lane 7: stool sample P29.

In Figure 5.5 (A), the positive control, lane 3 shows a clear band at 342 bp as expected as pNoVGII was used as the template. The negative control, lane 2, contains no bands as

expected as ddH<sub>2</sub>O was used as the template. Stool sample P2, lane 4, does not contain a 342 bp band but stool sample P1, lane 5, shows this band. Figure 5.5 (B) shows the presence of a 342 bp PCR product in the positive control, lane 3, while the negative control, lane 2 does not. Stool samples P17-P21, lanes 5-9, show the presence of a 342 bp band however, P14, lane 4, does not show this band. Figure 5.5 (C) shows a single band of 342 bp in the positive control, lane 2, and no bands in the negative control, lane 3, as expected. Stool samples P12, P13 and P15, lanes 4-6, do not show any bands but stool sample P29, lane 7, shows the presence of a band at 342 bp.

**Table 5.2: Presence of NoV GII in the Stool Samples Analysed.**

<b>Sample</b>	<b>NoV GII</b>	<b>Sample</b>	<b>NoV GII</b>	<b>Sample</b>	<b>NoV GII</b>
<b>P1</b>	Yes	<b>P11</b>	No	<b>P21</b>	Yes
<b>P2</b>	No	<b>P12</b>	No	<b>P22</b>	No
<b>P3</b>	No	<b>P13</b>	No	<b>P23</b>	No
<b>P4</b>	No	<b>P14</b>	No	<b>P24</b>	No
<b>P5</b>	Yes	<b>P15</b>	No	<b>P25</b>	No
<b>P6</b>	No	<b>P16</b>	No	<b>P26</b>	No
<b>P7</b>	Yes	<b>P17</b>	Yes	<b>P27</b>	No
<b>P8</b>	Yes	<b>P18</b>	Yes	<b>P28</b>	No
<b>P9</b>	Yes	<b>P19</b>	Yes	<b>P29</b>	Yes
<b>P10</b>	No	<b>P20</b>	Yes	<b>P30</b>	No

Using the nested RT-PCR assay, 30 stool samples were screened for NoV GII. RT-PCR products were obtained for 11 of the stool samples tested (shown in Table 5.2). The PCR products were sequenced and analysed using NCBI BLAST.

#### ***5.3.4 BLAST Analysis of the NoV GII Sequences***

Figure 6S to Figure 18S (Appendix II) show the nucleotide sequences of the RT-PCR products of wastewater, oysters and stool samples inserted into pGEM®-T Easy. The nucleotide sequences show that the RT-PCR products for NoV GII N/S Domain were correctly inserted into pGEM®-T Easy.

Table 5.3 below shows the results from the BLAST analysis of the PCR products from the NoV GII RT-PCR performed on the wastewater, oyster and stool samples. All the PCR products were determined to be NoV GII, strain GII.4. The wastewater and oyster PCR product showed a 99% identity to that of NoV GII (Accession no. KC631815.1). All but one of the PCR products from the stool samples showed a 99% identity to NoV GII (Accession no. KC631815.1), P7 showed a 98% identity to NoV GII (Accession no. KC631815.1).

**Table 5.3: The BLAST Analysis of the NoV GII PCR Products for Wastewater, Oyster and Stool Samples.**

Sample	Description	Query Coverage	E-Value	Identity	Accession No.
<b>Wastewater</b>	Norovirus Hu/GII.4MI002/2011/USAORF-1, ORF-2, and ORF-3 genes, complete cds	88%	5e-166	99%	KC631815.1
<b>Oyster</b>	Norovirus Hu/GII.4MI002/2011/USAORF-1, ORF-2, and ORF-3 genes, complete cds	94%	2e-165	99%	KC631815.1
<b>P1</b>	Norovirus Hu/GII.4MI002/2011/USAORF-1, ORF-2, and ORF-3 genes, complete cds	79%	6e-166	99%	KC631815.1
<b>P5</b>	Norovirus Hu/GII.4MI002/2011/USAORF-1, ORF-2, and ORF-3 genes, complete cds	91%	2e-169	99%	KC631815.1
<b>P7</b>	Norovirus Hu/GII.4MI002/2011/USAORF-1, ORF-2, and ORF-3 genes, complete cds	83%	5e-166	98%	KC631815.1
<b>P8</b>	Norovirus Hu/GII.4MI002/2011/USAORF-1, ORF-2, and ORF-3 genes, complete cds	92%	5e-171	99%	KC631815.1
<b>P9</b>	Norovirus Hu/GII.4MI002/2011/USAORF-1, ORF-2, and ORF-3 genes, complete cds	92%	2e-169	99%	KC631815.1
<b>P17</b>	Norovirus Hu/GII.4MI002/2011/USAORF-1, ORF-2, and ORF-3 genes, complete cds	78%	5e-166	99%	KC631815.1
<b>P18</b>	Norovirus Hu/GII.4MI002/2011/USAORF-1, ORF-2, and ORF-3 genes, complete cds	87%	6e-165	99%	KC631815.1
<b>P19</b>	Norovirus Hu/GII.4MI002/2011/USAORF-1, ORF-2, and ORF-3 genes, complete cds	88%	5e-166	99%	KC631815.1
<b>P20</b>	Norovirus Hu/GII.4MI002/2011/USAORF-1, ORF-2, and ORF-3 genes, complete cds	79%	1e-167	99%	KC631815.1
<b>P21</b>	Norovirus Hu/GII.4MI002/2011/USAORF-1, ORF-2, and ORF-3 genes, complete cds	79%	1e-167	99%	KC631815.1
<b>P29</b>	Norovirus Hu/GII.4MI002/2011/USAORF-1, ORF-2, and ORF-3 genes, complete cds	80%	1e-167	99%	KC631815.1

### 5.3.5 Multiple Alignment of the NoV GII Sequences

A multiple sequence alignment of the nucleotide sequences (Figure 19S, Appendix II) and amino acid sequences from the NoV GII positive wastewater, oyster and stool samples was performed using ClustalW, along with the NoV GII reference sequence reported by Mans *et al.* (2010) (Accession no. HQ008055.1). Figure 5.6 shows a multiple alignment of the amino acid sequences. Each amino acid group is represented in its own colour as follows: the amino acids with a positively charged side chain are shown in dark blue (R and K) or pink (H), the negatively charged side chains are shown in red (D and E). The amino acids with polar uncharged side chains are light blue (S, T, N and Q) while the amino acids with hydrophobic side chains are shown in dark green (L, M, I, V and W) or aqua (A, F and Y). The special cases are represented by grey for P and yellow for G. Table 5.4 shows the percentage identity and similarity of the amino acids sequences when compared to the reference strain and the NoV GII positive stool sample (positive control). Table 5.5 shows the amino acid changes between the reference strain, the NoV GII positive control (provided by Maureen Taylor), wastewater, oyster and stool sample amino acid sequences.

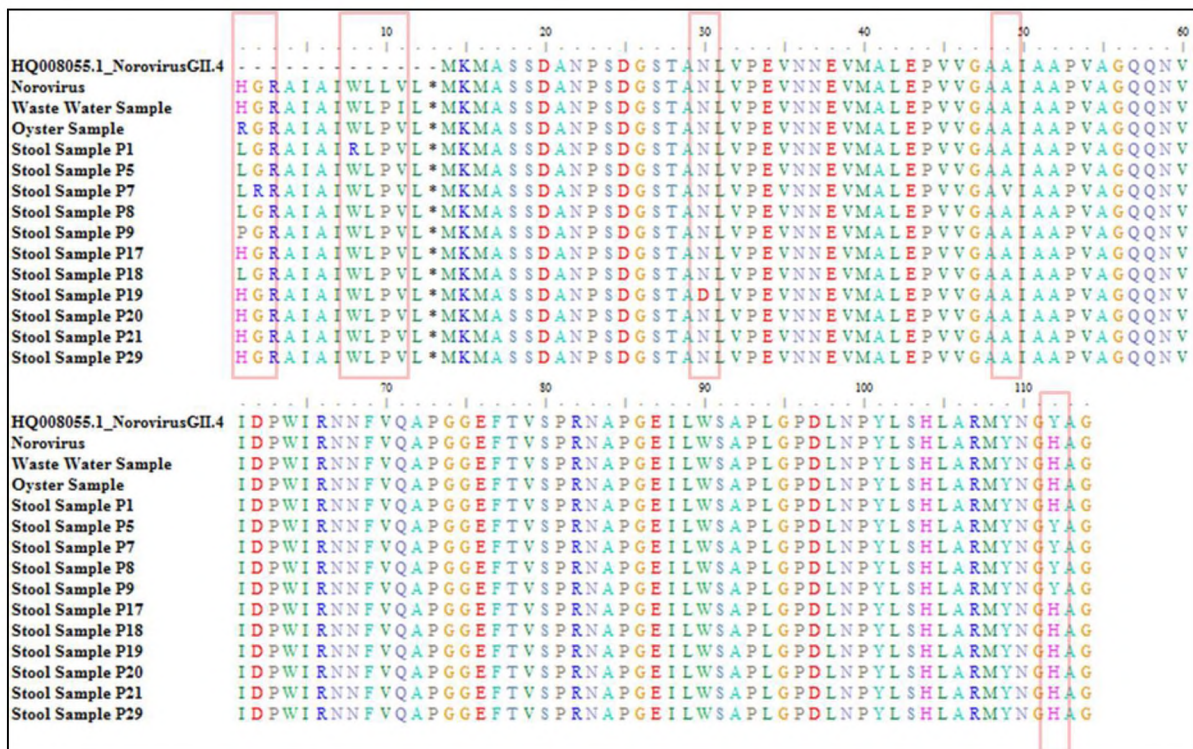


Figure 5.6: Multiple amino acid sequence Alignment of NoV GII sequences in comparison to the reference sequence (Accession no. HQ008055.1).

The VP1 N/S domain amino acid sequences from the NoV GII positive control, wastewater, oyster and stool samples show a high identity to the NoV GII reference strain (Accession no. HQ008055.1) as can be seen in Figure 5.6. The multiple sequence alignment showed a sequence identity and similarity of 88% - 89% between the NoV positive control, wastewater, oyster and stool samples sequences and the reference sequence (Accession no. HQ008055.1), as shown in Table 5.4. While the wastewater, oyster and stool samples sequences showed a 96% - 99% sequence identity and similarity to the NoV GII positive control sequence. There are seven amino acid changes present amongst the sequences, as shown in Table 5.5 below. Four of the amino acid changes are present before the start of the reference strain, the norovirus sequence from the pNoVGII was used as the reference for these changes as it was used as the positive control for the RT-PCR assay.

**Table 5.4: The Sequence Identity and Similarity of the NoV GII Amino Acid Sequences.**

	Sequence Identity		Sequence Similarity	
	HQ008055.1	NoV	HQ008055.1	NoV
<b>HQ008055.1</b>	-	88%	-	89%
<b>NoV</b>	88%	-	89%	-
<b>Wastewater</b>	88%	98%	89%	98%
<b>Oyster</b>	88%	98%	89%	98%
<b>P1</b>	88%	96%	88%	96%
<b>P5</b>	89%	97%	89%	97%
<b>P7</b>	88%	96%	89%	96%
<b>P8</b>	89%	97%	89%	97%
<b>P9</b>	89%	97%	89%	97%
<b>P17</b>	88%	99%	89%	99%
<b>P18</b>	88%	98%	89%	98%
<b>P19</b>	88%	99%	89%	99%
<b>P20</b>	88%	98%	88%	98%
<b>P21</b>	88%	99%	89%	99%
<b>P29</b>	88%	99%	89%	99%

**Table 5.5: Amino Acid Changes in the Nov GII Sequences for the Nov GII Positive Control, Wastewater, Oyster and Stool Samples.**

Sequence	Amino Acid Change			
NoV	112H	→	Y	
Wastewater	10L	→	P	112H → Y
Oyster	1H	→	R	10L → P 112H → Y
P1	1H	→	L	8W → R 10L → P 112H → Y
P5	1H	→	L	10L → P
P7	1H	→	L	2G → R 10L → P 49A → V
P8	1H	→	L	10L → P
P9	1H	→	P	10L → P
P17	10L	→	P	112H → Y
P18	1H	→	L	10L → P 112H → Y
P19	10L	→	P	30N → D 112H → Y
P20	10L	→	P	112H → Y
P21	10L	→	P	112H → Y
P29	10L	→	P	112H → Y

Table 5.5 shows the seven amino acid changes seen in the amino acid sequences of the NoV positive control, wastewater, oyster and stool sample. The first amino acid change is histidine (H) to arginine (R), lysine (L) or proline (P), resulting in either no change in amino acid

group (H to R), or a change from a positively-charged side chain to a hydrophobic side chain (L) or the special side chains (P). The next change observed is that of glycine (G) to arginine, which results in a change from a special side chain to a positively charged side chain. The third amino acid substitution is that of tryptophan (W) with arginine, resulting in the change of a hydrophobic side chain in to a positively charged side chain. Lysine to proline is the next change observed and results in a change from a hydrophobic to a special side chain. The fifth amino acid substitution is that of asparagines (N) with aspartic acid (D) resulting in a side chain change of polar uncharged to negatively charged. The sixth substitution is Alanine (A) and Valine (V), both of which are amino acids with hydrophobic side chains. The last change is that of histidine to tyrosine (Y) which results in a change from a positively charged side chain to a hydrophobic side chain. These amino acid substitutions may indicate seasonal variation of the GII.4 strain of NoV.

#### **5.4 Discussion**

Several studies have shown that NoV has been isolated it from a variety of sources including wastewater, shellfish and stool samples from symptomatic patients. RT-PCR assays were therefore developed to detect its presence in the wastewater, oyster and stool samples used in this study. Using a two-step nested RT-PCR assay, NoV of the genogroup GII was successfully identified in the wastewater, oyster and 11 of the stool samples. BLAST analysis of the nucleotide sequences showed that they belonged to the NoV GII.4 strain. The nucleotide sequences from all the samples were translated into amino acid sequences and a multiple alignment was performed. The multiple alignment showed that the sequences had an 88-89% identity and an 88-89% similarity of amino acids to the reference strain (Accession no. HQ008055.1) and an identity of 96-99% and similarity of 96-99% to that of the NoV GII positive control.

NoV is commonly identified in a variety of samples including those of wastewater, shellfish and stool samples through the use of RT-PCR assays. As wastewater is most likely to contain NoV GII, studies have used it as source for testing the presence of this enteric virus. Da Silver *et al.* (2007) was able to isolate NoV GII from 71 of 81 samples of influent collected from four wastewater treatment plants around France. The assay chosen in this study was a

conventional RT-PCR assay, whereas da Silver *et al.* (2007) used a real-time RT-PCR assay and the primer set QNIF2d/ COG2R and the QNIFS probe.

Atmar *et al.* (1993) developed a method for the detection of NoV from shellfish such as oysters using the whole tissue and RT-PCR assays. In a later study, Atmar *et al.* (1995), showed an increase in sensitivity when the stomach and digestive tracts of oysters and hard-shell clams was used rather than the whole tissues (Atmar *et al.*, 1995). Another study, by Loisy *et al.* (2005), was able to identify NoV GII from 46 out of 150 naturally-contaminated oyster samples using the G2SKF/R primer set in a RT-PCR assay. They were, however, able to identify a higher number (60 of 150) of NoV GII positive samples when using a real-time RT-PCR assay with the primer set the primer set QNIF2d/ COG2R and the QNIFS probe.

NoV has been found in stool samples all over the world including South Africa. Both Mans *et al.* (2010) and Wolfaard *et al.* (1997) used RT-PCR assays for the identification of NoV from stool samples. Wolfaard *et al.* (1997) was able to identify NoV GII from 29 of 1296 stool samples collected in South Africa. However, the primer set used in this RT-PCR was NV36/NV35 and NV36/NV51 instead of the G2SK F/R primer set. Mans *et al.* (2010) identified NoV GII in 35 of 245 stool samples using a real-time RT-PCR assay. Genotyping was performed on the NoV positive samples using the G2SK F/R primers and conventional RT-PCR and eight strains were identified. Of these GII.4 (48%), GII.6 (17 %) and GII.1 (9%) were detected most frequently (Mans *et al.*, 2010). This study differs from our own as once again only conventional RT-PCR was used to detect NoV GII from the stool samples. Currently, NoV GII.4 is the most prevalent in South Africa. This is shown by the studies performed by Mans *et al.* (2010) and Mans *et al.* (2013), where NoV was identified from water sources in Gauteng, South Africa. This corresponds to the results in this study, where all NoV positive samples were shown to be NoV GII.4.

In conclusion, the wastewater, oyster and 11 of 30 stool samples showed the presence of NoV GII.4 when screened using the RT-PCR assay designed by Kojima *et al.* (2002), which are highly similar to that of the reference strain (Accession no. HQ008055.1) and the NoV GII positive stool sample. The next chapter discusses the general conclusions and future work of this study.

## ***Chapter 6: General Conclusions and Future Work***

The overall aim of this study was to develop sample preparation techniques, including TEM, PEG precipitation, RNA extraction and RT-PCR assays for the identification of NoV, AiV and SAFV from a variety of samples, including wastewater, oysters and clinical samples. Using TMEV, as this virus can be grown in large volumes in tissue culture in the laboratory, it was determined that the use of filter-sterilisation and VIVA spin columns in conjunction with PEG precipitation, with PEG 6000 at a final concentration of 8% and NaCl at a final concentration of 0.25 M, yielded a high number of virus particles. TEM analysis was then used to screen for the presence of virus particles and showed small, 30 nm, non-enveloped viruses, from which RNA was extracted. Using this RNA, RT-PCR assays were developed for the 2B and VP1 coding regions of TMEV and the specificity was determined by detection of a RT-PCR product from as little as 2 ng/ $\mu$ l of RNA. In order to use the RT-PCR assay for the detection of viruses from the selected samples a positive control is required, this was successfully developed through the use of *in vitro* transcribed RNA from the pTMEV plasmid.

As stated previously, TMEV can be grown in large amounts in cell culture, which allows high volumes of RNA to be extracted from the culture. This is not the case for the environmental and clinical samples as it is unknown which viruses are present or if they will grow in cell culture. The number of virus particles present and extracted from the environmental and clinical samples are thus expected to be much lower than what is produced in cell culture, resulting in the extraction of lower amounts of RNA (Lewis *et al.*, 2010). TMEV is, however, a good model for developing the techniques chosen in this study.

While the VIVA spin columns have a 95% recovery rate, a portion of the viral particles cannot be recovered from the membrane. PEG precipitation was first shown to concentrate small, round viruses by Hebert (1963). Lewis and Metcalf (1988) utilised 8% PEG 6000 to concentrate hepatitis A virus, human rotavirus simian rotavirus and poliovirus from fresh water, estuarine water and oysters, and showed that PEG precipitation was more effective than organic flocculation for the concentration of hepatitis A virus and rotavirus. Lewis *et al.* (2010) utilised PEG precipitation for the recovery of enteroviruses and F-specific

bacteriophages from the digestive tracts of mussels and oysters. Due to the successful use of PEG precipitation for the concentration of viral particles, this technique was used in this study. PEG precipitation does, however, result in the loss of virus particles. While both of these techniques result in a lower concentration of virus particles, the recovered RNA has a higher concentration when compared to samples which did not undergo PEG precipitation. Thus, indicating the importance of concentrating the virus particles for this study.

Using the methods described above, RT-PCR assays were developed for the identification of NoV GII, AiV and SAFV and the sensitivity of these assays was determined to be 3.4 ng/ $\mu$ l of RNA for NoV GII, 3.5 ng/ $\mu$ l of RNA for AiV 5'UTR, 0.0 ng/ $\mu$ l of RNA for AiV 3CD and 4.8 ng/ $\mu$ l of RNA for SAFV. The sensitivity was determined as the concentration of the RNA extracted from the samples is expected to be lower than that of the concentration of the *in vitro* transcribed RNA used to develop the RT-PCR assays. If the RNA concentration from the samples is lower than what the RT-PCR assays can detect, a false negative result may be produced. By determining the RNA concentration in the samples, these false negatives could be avoided.

These RT-PCR assays were developed based on studies published by Kojima *et al.* (2002), Drexler *et al.* (2011), Pham *et al.* (2007) and Blinkova *et al.* (2009). There were, however, variations in the RT-PCR assay technique developed in this study compared to those in the literature. For example: Kojima *et al.* (2002) used one round of RT-PCR assays to detect NoV GII, where as nested RT-PCR assay was used in this study. This was due to the inability of the first round of the RT-PCR assay to detect an amplicon, which may be due to a lower amount of the NoV cDNA in the samples. For the AiV 3CD RT-PCR assay, Pham *et al.* (2007) used a nested RT-PCR assay where the first round amplified a 519 bp fragment of the 3CD junction of AiV and the second round amplified a 266 bp fragment within the 519 bp amplicon. In this study, a RT-PCR assay was developed for the amplification of the 266 bp fragment of the AiV 3CD junction, based on the work of Pham *et al.* (2007), as the 266 bp PCR product was available and could be used as a positive control for the RT-PCR assay. The 519 bp primers, developed by Pham *et al.* (2007), were not used in this study because they do not bind to the 266 bp PCR product which was available and a 519 bp PCR product

was not available. Therefore a positive control for the 519 bp RT-PCR assay could not be developed and the results of the 519 bp AiV 3CD RT-PCR assay could not be validated.

The PCR products from the NoV GII, AiV 5'UTR and AiV 3CD RT-PCR assays were cloned into the vector pGEM®-T Easy and RNA was transcribed *in vitro*. The RNA was then used for the development of the positive controls for the RT-PCR assays. The SAFV full cDNA sequence in pSAFV did not have to be cloned into pGEM®-T Easy, as pSP72+ also contains the T7 promoter (Promega, 2006). Using *in vitro* transcribed RNA from pNoVGII, pAiV5'UTR, pAiV3CD and pSAFV, positive controls for the RT-PCR assays were successfully developed allowing for the screening of the environmental and clinical samples for the presence of these viruses. Positive and negative controls are important for PCR assays as they validate the results from the RT-PCR assays. Negative controls detect contamination of reagents and non-specific amplification both of which may produce false positive results. Positive controls are used to verify negative amplification results as well as detecting non-specific amplification, by ensuring any PCR products correspond to the known sequence, which is included in the positive control reaction. Pham *et al.* (2010) used negative controls consisting of either distilled water or samples with mono-infections of group A rotavirus, adenovirus, norovirus (GI and GII), sapovirus or astrovirus for monoplex and multiplex RT-PCR assays. Aichi virus, human parechovirus, enteroviruses and human bocavirus sequences were used as positive controls, either as single virus positive controls or mixed virus positive controls (Pham *et al.* (2010). Drexler *et al.* (2008) used a SAFV sample as a positive control in a RT-PCR assay for the identification of SAFV-like viruses from 844 samples from patients from Germany and Brazil, but no negative controls were recorded in this publication.

The following experiments focused on the preparation of the wastewater, oysters and stool samples using the filter-sterilisation, concentration and PEG precipitation followed by TEM analysis. TEM showed a variety of particles in the samples, including small, 30-40 nm, round, non-enveloped particles, indicative of picornaviruses and caliciviruses. RNA was extracted from the wastewater, oysters and stool samples, thus the first three aims, 1) the preparation and screening of the clinical and environmental samples by TEM, 2) extraction of viral RNA from the selected samples and 3) the development of the RT-PCR assays and associated positive controls for NoV GII, AiV 5'UTR, AiV 3CD and SAFV were

successfully achieved. Achieving these first three aims is important as the RT-PCR assays cannot be performed on the wastewater, oyster and stool samples if, firstly contaminants which may affect downstream applications are present and, secondly, the virus particles are either not present or do not correspond to the size and morphology of the picornaviruses and caliciviruses. Thirdly, viral RNA is not extracted or does not meet the minimum amount required to perform the RT-PCR assay. Finally, the RT-PCR assays, based on the work of Kojima *et al.* (2002), Drexler *et al.* (2011) and Pham *et al.* (2007), have to be optimised and the positive controls have to be developed to ensure that the results of the RT-PCR assays performed on the environmental and stool samples are correct.

The fourth aim of this study was to perform RT-PCR assays for the amplification of SAFV, AiV and NoV sequences from the wastewater, oyster and stool samples using the extracted viral RNA. Unfortunately, this goal was not achieved due to time constraints, and is recommended for further research. The only RT-PCR assay performed on the wastewater, oysters and stool samples was the NoV GII, and this showed the presence of this virus in the wastewater, oysters and 11 of the 30 stool samples. The strain detected in all the samples was determined to be NoV GII.4. While it was possible to detect NoV GII in these samples, it would also be important to detect NoV GI as these strains are also a common cause of gastroenteritis in many countries including South Africa (Mans *et al.*, 2010). NoV GI strains show a similar detection rate to the NoV GII strains (31% GII vs. 29% GII), as well as mixed infections (GI and GII) in water sources in South Africa (Mans *et al.*, 2013).

A preliminary experiment was performed in this study to develop a RT-PCR assay for the amplification of NoV GI using the GISK primer set and RT-PCR assay described by Kojima *et al.* (2002), however no clear RT-PCR product was produced and the correct conditions of the RT-PCR assay could not be determined. Future work will thus be required to firstly, determine the correct conditions for the NoV GI RT-PCR assay and secondly, perform a preliminary study involving the screening of the wastewater, oyster and stool samples for NoV GI, SAFV and AiV. This would determine if these RT-PCR assays are able to detect these viruses from a variety of samples in South Africa.

While RT-PCR assays are commonly used for the identification of viruses, such as AiV, SAFV and NoV, many international research groups have chosen a variety of other techniques, such as real-time RT-PCR assays, clone libraries and next generation sequencing to identify viruses associated with gastroenteritis. Real-time RT-PCR assays have shown to be more sensitive and less labour intensive than traditional RT-PCR assays. This is due to the ability to detect amplicons using primers and either a fluorescent probe or dye, allowing not only for the detection of amplicons at a lower concentration but also the detection of the amplicons while the RT-PCR assay is in progress (Staggemeier *et al.*, 2012). Fluorescent dyes, such as SYBR® Green, bind non-specifically to dsDNA and produce a high level of fluorescence which is then detected. The fluorescent probe contains a fluorophore which is bound to an oligonucleotide sequence which binds to a specific DNA sequence and fluorescence only occurs once the probe has bound to the target region. Due to fluorescent probes sequence specificity, it can be used in multiplex qPCR assays unlike fluorescent dyes. Nielsen *et al.* (2013) used real-time RT-PCR assays for the detection of both AiV and SAFV along with two other viruses in 454 children screened both routinely (1007 samples) and during a gastroenteritis episode (386 samples). AiV and SAFV were detected in 6 and 38 samples, respectively, indicating the ability of this technique to detect known viruses. qRT-PCR assays are not only used to detect viral sequences, but can also be used to genotype the viruses (Liao *et al.*, 2013; Nakatani *et al.*, 2010). Genotyping of viruses can be achieved by designing primers which bind to conserved regions of the viral genome and fluorescent probes which bind to polymorphic regions of the viral genome. Different genotypes can be distinguished by using a different fluorophore for each probe allowing for detection and genotyping to be performed in one reaction (Liao *et al.*, 2013). Another method which can be employed for genotyping used a melting temperature curve, where probes are designed with different fluorophores and melting temperatures (Nakatani *et al.*, 2010). During the qPCR the annealing temperature will be ramped up from the lowest melting temperature to the highest with several amplification steps at each chosen temperature. qPCR assays are also used to quantify the number of DNA or RNA copies in a sample. This is achieved by comparison of the fluorescence observed in a unknown sample to that of a dilution series of standards with a known concentration. Drexler *et al.* (2011) utilised real-time RT-PCR assays not only for the detection of AiV from stool samples but also the quantification of viral concentrations. They showed the presence of 10 AiV positive samples out of 499 stool samples with a viral concentration of  $1.08 \times 10^2$  to  $1.30 \times 10^{12}$  RNA copies/g stool (Drexler *et al.*, (2011).

Determining the viral concentration can help in understanding the virulence of a virus as well as monitoring the therapy of a viral infection.

It is often the case, however, that the viral agent, such as AiV, SAFV and enteroviruses, which may be the cause of gastroenteritis is unknown and screening for each of the potential viruses by RT-PCR assay would be very labour intensive. It is possible to perform one RNA extraction and utilise this RNA for more than one RT-PCR assay, as the RNA is often eluted into approximately 60  $\mu$ l and only a portion of this is required for a single reaction, depending on the concentration of the extracted RNA. Single RT-PCR assays or multiple multiplex RT-PCR assays which may take several hours to run will, however, have to be performed and analysed for each potential virus making these techniques labour intensive (Garibyan and Avashi *et al.*, 2013). Techniques which allow for non-selective sequencing of the cDNA present in a sample include clone libraries and next generation sequencing both of which are better adapted for searching for unknown viruses (Finkbeiner *et al.*, 2008; Storch, 2000).

Clone libraries are created by cloning DNA, or cDNA which is synthesised from viral RNA, into a cloning vector followed by sequencing of the plasmid. This provides a broad view of what cDNA is present in the sample (Finkbeiner *et al.*, 2008). This technique can be very labour intensive as each new plasmid has to be selected for, extracted and sequenced (Finkbeiner *et al.*, 2008). If the clone library includes a large sample size, this could potentially be very costly as well. Due to the number of samples required and the costs involved, this technique was not selected for this study.

Next generation sequencing also provides a broad range of cDNA sequences present in the samples but, unlike clone libraries, next generation sequencing is able to sequence more than one sample at once and is therefore less labour intensive (Finkbeiner *et al.*, 2008). This technique involves the synthesis of cDNA, from extracted viral RNA, followed by sequencing. While this is a good technique and could have been applied in this study, it was not used as it is presently a costly technique, and the RNA concentrations and quality did not meet the requirements when a FlashGel analysis was performed.

With over 3000 reported deaths per year in children under the age of five attributed to gastroenteritis in South Africa and many more hospitalisations, it is important to determine the cause of the disease (WHO, 2015). Although rotavirus is the leading cause of this disease, the implementation of a vaccination programme in 2009 has led to a decrease of 65% in the number of rotavirus positive cases (Tshangela *et al.*, 2012). While NoV is the second leading cause of this disease, the actual number of cases is unknown since, unlike rotavirus, routine testing and surveillance is not performed (Mans *et al.*, 2010). The surveillance of rotavirus has shown that many cases are of unknown aetiology (reviewed by Knox *et al.*, 2012). These cases may be caused by viruses such as AiV, which has a high prevalence of disease, SAFV or other viruses associated with gastroenteritis. Through the use of the techniques developed in this study, it would be possible to identify viruses associated with gastroenteritis in South Africa which would allow for better surveillance of this disease. Vaccines could potentially be developed for viruses which are shown to have a high burden of disease allowing for the decrease of the burden of this disease in South Africa.

Other future work should consider looking at improving sample collection and preparation in order to increase the number of virus particles present in the samples. This may include utilising different collection methods, such as swabbing the grids and other surfaces at wastewater treatment plants rather than collecting wastewater; or increasing the amount of the sample used in the case of oysters and stool samples. Finally, the future work would have to include an increase in sample size. While NoV has a high detection rate in stool and other samples, the same cannot be said for SAFV or AiV. Pham *et al.* (2007) had a sample size of 912 stool samples for the study on the identification of AiV from patients from Japan, Bangladesh, Thailand and Vietnam. In this study, a detection rate of 3.1% was reported, where AiV was only detected in 28 of these samples. Drexler *et al.* (2011) showed a similar detection rate of 2% (10 of 499 stool samples) when determining the shedding concentrations of AiV from patients in northern Germany and Chuchaona *et al.* (2016) showed a detection rate of 2.6 % (24 of 923 stool samples) when determining the epidemiology of AiV in children admitted to hospital with gastroenteritis in Thailand. SAFV has a similar detection rate shown by Nielsen *et al.* (2012) where SAFV was detected in 38 of 1393 (2.7%) samples screened, but AiV was only detected in six of all the samples (0.4%) (Nielsen *et al.*, 2012). Khamrin *et al.* (2011), showed a similar detection rate of 2.7% (4 of 150 samples) when detecting SAFV from children with diarrhoea in Thailand. Increasing the sample size used

would increase the probability of detecting these and other viruses, thus aiding in the study of the viral causative agents associated with gastroenteritis.

In conclusion, this study successfully prepared the rotavirus-negative stool samples, wastewater and oyster samples, showed the presence of viral particles by TEM analysis and successfully extracted RNA from these samples. The first two aims of this study were thus achieved. RT-PCR assays were successfully developed for the amplification of NoV GII N/S domain, AiV 5'UTR, AiV 3CD and SAFV 2C sequences, along with the corresponding positive controls, successfully fulfilling the third aim of this study. The fourth aim was to screen the wastewater, oyster and stool samples for the presence of NoV GII, AiV and SAFV utilising the developed RT-PCR assays. This aim was only partially achieved as the samples were only screened for the presence of NoV GII and not AiV and SAFV due to time constraints. This study can contribute to further research as it has developed sample preparation techniques which allow for the successful extraction of viral particles and RNA from selected samples as well as RT-PCR assays and positive controls which allow the screening of samples for the presence of AiV, NoV GII and SAFV. All of the methods can be applied to other samples allowing for further study of the presence of AiV and SAFV in South Africa.

## *References*

- Agilent Technologies Inc. (2008).** pBluescript II Phagemid Vectors Instruction Manual, 1-23.
- Anderson, E. J. & Weber, S. G. (2004).** Rotavirus Infections in Adults. *Lancet Infectious Disease* **41**, 91-99.
- Arias, C.F. & DuBois, R. M. (2017).** The Astrovirus Capsid: A Review. *Viruses* **9**, 15.
- Atmar, R. L., Metcalf, T. G., Neill, F. H. & Estes, M. K. (1993).** Detection of enteric viruses in oysters by using the polymerase chain reaction. *Applied and Environmental Microbiology* **59**, 631–635.
- Atmar, R. L., Neill, F. H., Romalde, J. L., Le Guyader, F., Woodley, C. M., Metcalf, T. G. & Estes, M. K. (1995).** Detection of Norwalk Virus and Hepatitis A Virus in Shellfish Tissue with the PCR. *Applied and Environmental Microbiology* **61**, 3014-3018.
- Ball, A. (2007).** Virus Replication Strategies. In *Fields' Virology*, volume 1, 5th edition, pp.119-140. Edited by Howley, P. M. and Knipe, D. M. Philadelphia: USA. Lippincott Williams & Wilkins.
- Bennett, B. (1998).** Gastroenteritis. *Medical Update for Psychiatrists* **4**, 95-98.
- Berk, A. J. (2007).** *Adenoviridae: The Viruses and Their Replication*. In *Fields' Virology*, volume 2, 5<sup>th</sup> edition, pp.2355-2394. Edited by Howley, P. M. and Knipe, D. M. Philadelphia: USA. Lippincott Williams & Wilkins.
- Bernstein, D. I. (2009).** Rotavirus Overview. *The Pediatric Infectious Disease Journal* **28**, S50-S53.
- Bernstein, D. I., Atmar, R. L., Lyon, G. M., Treanor, J. J., Chen, W. H., Jiang, X., Vinjé, J., Gregoricus, N., Freck, R. W. & other authors. (2015).** Norovirus vaccine against experimental human GII.4 virus illness: a challenge study in healthy adults. *Journal of Infectious Diseases* **6**, 870-878.
- Besser, R. E. (1999).** *Escherichia coli* O157:H7 Gastroenteritis and the Hemolytic Uremic Syndrome: An Emerging Infectious Disease. *Annual Review of Medicine* **50**, 355-367.
- Bibby, K. (2013).** Metagenomic Identification of viral pathogens. *Trends in Biotechnology* **31**, 275-279.

**Blinkova, O., Rosario, K., Li, L., Kapoor, A., Slikas, S., Bernardin, F., Breitbart, M. & Delwart, E. (2008).** Frequent Detection of Highly Diverse Variants of *Cardiovirus*, *Cosavirus*, *Bocavirus* and *Circovirus* in Sewage Samples Collected in the United States. *Journal of Clinical Microbiology* **47**, 3507-3513.

**Blinkova, O., Kapoor, A., Victoria, J., Jones, M., Wolfe, N., Naeem, A., Shaukat, S., Sharif, S., Alam, M. M. & other authors. (2009).** Cardioviruses are Genetically Diverse and Cause Common Enteric Infections in South Asian Children. *Journal of Virology* **83**, 4631-4641.

**Bosch, A., Pintó, R. M. & Guix, S. (2014).** Human Astroviruses. *Clinical Microbiology Reviews* **27**, 1048-1074.

**Campbell, A. M. (2007).** Bacteriophages. In *Fields' Virology*, volume 1, 5<sup>th</sup> edition, pp.769-794. Edited by Howley, P. M. and Knipe, D. M. Philadelphia: USA. Lippincott Williams & Wilkins.

**Casas, N. & Sunén, E. (2001).** Detection of Enterovirus and Hepatitis A Virus RNA in Mussels (*Mytilus* spp.) by Reverse Transcriptase-Polymerase Chain Reaction. *Journal of Applied Microbiology* **90**, 89-95.

**Chang, J. -T., Chen, Y. -S., Chen, B. -C., Chao, D. & Chang, T. -H. (2013).** Complete Genome Sequence of the First Aichi Virus Isolated in Taiwan. *Genome Announcements* **1**, 1.

**Chau, K. B., Voon, K., Yu, M., Ali, W. N. A. W., Kasri, A. R. & Wang, L. F. (2011).** Saffold Virus Infection in Children, Malaysia 2009. *Emerging Infectious Diseases* **17**, 1562-1564.

**Cohen, C., du Plessis, D., Frean, J., Keddy, K., Kistiah, K., Kruger, T., Mogoye, B., Moyes, J., Msimang, V. & other authors. (2010).** Rotavirus Surveillance in South Africa, 2009. *Communicable Disease Surveillance Bulletin* **8**, 11-14.

**Chuchaona, W., Khamrin, P., Yodmeeklin, A., Kumthip, K., Saikruang, W., Thongprachum, A., Okitsu, S., Ushijima, H. & Maneekarn, N. (2016).** Detection and characterization of Aichi virus 1 in pediatric patients with diarrhea in Thailand. *Journal of Medical Virology* **88**, 1-5.

**da Silva, A. K., Le Saux, J. –C., Parnaudeau, S., Pommepuy, M., Elimelech, M. & Le Guyader, F. S. (2007).** Evaluation of Removal of Noroviruses during Wastewater Treatment, Using Real-Time Reverse Transcription-PCR: Different Behaviours of Genogroups I and II. *Applied and Environmental Microbiology* **73**, 7891-7897.

**Dennehy, P. H. (2008).** Rotavirus Vaccines: an Overview. *Clinical Microbiology Reviews* **21**, 198-208.

**Di Martino, B., Di Profio, F., Ceci, C., Di Felice, E. & Marsillio, F. (2013).** Molecular detection of Aichi virus in raw sewage in Italy. *Archives of Virology* **158**, 2001-2005.

**Dinges, M. M., Orwin, P. M. & Schlievert, P. M. (2000).** Exotoxins of *Staphylococcus aureus*. *Clinical Microbiology Reviews* **13**, 16-34.

**Doerfler, W. (1996).** Adenoviruses. In *Medical Microbiology*, 4th edition, Chapter 67. Edited by Baron, S. Galveston: USA. University of Texas Medical Branch at Galveston.

**Donaldson, E. F., Lindesmith, L. C., LoBue, A. D. & Baric, R. S. (2010).** Viral shape-shifting: norovirus evasion of the human immune system. *Nature Reviews Microbiology* **8**, 231-241.

**Drexler, J. F., de Souza Luna, L. K, Stöcker, A., Almeida, P. S., Ribeiro, T. C. M., Petersen, N., Herzog, P., Pedrosa, C., Huppertz, H. I. & other authors (2008).** Circulation of 3 Lineages of a Novel Saffold Cardiovirus in Humans. *Emerging Infectious Disease* **14**, 1398-1405.

**Drexler, J. F., Baumgarte, S., de Souza Luna, L. K., Eschbach-Bludau, M., Lukashev, A. N. & Drosten, C. (2011).** Aichi Virus Shedding in High Concentrations in Patients with Acute Diarrhea. *Emerging Infectious Disease* **17**, 1544-1548.

**Eden, J- S., Bull, R. A., Tu, E., McIver, C. J., Lyon, M. J., Marshall, J. A., Smith, D. W., Musto, J., Rawlinson, W. D. & White, P. A. (2010).** Norovirus GII.4 Variant 2006b Caused Epidemics of Acute Gastroenteritis in Australia During 2007 and 2008. *Journal of Clinical Virology* **49**, 265-271.

**Edwards, R. A. & Rohwer, F. (2005).** Virus Metagenomics. *Nature Reviews Microbiology*, 6-11.

**Ehlers, M. M., Grabow, W. O. K. & Pavlov, D. N. (2005).** Detection of enteroviruses in untreated and treated drinking water supplies in South Africa. *Water Research* **39**, 2253-2258.

- Elnifro, E. M., Ashshi, A. M., Cooper, R. J. & Klapper, P. E. (2000).** Multiplex PCR: Optimization and Application in Diagnostic Virology. *Clinical Microbiology Reviews* **13**, 559-570.
- Esposito, S., Ascolese, B., Senatore, L. & Codecà, C. (2013).** Pediatric norovirus infection. *European Journal of Clinical Microbiology* **33**, 285-290.
- Ferson, M. J., Ressler, K.-A., McIver, C. J., Isaacs, M. & Rawlinson, W. D. (2000).** Norwalk-like virus as a cause of a gastroenteritis outbreak in a childcare centre. *Australian and New Zealand Journal of Public Health* **24**, 342-343.
- Finkbeiner, S. R., Allred, A.F., Tarr, P. I., Klein, E. J., Kirkwood, C. D. & Wang, D. (2008).** Metagenomic Analysis of Human Diarrhea: Viral Detection and Discovery. *PLoS Pathogens* **4**, 1-9.
- Formiga-Cruz, M., Hundesa, A., Clemente-Casares, P., Albiñana-Gimenez, N., Allard, A. & Girones, R. (2005).** Nested multiplex PCR assay for detection of human enteric viruses in shellfish and sewage. *Journal of Virological Methods* **125**, 111-118.
- Fuhrman, J.A., Liang, X. & Noble, R. T. (2005).** Rapid Detection of Enteroviruses in Small Volumes of Natural Waters by Real-Time Quantitative Reverse Transcriptase PCR. *Applied and Environmental Microbiology* **71**, 4523-4530.
- Gan, S. D. & Patel, K. R. (2013).** Enzyme Immunoassay and Enzyme-Linked Immunosorbent Assay. *Journal of Investigative Dermatology* **133**, 1-4.
- Garibyan, L. & Avashia, N. (2013).** Polymerase Chain Reaction. *Journal of Investigative Dermatology* **133**, 1-4.
- Ghadage, D. P., Mali, R., Wankhade, A. B. & Bhore, A. V. (2014).** Case Report: Gastroenteritis due to *Isospora belli* in immunocompromised teenager. *International Journal of Healthcare and Biomedical Research* **2**, 64-66.
- Granum, P. E. & Lund, T. (1997).** *Bacillus cereus* and its food poisoning toxins. *FEMS Microbiology Letters* **157**, 223-228.
- Green, K. Y., Ando, T., Balayan, M. S., Berke, T., Clarke, I. N., Estes, M. K., Matson, D. O., Nakata, S., Neill, J. D., & other authors. (2000).** Taxonomy of the Caliciviruses. *The Journal of Infectious Disease* **181**, S322-S330.
- Green, K. Y. (2007).** *Caliciviridae: The Noroviruses*. In *Fields' Virology*, volume 1, 5<sup>th</sup> edition, pp. 949 – 981. Edited by Howley, P. M. and Knipe, D. M. Philadelphia: USA. Lippincott Williams & Wilkins.

- Griffin, D. W., Donaldson, K. A., Paul, J. H. & Rose, J. B. (2003).** Pathogenic Human Viruses in Coastal Waters. *Clinical Microbiology Reviews* **16**, 129-143.
- Herbert, T. T. (1963).** Precipitation of Plant Viruses by Polyethylene Glycol. *Phytopathology* **53**, 362.
- Holtz, L. R., Finkbeiner, S. R., Kirkwood, C. D. & Wang, D. (2008).** Identification of a novel picornavirus related to cosavirus in a child with acute diarrhea. *Virology Journal* **5**, 1-5.
- Hoseini, S. S. & Sauer, M. G. (2015).** Molecular cloning using polymerase chain reaction, an educational guide for cellular engineering. *Journal of Biological Engineering* **9**, 1-12.
- International Committee on Taxonomy of Viruses. (2012).** Family Picornaviridae. In *Virus Taxonomy: Classification and Nomenclature of Viruses: Ninth Report of the International Committee on Taxonomy of Viruses*, pp. 855-890. Edited by King A. M. Q., Adams M. J., Carstens E. B. & Lefkowitz E. J. San Diego: Elsevier Academic Press.
- Iyaloo, S., Keddy, K., Page, N., Poonsamy, B., Cohen, C., & Frean, J. (2015).** Non-viral causes of diarrhoea in children less than 5 years from sentinel sites in South Africa, 2009 – 2013. *Communicable Diseases Surveillance Bulletin* **13**, 65-72.
- Jeong, H. S., Jeong, A. & Cheon, D- S (2012).** Epidemiology of Asrtovirus Infection in Children. *Korean Journal of Paediatrics* **55**, 77-82.
- Jones, M. S., Lukashov, V. V., Ganac, R. D. & Schnurr, D. P. (2007).** Discovery of a Novel Human Picornavirus in a Stool Sample from a Pediatric Patient Presenting with Fever of Unknown Origin. *Journal of Clinical Microbiology* **45**, 2144-2150.
- Kageyama, T., Kojima, S., Shinohara, M., Uchida, K., Fukushi S., Hoshino, F. B., Takeda, N. & Katayama, K. (2003).** Broadly Reactive and Highly Sensitive Assay for Norwalk-Like Viruses Based on Real-Time Quantitative Reverse Transcription-PCR. *Journal of Clinical Microbiology* **41**, 1548-1557.
- Kapikian, A. Z., Wyatt, R. G., Dolin, R., Thornhill, T. S., Kalica, A. R. & Chanock, R. M. (1972).** Visualization by Immune Electron Microscopy of a 27-nm Particle Associated with Acute Infectious Nonbacterial Gastroenteritis. *Journal of Virology* **10**, 1075-1081.
- Kapoor, A., Victoria, J., Simmonds, P., Slikas, E., Chieochansin, T., Naeem, A., Shaukat, S., Sharif, S., Alam, M. M., & other authors (2008).** A highly prevalent and genetically diversified *Picornaviridae* genus in South Asian children. *PNAS* **105**, 1-6.

- Khamrin, P., Chaimongkol, N., Nantachit, N., Okitsu, S., Ushijima, H. & Maneekern, N. (2011).** Saffold Cardioviruses in Children with Diarrhea, Thailand. *Emerging Infectious Disease* **17**, 1150-1152.
- Knowles, N. J., Hovi, T., Hyypiä, T., King, A. M. Q., Lindberg, A. M., Pallansch, M. A., Palmenberg, A. C., Simmonds, P., Skern, T., & other authors. (2012).** *Picornaviridae*. In: *Virus Taxonomy: Classification and Nomenclature of Viruses: Ninth Report of the International Committee on Taxonomy of Viruses*, pp 855-880. Edited by King, A. M. Q., Adams, M.J., Carstens, E. B. and Lefkowitz, E. J. San Diego. USA, Elsevier Academic Press.
- Knox, C. M., Luke, G. A., Dewar, J., de Felipe, P. & Williams, B. J. (2012).** Rotaviruses and Emerging Picornaviruses as Aetiological Agents of Acute Gastroenteritis. *South African Journal of Epidemiological Infection* **27**, 141-148.
- Kojima, S., Kageyama, T., Fukushi, S., Hoshino, F. B., Shinohara, M., Uchida, K., Natori, K., Takeda, N. & Katayama, K. (2002).** Genogroup-specific PCR primers for detection of Norwalk-like viruses. *Journal of Virological Methods* **100**, 107-114.
- Kumar, G., Sen, M. & Roy, A. (2015).** Stool Microscopy Examination to HIV Diagnosis: A Case Report of Gastroenteritis by Isosporiasis. *International Journal of Current Microbiology and Applied Sciences* **4**, 438-441.
- La Rosa, G., Pourshaban, M., Iaconelli, M. & Muscillo, M. (2008).** Detection of Genogroup IV Noroviruses in Environmental and Clinical Samples and Partial Sequencing Through Rapid Amplification of cDNA Ends. *Archives Virology* **153**, 2077-2083.
- Lanata, C., Fischer-Walker, C., Olascoaga, A., Torres, C., Aryee, M. & Black, R. (2013).** Global causes of diarrheal disease mortality in children <5 Years of Age: A Systematic Review. *PLoS ONE* **8**, 1-11.
- Le Guyader, F.S., Le Saux, J. –C., Ambert-Balay, K., Krol, J., Serais, O., Parnaudeau, S., Giraudon, H., Delmas, G., Pommepuy, M. & other authors. (2008).** Aichi Virus, Norovirus, Astrovirus, Enterovirus and Rotavirus Involved in Clinical Cases from a French Oyster-Related Gastroenteritis Outbreak. *Journal of Clinical Microbiology* **46**, 4011-4017.
- Le Pendu, J., Ruvoën-Clouet, N., Kindberg, E. & Svensson, L. (2006).** Mendelian resistance to human norovirus infections. *Seminars in Immunology* **18**, 375-386.

- Lewis, G. D. & Metcalf, T. G. (1988).** Polyethylene Glycol Precipitation for Recovery of Pathogenic Viruses, Including Hepatitis A Virus and Human Rotavirus, from Oyster, Water, and Sediment Samples. *Applied and Environmental Microbiology* **54**, 1983-1988.
- Lewis, G. D., Hough, A., Green, D. H., Hay, J. E. & Ferguson, L. R. (2010).** Modification of the Polyethylene Glycol 6000 Precipitation Method for Recovering Human and Indicator Viruses from Oysters and Mussels. *New Zealand Journal of Marine and Freshwater Research* **30**, 443-447.
- Liao, Y., Zhou, Y., Guo, Q., Xie, X., Luo, E., Li, L. & Li, Q. (2013).** Simultaneous Detection, Genotyping, and Quantification of Human Papillomaviruses by Multicolor Real-Time PCR and Melting Curve Analysis. *Journal of Clinical Microbiology* **52**, 429-435.
- Lim, J. Y., Yoon, J. W. & Hovde, C. J. (2010).** A Brief Overview of Escherichia coli O157:H7 and its Plasmid O157. *Journal of Microbial Biotechnology* **20**, 5-14.
- Lipton, H. L. & Friedman, A. (1980).** Purification of Theiler's murine encephalomyelitis virus and analysis of the structural virion polypeptides: correlation of the polypeptide profile with virulence. *Journal of Virology* **33**, 1165-1172.
- Lipton, H. L., Pritchard, A. E. & Calenoff, M. A. (1998).** Attenuation of neurovirulence of Theiler's murine encephalomyelitis virus strain GDVII is not sufficient to establish persistence in the central nervous system. *Journal of General Virology* **79**, 1001-1004.
- Lipton, H. L. (2008).** Human Vilyuisk encephalitis. *Reviews in Medical Virology* **18**, 347-352.
- Lodder, W. J., Rutjies, S. A., Takumi, K. & de Roda Husman, A. M. (2013)** Aichi Virus in Sewage and Surface Water, the Netherlands. *Emerging Infectious Diseases* **19**, 1222-1230.
- Loisy, F., Atmar, R. L., Guillon, P., Le Cann, P., Pommeputy, M. & Le Guyader, F. S. (2005).** Real-time RT-PCR for norovirus screening in shellfish. *Journal of Virological Methods* **123**, 1-7.
- Magwalivha, M., Wolfaardt, M., Kiulia N. M., van Zyl W. B., Mwenda, J. M. & Taylor M. B. (2010).** High Prevalence of Species D Human Adenoviruses in Fecal Specimens From Urban Kenyan Children With Diarrhea. *Journal of Medical Virology* **82**, 77-84.
- Majowicz, S. E., Musto, J., Scallan, E., Angulo, F. J., Kirk, M., O' Brien, S. J., Jones, T. F., Fazil, A. & Hoekstra, R. M. (2010).** The Global Burden of Non-Typhoidal Salmonella Gastroenteritis. *Clinical Infectious Disease* **50**, 882-889.

- Mans, J., de Villiers, C., du Plessis, N. M., Avenant, T. & Taylor, M. B. (2010).** Emerging norovirus GII.4 2008 variant detection in hospitalised paediatric patients in South Africa. *Journal of Clinical Virology* **49**, 258-264.
- Mans, J., Netshikweta, R., Magwalivha, M., Van Zyl, W. B. & Taylor, M. B. (2013).** Diverse norovirus genotypes identified in sewage-polluted river water in South Africa. *Journal of Epidemiological Infection* **141**, 303-313.
- Mans, J., Murray, T. Y & Taylor, M. B. (2014).** Novel Norovirus Recombinants Detected in South Africa. *Virology Journal* **11**, 168.
- Matthijnssens, J., Ciarlet, M., Rahman, M., Attoui, H., Bányai, K., Estes, M. K., Gentsch, J. R., Iturriza-Gómara, M., Kirkwood, C. & other authors. (2009)** Recommendations for the classification of group A rotaviruses using all 11 genomic RNA segments. *Archives of Virology* **153**, 1621-1629.
- Midthun, K. & Kapikian, A. Z. (1996).** Rotavirus vaccines: an overview. *Clinical Microbiology Reviews* **9**, 423-434.
- Murray, L. (2007).** *Localisation of Theiler's Murine Encephalomyelitis Virus non-structural proteins 2B, 2C, 2BC and 3A in BHK-21 cells, and the effect of amino acid substitutions in 2C on localisation and virus replication.* Dissertation, pp 1-136.
- Naeem, A., Hosomi, T., Nishimura, Y., Alam, M. M., Oka, T., Zaidi, S. S. & Shimizu, H. (2014).** Genetic diversity of circulating Saffold viruses in Pakistan and Afghanistan. *Journal of General Virology* **95**, 1945-1957.
- Nakatani, S. M., Santos, C. A., Riediger, I. N., Krieger, M. A., Duarte, C. A., Lacerda, M. A., Biondo, A.W., Carilho, F. J. & Ono-Nita, S. K. (2010).** Development of Hepatitis C Virus Genotyping by Real-Time PCR Based on the NS5B Region. *PLoS ONE* **5**, 1-6.
- National Health Service. (2013b).** Quality Report For the Year 2012-2013. *Derby Hospitals NHS Foundation Trust*, 1-73.
- Nemerow, G. R., Stewart, P. L. & Reddy, V. S. (2012).** Structure of Human Adenovirus. *Current Opinion in Virology* **2**, 115-121.
- Nielsen, A. C. Y., Böttiger, B., Banner, B., Hoffmann, T. & Nielsen, L. P. (2012).** Serious Invasive Saffold Virus Infections in Children, 2009. *Emerging Infectious Disease* **18**, 7-12.

- Nielsen, A. C. Y., Gyhrs, M. L., Nielsen, L. P., Pedersen, C. & Böttiger, B. (2013). Gastroenteritis and the Novel Picornaviruses Aichi virus, Cosavirus, Saffold Virus, and Salivirus in Young Children. *Journal of Clinical Virology* **57**, 239-242.
- Odell, I. D. & Cook, D. (2013). Immunofluorescence Techniques. *Journal of Investigative Dermatology* **133**, 1-4.
- Oh, D. -Y., Silva, P.A., Hauroeder, B., Diedrich, S., Cardoso, D.D.P. & Schreier, E. (2006). Molecular characterization of the first Aichi viruses isolated in Europe and in South America. *Archives of Virology* **151**, 1199-1206.
- Oleszak, E. L., Chang, J. R., Friedman, H., Katsetos, C. D. & Platsoucas, C. D. (2004). Theiler's Virus Infection: a Model for Multiple Sclerosis. *Clinical Microbiology Reviews* **17**, 174-207.
- Ozoemena, L. C., Minor, P. D. & Afzal, M. A. (2004). Comparative Evaluation of Measles Virus Specific TaqMan PCR and Conventional PCR Using Synthetic and Natural RNA Templates. *Journal of Medical Virology* **73**, 79-84.
- Page, N., Mapuroma, F., Seheri, M., Kruger, T., Peenze, I., Walaza, S., Cohen, C., Groome, M. & Madhi, S. (2014). Rotavirus Surveillance Report, South Africa, 2013. *Communicable Diseases Surveillance Bulletin* **12**, 130-135.
- Parashar, U. D., Hummelman, E. G., Bresee, J. S., Miller, M. A. & Glass, R. I. (2003). Global Illness and Death Caused by Rotavirus Disease in Children. *Emerging Infectious Disease* **9**, 565-572.
- Petrosino, J. F., Highlander, S., Luna, R. A., Gibbs, R. A. & Versalovic, J. (2009). Metagenomic Pyrosequencing and Microbial Identification. *Clinical Chemistry* **55**, 856-866.
- Pham, N. T. K., Khamrin, P., Nguyen, T. A., Kanti, D. S., Phan, T. G., Okitsu, S. & Hiroshi Ushijima. (2007). Isolation and Molecular Characterization of Aichi Virus from Fecal Specimens Collected in Japan, Bangladesh, Thailand, and Vietnam. *Journal of Clinical Microbiology* **35**, 2287-2288.
- Pham, N.T.K., Trinh, Q. D., Chan-It, W., Khamrin, P., Shimizu. H., Okitsu, S., Mizuguchi, M. & Ushijima, H. (2010). A novel RT-multiplex PCR for detection of Aichi virus, human parechovirus, enteroviruses, and human bocavirus among infants and children with acute gastroenteritis. *Journal of Virological Methods* **169**, 193-197.
- Promega. (2006). pSP72 Vector Instructions for Use. *Technical Bulletin*, 1-7.

**Promega. (2010).** pGEM®-T and pGEM®-T Easy Vector Systems Instructions for Use. *Technical Bulletin*, 1-27.

**Racaniello, V.R. (2007).** Picornaviridae: The Viruses and Their Replication. In *Fields' Virology*, volume 1, 5<sup>th</sup> edition, pp. 795-838. Edited by Howley, P. M. and Knipe, D. M. Philadelphia: USA. Lippincott Williams & Wilkins.

**Rahman, M. (2012).** Salmonella: Taxonomy, Genomics and Antimicrobial Resistance. In *Foodborne and Waterborne Bacterial Pathogens*, pp. 113-119. Edited by Faruque, S. M. Norfolk: UK. Caister Academic Press.

**Rahman, M., Banik, S., Faruque, A. S. G., Taniguchi, K., Sack, D. A., Van Ranst, M. & Azim, T. (2005).** Detection and Characterisation of Human Group C Rotavirus in Bangladesh. *Journal of Clinical Microbiology* **43**, 4460-4465.

**Reuter, G., Boldizsár, A., Papp, G. & Pankovics, P. (2009).** Detection of Aichi virus shedding in a child with enteric and extraintestinal symptoms in Hungary. *Archives of Virology* **154**, 1529-1532.

**Reuter, G., Boros, Á. & Pankovics, P. (2011).** Kobuviruses- a comprehensive review. *Reviews in Medical Virology* **21**, 32-41.

**Robilotti, E., Deresinski, S. & Pinsky B. A. (2015).** Norovirus. *Clinical Microbiology Reviews* **28**, 134-164.

**Russell, W. C. (2000).** Update on Adenovirus and its Vectors. *Journal of General Virology* **81**, 2573-2604.

**Sanekata, T., Ahmed, M. U., Kader, A., Taniguchi, K. & Kobayashi, N. (2003).** Human Group B Rotavirus Infections Causes Severe Diarrhea in Children and Adults in Bangladesh. *Journal of Clinical Microbiology* **41**, 2187-2190.

**Staggemeier, R., Almeida, S. E. M. & Spilki, F. R. (2012).** Methods of Virus Detection in Soils and Sediments. *Virus Reviews and Research*, 1-7.

**Steele, D., Reynecke, E., de Beer, M., Bos, P. & Smuts, I. (2002).** Characterization of Rotavirus Infection in a Hospital Neonatal Unit in Pretoria, South Africa. *Journal of Tropical Pediatrics* **48**, 167-171.

**Storch, G. A. (2000).** Diagnostic Virology. *Clinical Infectious Disease* **31**, 739-751.

- Stranneheim, H. & Lundeberg, J. (2012).** Stepping Stones in DNA Sequencing. *Biotechnology Journal* **7**, 1063-1073.
- Tan, S. C. & Yiap, B. C. (2009).** DNA, RNA, and Protein Extraction: The Past and The Present. *Journal of Biomedicine and Biotechnology* **2009**, 1-10.
- Tate, J. E., Burton, A. H., Boschi-Pinto, C. & Parashar, U. D. (2016).** Global, Regional, and National Estimates of Rotavirus Mortality in Children <5 Years of Age, 2000-2013. *Clinical Infectious Diseases* **62**, S96-S105.
- Tshangela, A., Moyes, J., Kruger, T., Mapuroma, F., Peenze, I., Seheri, M., Walaza, S., Cohen, C. & Page, N. (2012).** Rotavirus Surveillance in South Africa, 2011. *Communicable Disease Surveillance Bulletin* **10**, 42-46.
- Verweij, J. J., Blange, R. A., Templeton, K., Schinkel, J., Brienen, E. A. T., van Rooyen, M. A. A., van Lieshout, L. & Polderman, A. M. (2004).** Simultaneous Detection of *Entamoeba histolytica*, *Giardia lamblia*, and *Cryptosporidium parvum* in Fecal Samples by Using Multiplex Real-Time PCR. *Journal of Clinical Microbiology* **42**, 1220-1223.
- Wacker, M. J. & Godard, M. P. (2005).** Analysis of One-Step and Two-Step Real-Time RT-PCR Using SuperScript III. *Journal of Biomolecular Techniques* **16**, 266-271.
- Wilhelmi, I., Roman, E. & Sánchez-Fauquier, A. (2003).** Viruses causing gastroenteritis. *Clinical Microbiology and Infection* **9**, 247-262.
- Wolfaard, M., Taylor, M. B., Booysen, H. F., Engelbrecht, L., Grabow, W. O. K. & Jiang, X. (1997).** Incidence of Human Calicivirus and Rotavirus Infections in Patients With Gastroenteritis in South Africa. *Journal of Medical Virology* **51**, 290-296.
- World Health Organisation. (2013).** Rotavirus surveillance data reporting period: January-June 2012. *Global Rotavirus Information and Surveillance Bulletin* **7**, 1-11.
- World Health Organisation. (2015).** World Health Statistic 2015. *WHO Library Cataloguing-in-Publication Data*, 56-75.
- Yamashita, T., Kobayashi, S., Sakae, K., Nakata, S., Chiba, S., Ishihara, Y. & Isomura, S. (1991).** Isolation of Cytopathic Small Round Viruses with BS-C-1 Cells from Patients with Gastroenteritis. *The Journal of Infectious Disease* **164**, 954-957.
- Yamashita, T., Sakae, K., Ishihara, Y., Isomura, S. & Utagawa, E. (1993).** Prevalence of Newly Isolated, Cytopathic Small Round Virus (Aichi Strain) in Japan. *Journal of Clinical Microbiology* **31**, 2938-2943.

**Yamashita, T., Sakae, K., Kobayashi, S., Ishihara, Y., Miyake, T., Mubina, A. & Isomura, S. (1995).** Isolation of Cytopathic Small Round Virus (Aichi Virus) from Pakistani Children and Japanese Travellers from Southeast Asia. *Microbiology and Immunology* **39**, 433-435.

**Yamashita, T., Sakae, K., Tsuzuki, H., Suzuki, Y., Ishikawa, N., Takeda, N., Miyamura, T. & Yamazaki, S. (1998).** Complete Nucleotide Sequence and Genetic Organization of Aichi Virus, a Distinct Member of the *Picornaviridae* Associated with Acute Gastroenteritis in Humans. *Journal of Virology* **72**, 8408-8412.

**Yamashita, T., Sugiyama, M., Tsuzuki, H., Sakae, K., Suzuki, Y. & Miyazaki, Y. (2000).** Application of a Reverse Transcription-PCR for Identification and Differentiation of Aichi Virus, a New Member of the Picornavirus Family Associated with Gastroenteritis in Humans. *Journal of Clinical Microbiology* **38**, 2955-2961.

**Zakikhany, K., Allen, D. J., Brown, D. & Iturriza-Gómara, M. (2012).** Molecular Evolution of GII-4 Norovirus Strains. *PLoS ONE* **7**, 1-8.

**Zheng, D. P., Ando, T., Fankhauser, R. L., Beard, R. S., Glass, R. I. & Monroe, S. S. (2006).** Norovirus classification and proposed strain nomenclature. *Virology* **346**, 312–323.

**Zoll J., Hulshof S. E., Lanke K., Lunel F. V., Melcher W. J. G., Schoondermark –van de Ven E., Roivainen M., Galama J. M. G. & van Kuppeveld F.J. M. (2009).** Saffold Virus, a Human Theiler's-Like Cardiovirus, Is Ubiquitous and Causes Infection Early in Life. *PLoS Pathogens* **5**, 1-10.

**Norovirus. Centre for Disease Control and Prevention (reviewed 2013).** <http://www.cdc.gov/norovirus.html>. Updated 10/12/2015. Accessed 12/01/2016.

**Virus Taxonomy: 2014 Release. International Committee on Taxonomy of Viruses (2014).** <http://www.ictvonline.org/virusTaxonomy.asp>. Updated February 2015. Accessed 25/1/2016.

**Salmonella (Non-Typhoidal) Fact Sheet. (World Health Organisation. (2016).** <http://www.who-int/mediacentre/factsheets/fs139/en>. Updated December 2016. Accessed 25/3/2016.

**Rotavirus Vaccine. National Health Service (2013).**

[www.nhs.uk/conditions/vaccinations/pages/rotavirus-vaccine.aspx](http://www.nhs.uk/conditions/vaccinations/pages/rotavirus-vaccine.aspx). Updated 16 April 2014. Accessed 12/1/2016.

**Figure 1.4:** Viral Zone. (2015). [www.viralzone.expasy.org](http://www.viralzone.expasy.org) (Accessed: 06/12/2015)

**Figure 1.7:** Viral Zone. (2015). [http://viralzone.expasy.org/all\\_by\\_species/27.html](http://viralzone.expasy.org/all_by_species/27.html)  
(Accessed: 25/03/2017)

**Figure 4.1:** Invertebrate Anatomy OnLine: *Crassostrea virginica* © American oyster. (2007)  
<http://lanwebs.lander.edu/faculty/rsfox/invertebrates/crassostrea.html>  
(accessed on: 4/07/2013).

## Appendix I: Aichivirus Nucleotide Sequences and Multiple Alignments

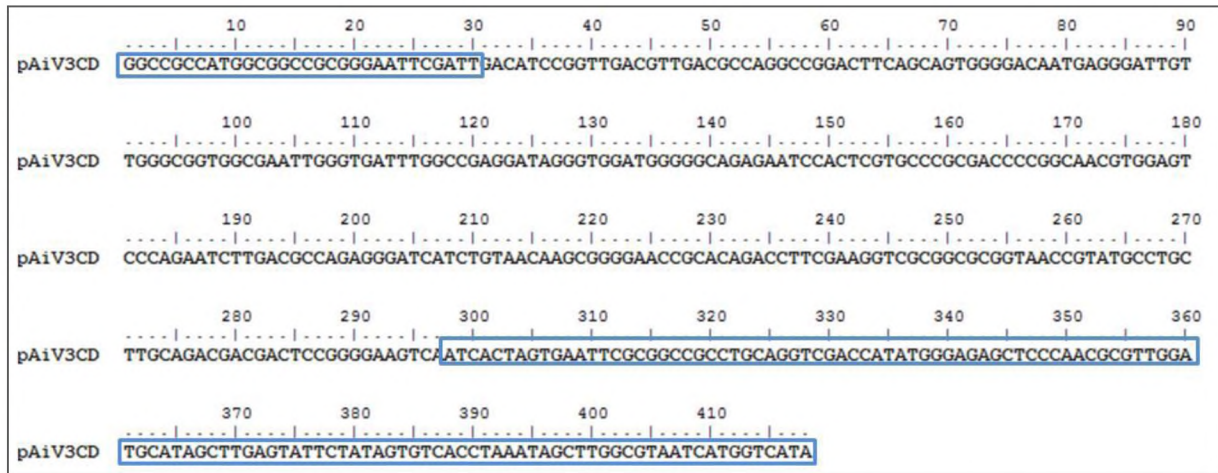


**Figure 1S:** The nucleotide sequence of the AiV 3CD insert in pAiV3CD. The blue boxes highlight the pGEM®-T Easy nucleotide sequence which surrounds the AiV 3CD insert.

```

      10      20      30      40      50      60      70      80      90
pAiV5'UTR  TTAACCCCTCACTAAAGGGACTAGTCTGCAGGTTTAAACGAATTCGCCCTTGTAACTCCATTAGCTTCTTCGGAACCTGTTCCGGAGGAA
      100     110     120     130     140     150     160     170     180
pAiV5'UTR  TTAACGGGCACCCATACTCCCCCACCCTTTTGTAACTAAGTATGTGTGCTCGTGACCTTGACTCCCACGGAACGGACCGATCC
      190     200     210     220     230     240     250     260     270
pAiV5'UTR  GTTGGTGAACAAACAGCTAGGTCCACATCCTCCCTTCCCTGGGAGGGTCCCCGCCCTCCACATCCTCCCCCAGCCTGACGTATCAC
      280     290     300     310     320     330     340     350     360
pAiV5'UTR  AGGCTGTGTGAAGCCCCGCGAAAGCTGCTCACGTGGCAATTGTGGTCCCCCTTCATCAAGACACCAGGTCTTTCCTCCTTAAGGCTA
      370     380     390     400     410     420     430     440     450
pAiV5'UTR  GCCCCGGCGTGTGAACCTCACGTTGGGCAACTAGTGGTGTCACTGTGCGCTCCCAATCTCGGCCGCGGAGTGTGTTCCCAAGCCAAC
      460     470     480     490     500     510     520     530     540
pAiV5'UTR  CCTGGCCCTTCACTATGTGCCTGGCAAGCATATCTGAGAAGGTGTTCCGCTGTGGCTGCCAGCCTGGTAACAGGTGCCCCAGTGTGCGTA
      550     560     570     580     590     600     610     620     630
pAiV5'UTR  ACCTTCTCCGTCTTCGGACGGTAGTGATTGGTTAAGATTTGGTGAAGTTTCATGTCCAACGCCCTGTGCGGGATGAAACCTCTACTG
      640     650     660     670     680     690     700     710     720
pAiV5'UTR  CCCTAGGAATGCCAGGCAGGTACCCACCTCCGGTGGGATCTGAGCCTGGGCTAATTGTCTACGGTAGTTTCATTTCCAATTCTTTCA
      730     740     750     760     770     780     790     800     810
pAiV5'UTR  TGTCGGAGTCATGGCTGCAACACGGGTTTACGATCTGTGCTCGTGTGGCTCACTCTGCTGCTCACCGCACCTACCACACTGTCTT
      820     830     840     850     860     870     880     890     900
pAiV5'UTR  TGACTGCTATGATAGGCTCTACCTCAACACCAACCCCATCTCTCCTATCCCCTTCCCAAAAATTCCTCCTTCCCTTGCCCGTTCTGCC
      910     920     930     940     950     960     970     980     990
pAiV5'UTR  AGTACGACGAGCAGAAATGAAGTCTCTCCACAGAGTCTCTCTGCGGTGAGGGGGCCGAACCCCTGCTGGAAGTGCTCACAGGACAAGCCCC
      1000    1010    1020    1030    1040    1050    1060    1070    1080
pAiV5'UTR  GCCGCAACACAACACCACCCCTCCTGAAGACTGGCTCTATGATTCTGATGTCCAATCCTGAAGGGCGAATTCGGGCCGCTAAATTCAA

```

**Figure 2S:** The nucleotide sequence of the AiV 5'UTR insert in pAiV5'UTR. The blue boxes highlight the pGEM®-T Easy nucleotide sequence which surrounds the AiV 5'UTR insert.



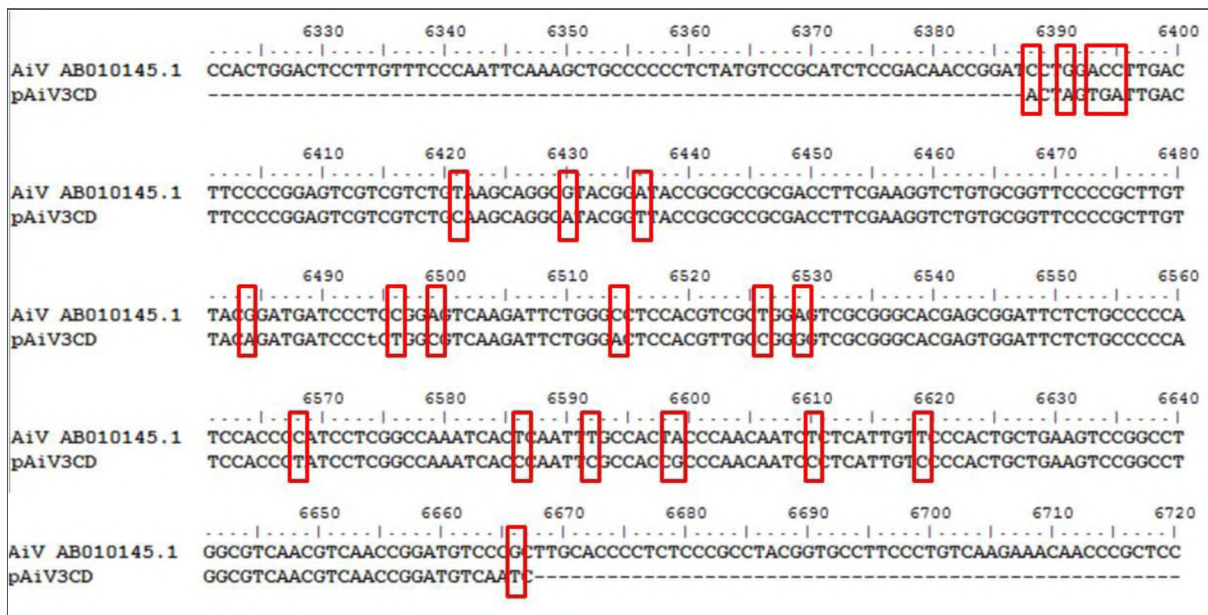


**Figure 4S:** A multiple sequence alignment of the nucleotide sequence of the AiV 3CD insert of pAiV3CD to the AiV reference strain (Accession no. AB010145.1). The red blocks indicate changes in the bases of the nucleotide sequences nucleotide.

## *Appendix II: Norovirus Nucleotide Sequences and Multiple Alignments*

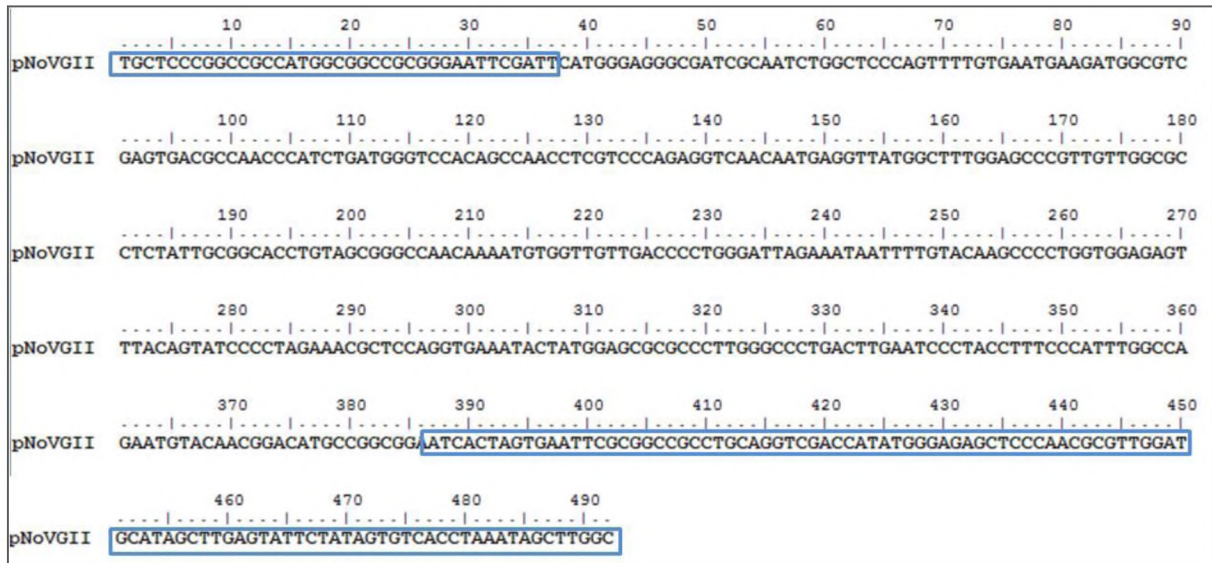


**Figure 5S:** The nucleotide sequence of the NoV GII N/S Domain PCR product insert in pNoVGII. The blue boxes highlight the pGEM®-T Easy nucleotide sequence which surrounds the NoV GII N/S Domain insert.

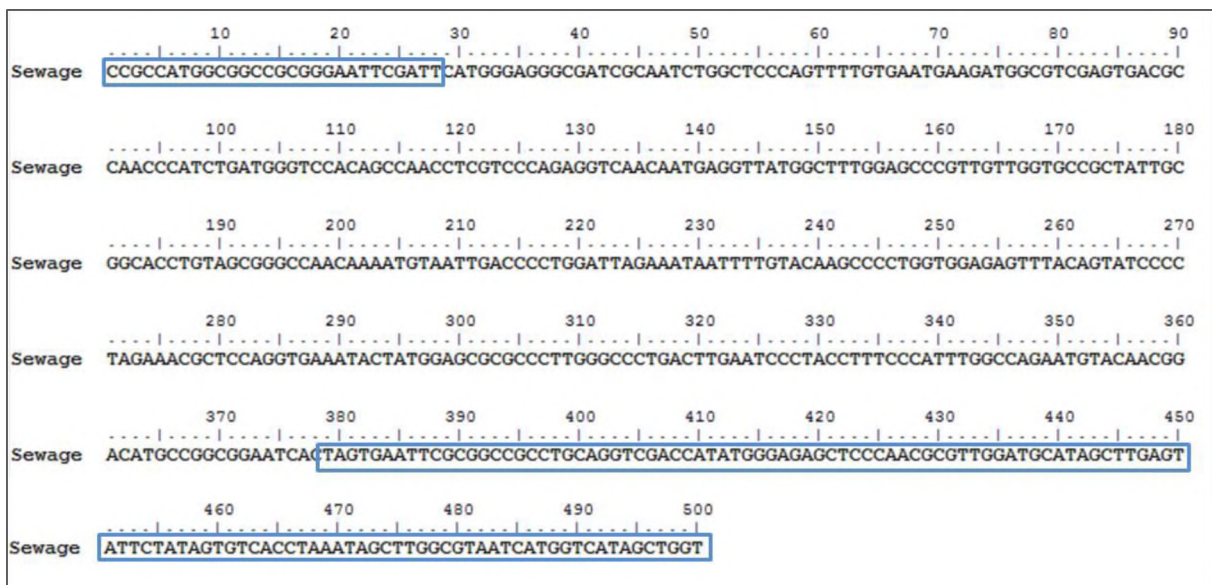


**Figure 6S:** The nucleotide sequence of the NoV GII N/S Domain PCR product from the sewage sample inserted into pGEM®-T Easy. The blue boxes highlight the pGEM®-T Easy nucleotide sequence which surrounds the NoV GII N/S Domain insert.



**Figure 7S:** The nucleotide sequence of the NoV GII N/S Domain PCR product from the oyster sample inserted into pGEM®-T Easy. The blue boxes highlight the pGEM®-T Easy nucleotide sequence which surrounds the NoV GII N/S Domain insert.



**Figure 8S:** The nucleotide sequence of the NoV GII N/S Domain PCR product from the P1 stool sample inserted into pGEM®-T Easy. The blue boxes highlight the pGEM®-T Easy nucleotide sequence which surrounds the NoV GII N/S Domain insert.



**Figure 9S:** The nucleotide sequence of the NoV GII N/S Domain PCR product from the P5 stool sample inserted into pGEM®-T Easy. The blue boxes highlight the pGEM®-T Easy nucleotide sequence which surrounds the NoV GII N/S Domain insert.

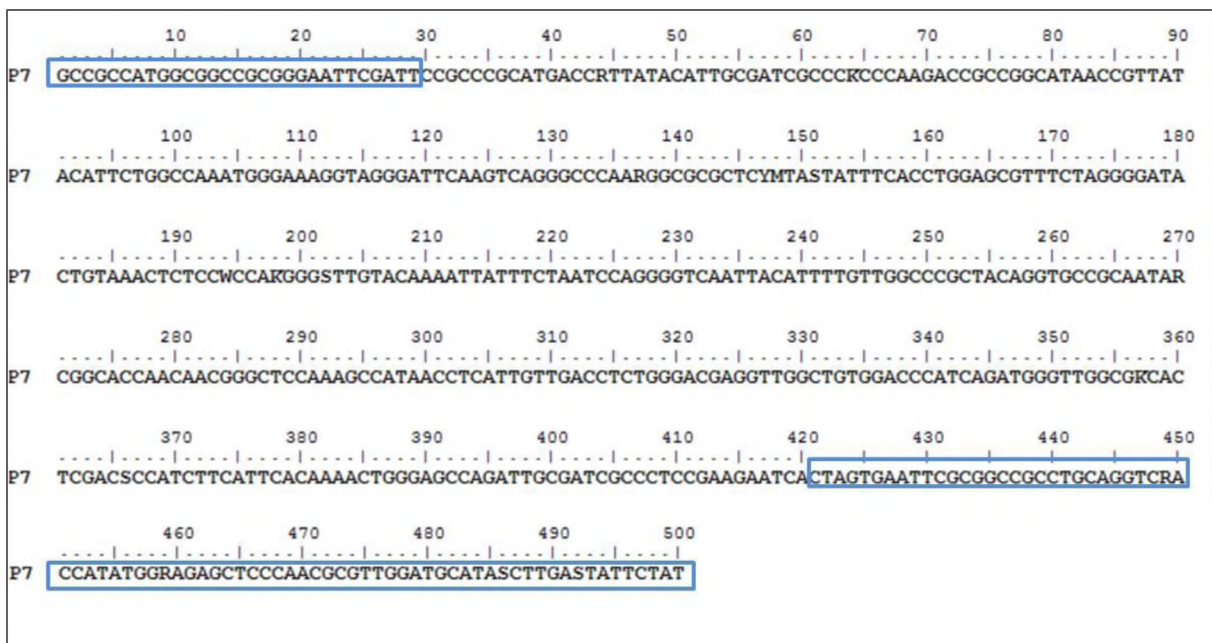


**Figure 10S:** The nucleotide sequence of the NoV GII N/S Domain PCR product from the P7 stool sample inserted into pGEM®-T Easy. The blue boxes highlight the pGEM®-T Easy nucleotide sequence which surrounds the NoV GII N/S Domain insert.

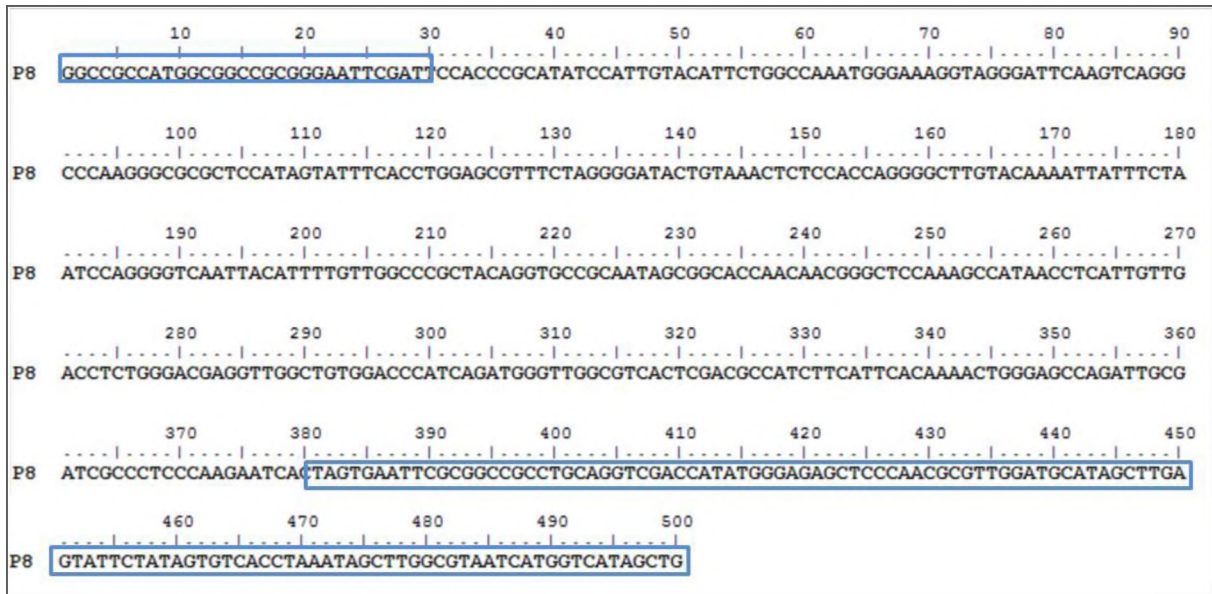


**Figure 11S:** The nucleotide sequence of the NoV GII N/S Domain PCR product from the P8 stool sample inserted into pGEM®-T Easy. The blue boxes highlight the pGEM®-T Easy nucleotide sequence which surrounds the NoV GII N/S Domain insert.

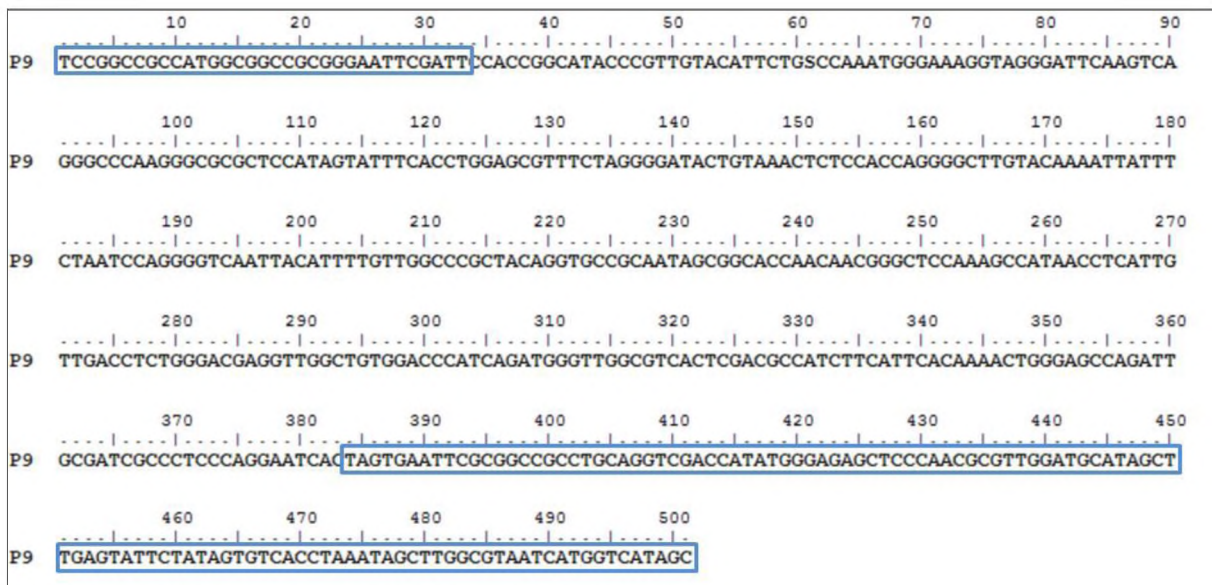


**Figure 12S:** The nucleotide sequence of the NoV GII N/S Domain PCR product from the P9 stool sample inserted into pGEM®-T Easy. The blue boxes highlight the pGEM®-T Easy nucleotide sequence which surrounds the NoV GII N/S Domain insert.



**Figure 13S:** The nucleotide sequence of the NoV GII N/S Domain PCR product from the P17 stool sample inserted into pGEM®-T Easy. The blue boxes highlight the pGEM®-T Easy nucleotide sequence which surrounds the NoV GII N/S Domain insert.

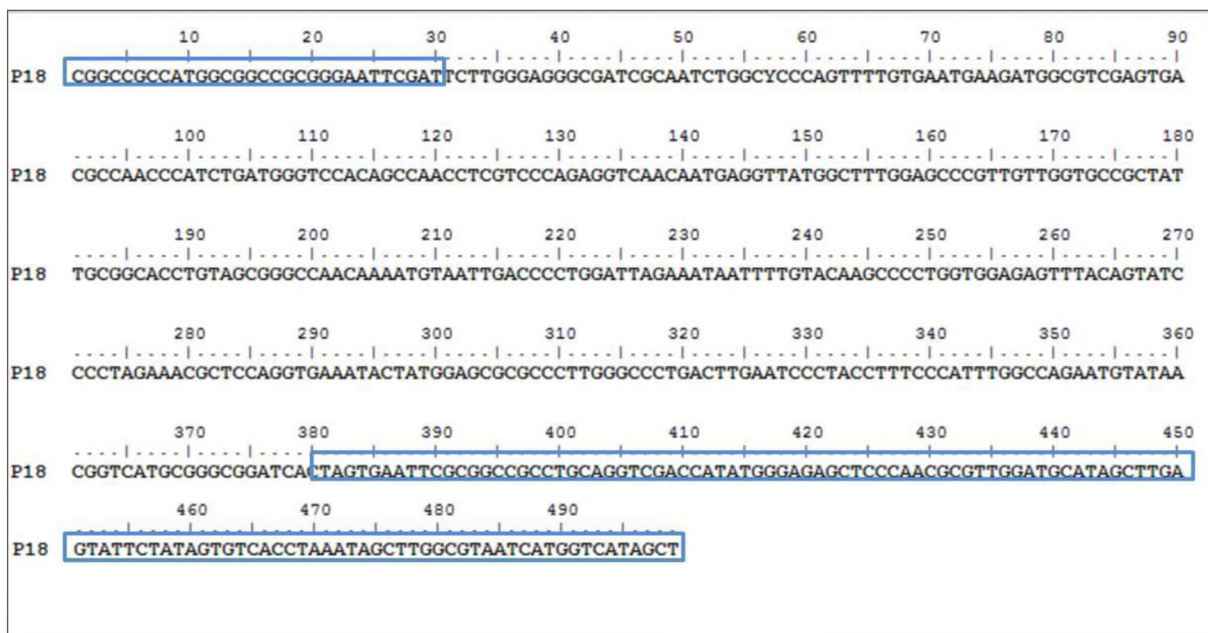


**Figure 14S:** The nucleotide sequence of the NoV GII N/S Domain PCR product from the P18 stool sample inserted into pGEM®-T Easy. The blue boxes highlight the pGEM®-T Easy nucleotide sequence which surrounds the NoV GII N/S Domain insert.



**Figure 15S:** The nucleotide sequence of the NoV GII N/S Domain PCR product from the P19 stool sample inserted into pGEM®-T Easy. The blue boxes highlight the pGEM®-T Easy nucleotide sequence which surrounds the NoV GII N/S Domain insert.

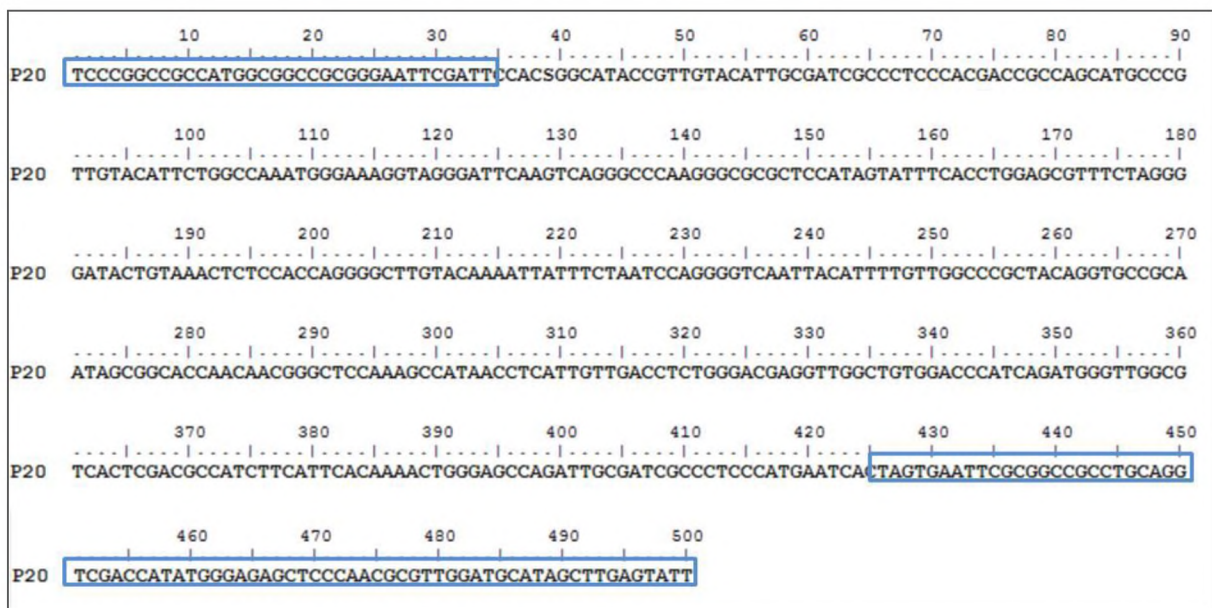


**Figure 16S:** The nucleotide sequence of the NoV GII N/S Domain PCR product from the P20 stool sample inserted into pGEM®-T Easy. The blue boxes highlight the pGEM®-T Easy nucleotide sequence which surrounds the NoV GII N/S Domain insert.



**Figure 17S:** The nucleotide sequence of the NoV GII N/S Domain PCR product from the P21 stool sample inserted into pGEM®-T Easy. The blue boxes highlight the pGEM®-T Easy nucleotide sequence which surrounds the NoV GII N/S Domain insert.



**Figure 18S:** The nucleotide sequence of the NoV GII N/S Domain PCR product from the P29 stool sample inserted into pGEM®-T Easy. The blue boxes highlight the pGEM®-T Easy nucleotide sequence which surrounds the NoV GII N/S Domain insert.

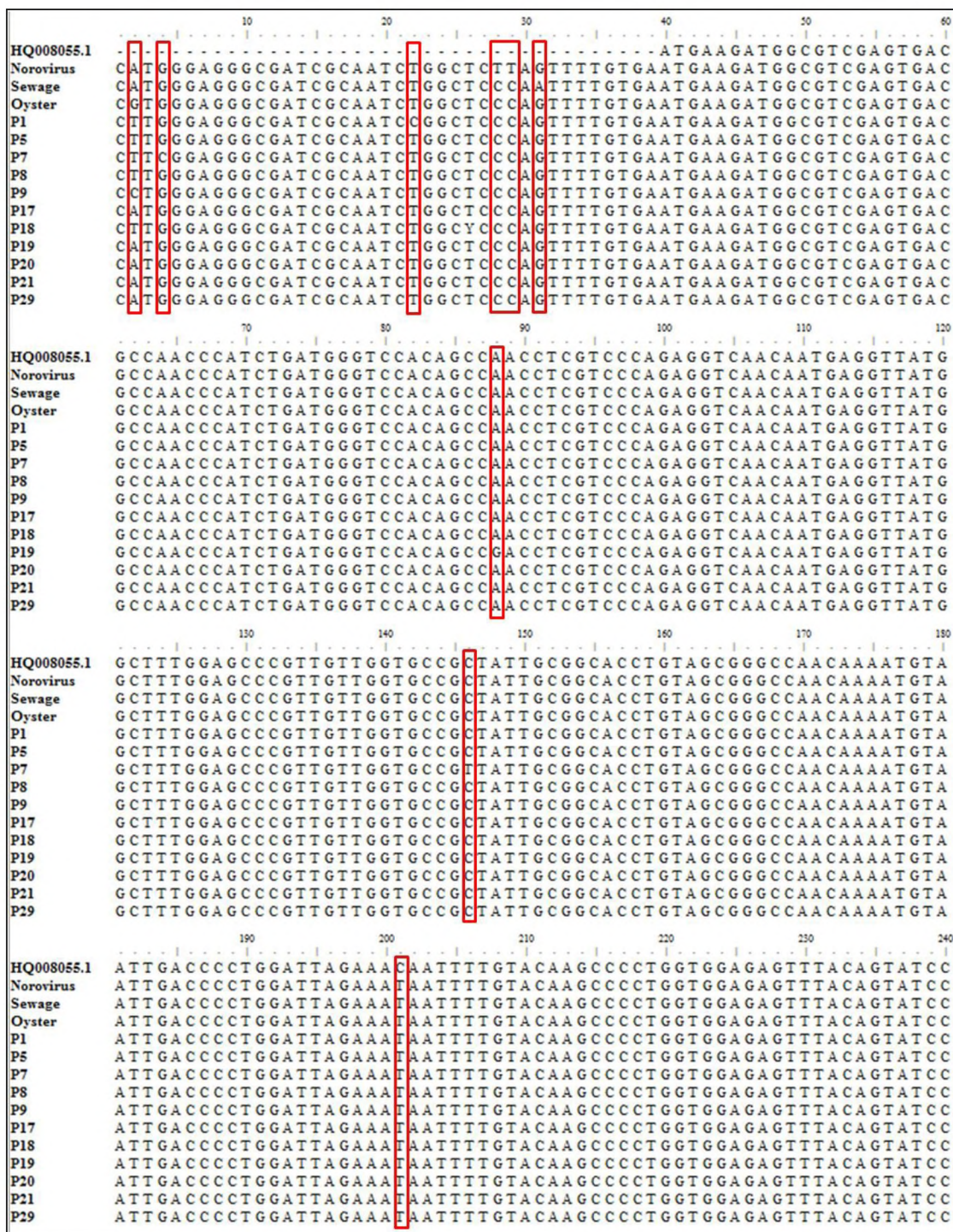


**Figure 19S:** A multiple alignment of the NoV GII PCR product nucleotide sequences from the NoV GII positive sample, wastewater, oyster and 11 stool samples and the reference strain (Accession no. HQ008055.1). The red blocks highlight changes in the bases of the nucleotide sequences. Continues on next page.



Figure 19S: (Continued from previous page) A multiple alignment of the NoV GII PCR product nucleotide sequences from the NoV GII positive sample, wastewater, oyster and 11 stool samples and the reference strain (Accession no. HQ008055.1). The red blocks highlight changes in the bases of the nucleotide sequences.